Characterizing the Role of Endofin/*ZFYVE16* in Cell Surface Receptor Trafficking and Tumor Suppression.

Jalal M. Kazan

Department of Biochemistry

Goodman Cancer Institute

McGill University

Montreal, Quebec, Canada

December 2021

A thesis submitted to McGill University in partial fulfillment of the requirements of the degree of Doctor of Philosophy

Table of Contents:

Abstract:

Cell surface receptors regulate several processes such as cell proliferation, survival, differentiation and migration/invasion. In cancer, several cell surface receptors are candidates for targeted therapy since they play critical roles in tumorigenesis and cancer progression. Internalized and ubiquitinated signaling receptors are silenced upon multivesicular body formation, a cellular process catalyzed by the Endosomal Sorting Complexes Required for Transport (ESCRT) machinery. HD-PTP/*PTPN23* is an ESCRT protein, it binds to different subunits of the ESCRT machinery and it is involved in the lysosomal delivery of several activated cell surface receptors such as integrin α5 and EGFR. Moreover, HD-PTP is a haploinsufficient tumor suppressor and its heterozygous deletion in mice induces spontaneous B cell lymphoma and upregulates integrin β1 receptor at the plasma membrane of lymphoma B cells. In addition, HD-PTP suppression in mammary epithelial cells triggers an invasive phenotype and predisposes breast tumorigenesis. HD-PTP directly binds to Endofin/*ZFYVE16*, a FYVE-domain protein recruited to early endosomes with poorly understood roles.

In this study, we show that Endofin forms a complex with ESCRT proteins and EGFR on early endosomes. Endofin depletion in HeLa cells increased integrin α5 and EGFR plasma membrane density and stability by hampering their lysosomal delivery, which in turn sustained receptor signaling and increased cell migration. Complementation of Endofin- or HD-PTP-depleted HeLa cells with wild-type Endofin or HD-PTP, but not with mutants harboring impaired Endofin/HD-PTP interaction or cytosolic Endofin, restored EGFR lysosomal delivery. Endofin also promoted Hrs indirect interaction with HD-PTP on early endosomes.

Cell surface proteomics and RNA-sequencing showed that Endofin and HD-PTP depletion in HeLa cells upregulated several cell surface receptors and gene expression well-known to be

involved in cancer metastasis. Interestingly, bioinformatics showed that *ZFYVE16* and *PTPN23* heterozygous deletions are frequent in breast cancer patients with basal-like subtype. This coincides with the increase in total integrin α5 receptor levels, signaling and cell migration/invasion upon Endofin and HD-PTP depletion in MDA-MB-231 triple negative basal-like breast cancer cells. Importantly, HD-PTP depletion in 4T1 triple negative murine breast cancer cells, increased lung metastasis in a syngeneic tumor mouse model.

Jointly, our results indicate that Endofin is required for HD-PTP and ESCRT-0 interdependent sorting of ubiquitinated transmembrane cargoes, ensuring efficient receptor desensitization and lysosomal delivery. Moreover, our data demonstrates that HD-PTP plays an important role in breast cancer metastasis, and Endofin depletion induces an invasive phenotype in triple negative breast cancer cells. Hence, Endofin might exert a tumor suppressor activity.

Résumé:

Les récepteurs de surface cellulaire régulent plusieurs processus cellulaires tels que la prolifération, la survie, la différenciation et la migration/invasion. Plusieurs récepteurs de surface cellulaire jouent un rôle essentiel dans la progression du cancer et sont des candidats pour une thérapie ciblée contre le cancer. Les récepteurs de signalisation internalisés et ubiquitinés sont réduits au silence lors de la formation du corps multivésiculaire, un processus cellulaire catalysé par la machinerie des complexes de tri endosomaux requis pour le transport (ESCRT). HD-PTP/PTPN23, une protéine ESCRT, se lie à différentes protéines ESCRT et est impliquée dans la délivrance lysosomale de plusieurs récepteurs de surface cellulaire activés, notamment l'intégrine α5 et l'EGFR. De plus, HD-PTP est un suppresseur de tumeur haplo-insuffisant et sa délétion hétérozygote chez la souris induit un lymphome B spontané. De plus, la suppression de HD-PTP dans les cellules épithéliales mammaires déclenche un phénotype invasif et prédispose à la tumorigenèse mammaire. HD-PTP se lie directement à Endofin/ZFYVE16, une protéine du domaine FYVE recrutée dans les endosomes précoces avec des rôles mal compris.

Dans cette étude, nous montrons qu'Endofin forme un complexe avec les protéines ESCRT et EGFR sur les endosomes précoces. L'épuisement des endofines dans les cellules HeLa a augmenté la densité et la stabilité de l'intégrine 5 et de la membrane plasmique EGFR en entravant leur délivrance lysosomale, ce qui a à son tour soutenu la signalisation des récepteurs et augmenté la migration cellulaire. La complémentation de cellules HeLa appauvries en Endofin ou HD-PTP avec Endofin ou HD-PTP de type sauvage, mais pas avec des mutants présentant une association Endofin/HD-PTP altérée ou Endofin cytosolique, a restauré l'administration lysosomale d'EGFR. Endofin a également promu l'interaction indirecte de Hs avec HD-PTP.

La protéomique de la surface cellulaire et le séquençage de l'ARN ont montré que la déplétion d'Endofin et de HD-PTP dans les cellules HeLa régulait positivement plusieurs récepteurs de surface cellulaire et l'expression de gènes bien connus pour être impliqués dans les métastases cancéreuses. Fait intéressant, la bioinformatique a montré que les délétions hétérozygotes ZFYVE16 et PTPN23 sont fréquentes chez les patientes atteintes d'un cancer du sein présentant un sous-type de type basal. Cela coïncide avec l'augmentation des niveaux totaux de récepteurs de l'intégrine 5, de la signalisation et de la migration/invasion cellulaire lors de l'épuisement d'Endofin et de HD-PTP dans les cellules cancéreuses du sein de type basal triple négatives MDA-MB-231. Il est important de noter que l'épuisement de HD-PTP dans 4T1, cellules de cancer du sein murin triple négatif, a augmenté les métastases pulmonaires dans un modèle de souris tumorale syngénique.

Conjointement, nos résultats indiquent qu'Endofin est requis pour le tri interdépendant HD-PTP et ESCRT-0 des cargaisons transmembranaires ubiquitinées, assurant une désensibilisation efficace des récepteurs et une délivrance lysosomale. De plus, nos données démontrent que la HD-PTP joue un rôle important dans les métastases du cancer du sein et que la déplétion d'Endofin induit un phénotype invasif dans les cellules cancéreuses du sein triple négatives. Par conséquent, Endofin pourrait exercer une activité suppressive de tumeur.

Acknowledgements:

I would like to thank:

- My supervisor and co-supervisor, Dr. Arnim Pause and Dr. Gergely L. Lukacs, for their mentorship.
- My research advisory committee members, Dr. Peter Siegel, Dr. Janusz Rak and Dr. Jason C. Young, for their guidance through out my research projects.
- The collaborators, Dr. Anne-Claude Gingras, Dr. Philippe P. Roux and Dr. Peter Siegel, and their lab members, Dr. Claire E. Martin, Geneviève Lavoie and Sebastien Tabaries, respectively.
- All my lab colleagues who contributed to this work, for their help, advice and for sharing their scientific thoughts, Guillaume Desrochers, Paola Blanchette, Leeanna El-Houjeiri, Mathieu Paquette, Rafael Cuesta Sanchez and Hyeonju Jeong.
- My family and friends for their unlimited support and encouragement.
- My fiancée for standing by myside and being an endless source of support, love and encouragement. Your presence made everything easier and meaningful.

Thank you everyone…

Funding:

This project was supported by Lui in Tso Doctoral Fellowship, Fonds de Recherche Sante (FRQS) Doctoral Award and Graduate Excellence Doctoral Fellowship (GEF) for Merit. In addition to the grants awarded to Dr. Arnim Pause lab: Canadian Institutes for Health Research (CIHR) grant 245969 and the Canadian Cancer Society Research Institute (CCSRI) grant 245095.

Preface:

This thesis is written in a manuscript format and resulted in one published paper, three published review papers, one paper under preparation and two papers published in collaboration.

1. **Jalal M. Kazan**, Guillaume Desrochers, Claire E. Martin, Hyeonju Jeong, Dmitri Kharitidi, Pirjo M. Apaja, Ariel Roldan, Nicole St. Denis, Anne-Claude Gingras, Gergely L. Lukacs and Arnim Pause. Endofin is Required for HD-PTP and ESCRT-0 Interdependent Endosomal Sorting of Ubiquitinated Transmembrane Cargoes. *iScience*. **2021** Oct. doi.org/10.1016/j.isci.2021.103274. (Used by the author to write chapter1).

2. **Jalal M. Kazan**, Gergely L. Lukacs, Pirjo M. Apaja and Arnim Pause. Single cell fluorescence ratio image analysis for studying ESCRT function in receptor trafficking. *Methods Mol Biol*. **2019**; 1998:93-103. doi: 10.1007/978-1-4939-9492-2_7.

3. **Jalal M. Kazan**, Sébastien Tabariès, Ariadna Pollato Blanco, Guillaume Desrochers, Geneviève Lavoie, Philippe P. Roux, Peter M. Siegel and Arnim Pause. Loss of the ESCRT Complex Components Endofin and HD-PTP Enhances the Malignant Phenotypes of Triple Negative Breast Cancer Cells. Manuscript in preparation.

4. Leeanna El-Houjeiri*, Elite Possik*, Tarika Vijayaraghavan, Mathieu Paquette, Jose´ A. Martina, **Jalal M. Kazan**, Eric H. Ma, Russell Jones, Paola Blanchette, Rosa Puertollano and Arnim Pause. The Transcription Factors TFEB and TFE3 Link the FLCN-AMPK Signaling Axis to Innate Immune Response and Pathogen Resistance. *Cell Rep*. **2019** Mar 26;26(13):3613-3628.e6. doi: 10.1016/j.celrep.2019.02.102.

5. Lahaie S, Morales D, Bagci H, Hamoud N, Castonguay CE, **Jalal M. Kazan**, Desrochers G, Klar A, Gingras AC, Pause A, Côté JF and Kania A. The endosomal sorting adaptor HD-PTP is required for ephrin-B:EphB signalling in cellular collapse and spinal motor axon guidance. *Sci Rep*. **2019** Aug 16;9(1):11945. doi: 10.1038/s41598-019-48421-9.

6. Guillaume Desrochers, **Jalal M. Kazan** and Arnim Pause. Structure and functions of His domain protein tyrosine phosphatase in receptor trafficking and cancer. *Biochem Cell Biol*. **2018** Jun 7:1-5. doi: 10.1139/bcb-2017-0322. (Used by the author to write chapter1).

7. Marie-Claude Gingras, **Jalal M. Kazan** and Arnim Pause. Role of ESCRT component HD-PTP/PTPN23 in cancer. *Biochem Soc Trans*. **2017**; 45(3):845-854. DOI: 10.1042/BST20160332. (Used by the author to write chapter1).

Authors' Contribution:

Chapter 1: Jalal M. Kazan, Guillaume Desrochers and Marie-Claude Gingras designed and drafted the reviews.

Chapter 2: I have designed, performed and analyzed all the experiments except for the BioID and APMS proteomics experiments (figure 1 A and C and figure 4 C) which were performed by Claire E. Martin and Nicole St. Denis in collaboration with Dr. Anne-Claude Gingras's lab, co-IP experiments (figure 3 A, supplemental figure 5 C and supplemental figure 6 E and F), the signaling and double knock-down experiments (figure 5 C, D, F and G) which were performed by Guillaume Desrochers. I wrote the first draft of the manuscript, which was edited and corrected by Dr. Gergely Lukacs and Dr. Arnim Pause.

Chapter 3: I have designed, performed and analyzed all the experiments except for the cell surface proteomics and RNAseq experiments (figure 1 and 2) which were performed by Geneviève Lavoie in collaboration with Dr. Philippe Roux's lab. The *in vivo* mammary fat pad injections and tumor volume measurements were performed by Sebastien Tabaries in collaboration with Dr. Peter Siegel's lab. I wrote the first draft of the manuscript, which was edited and corrected by Dr. Peter Siegel and Dr. Arnim Pause.

List of Abbreviations:

AJCC	American joint committee on cancer
BirA*	biotin ligase
CAMs	cell adhesion molecules
CHX	cycloheximide
CK	cytokeratin
CME	clathrin-mediated endocytosis
Co-IP	co-immunoprecipitation
cs-ELISA	cell surface-ELISA
DDA	data dependent acquisition
DUB	deubiquitinating enzyme
ECM	extracellular matrix
EE	early endosomes
EGFR	epidermal growth factor receptor
EMT	epithelial-to-mesenchymal transition
ER	estrogen receptor
ESCRT	endosomal sorting complexes required for transport
FDR	false discovery rate
FITC	fluorescein isothiocyanate
FRIA	florescence ratiometric image analysis
GCRs	glucocorticoid receptors
GFP	green fluorescence protein
GPCRs	G protein-coupled receptors
HCC	hepatocellular carcinoma
HE	high exposure
HRP	horseradish peroxidase
ILV	intraluminal vesicles
LE	late endosomes

LE	low exposure
LIMS	laboratory information management system
Lys	lysosomes
MCC	mander’s colocalization coefficient
MFI	mean fluorescence intensity
MVBs	multivesicular bodies
NSCLC	non-small-cell lung cancer
NT	non-target
pHv	vesicular pH
PM	plasma membrane
PR	progesterone receptor
PSMs	peptide-spectrum matches
RCP	Rab-coupling protein
RE	recycling endosomes
RFP	red fluorescence protein
RNAseq	RNA sequencing
RTCA	real time cell analysis
RTKs	receptor tyrosine kinases
SEM	standard error of the mean
SNX	sorting nexin
STKRs	serine/threonine kinase receptors
SWATH	data independent acquisition
TPM	transcript per million
TSG	tumor suppressive gene
Ub	ubiquitin
VEGF	vascular endothelial growth factor
WCL	whole cell lysate
WT	wild-type

List of Figures:

Chapter 1:

Chapter 2:

Chapter 3:

Chapter 1 – Literature Review

1.1. General introduction on endosomal sorting:

Internalization of activated cell surface receptors and their subsequent endosomal sorting is a key eukaryotic cellular process. The endosomal system is a dynamic trafficking pathway connecting multiple cellular compartments including the plasma membrane (PM), endocytic vesicles, endosomes, trans-Golgi network and lysosomes. Endosomal sorting is implicated in several human diseases including cancer, immune disorders, lysosomal storage diseases, neurodegeneration and others. Here, we describe the general concepts of endocytic sorting of cell surface receptors starting from their internalization at the PM until their lysosomal degradation.

1.2. Overview of receptor trafficking:

The steady-state components of the PM are regulated through receptor-mediated endocytosis and consequent cargo sorting in the endolysosomal system. Upon ligand-activation, a cell surface receptor is ubiquitinated and internalized by clathrin-dependent or independent mechanisms. Next, the internalized receptor is sorted towards Rab5-positive early endosomes. At this stage, receptors are either recycled back to the PM which triggers receptor resensitization, or it is sorted towards lysosomal degradation to terminate receptor signaling. The sorting process is complex and depends on sorting signals, post-translational modifications, ligand interaction, sorting adaptor molecules and endosomal pH. Receptors are recycled back to the PM either via Rab4 (quick recycling) or Rab11 (slow recycling). However, ubiquitinated receptors are incorporated within the endosomal lumen during the formation of multivesicular bodies (MVBs). Then MVB fuse with lysosomes and its content gets degraded. Thus, endocytic sorting regulates PM components, their localization, levels and receptor signaling (Figure 1).

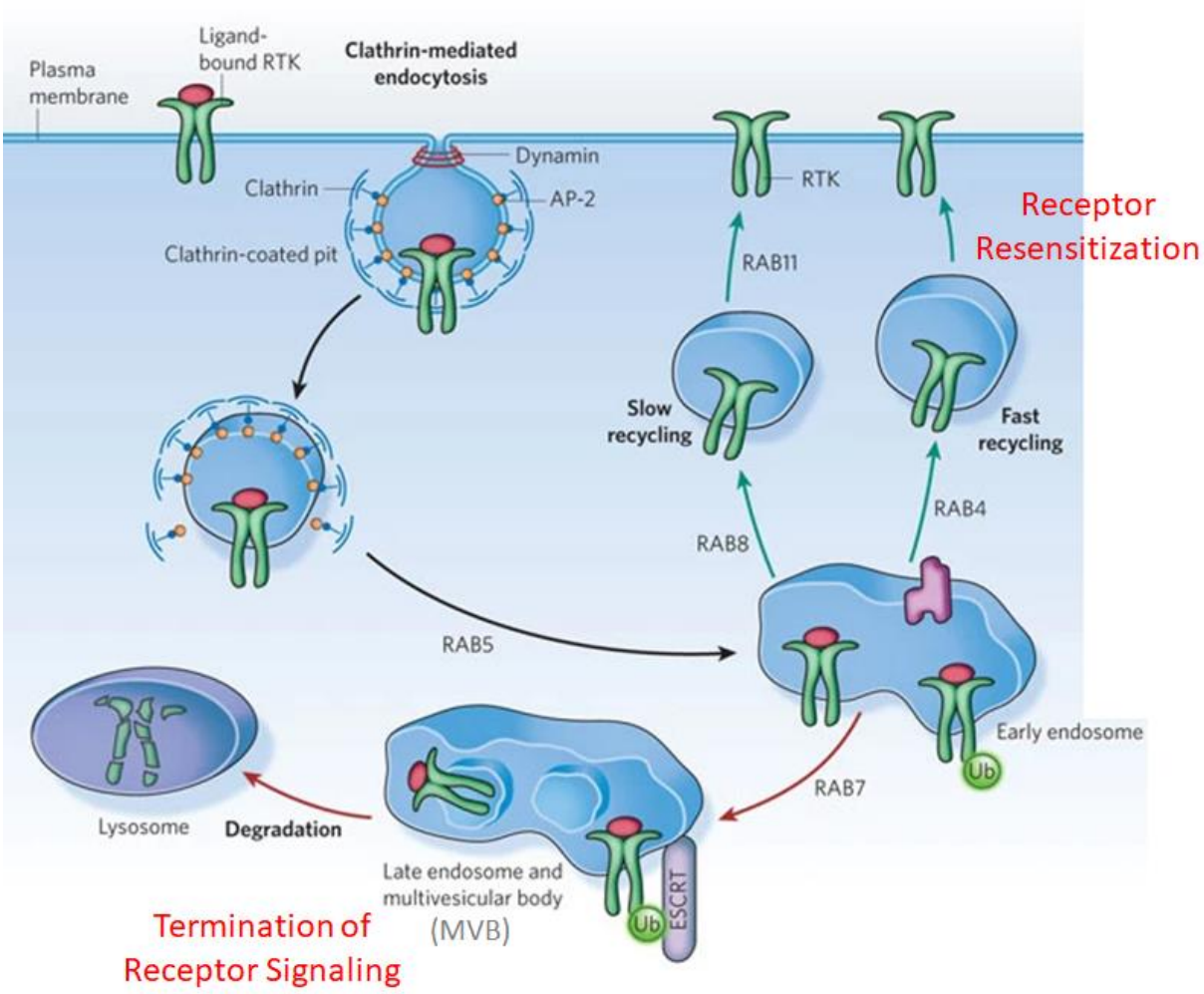

Figure 1: General overview of endosomal trafficking pathways:

Cell surface receptor endocytosis is initiated upon ligand activation of the receptor followed by receptor recruitment into clathrin coated pit. Other endocytic pathways exist (i.e. caveolae, pinocytosis, phagocytosis, etc), but are not shown here. The cargo containing clathrin vesicle undergoes uncoating and fuses with Rab5-positive early endosome. At this stage, receptors may be sorted to rapid (Rab4-mediated) or slow (Rab11-mediated) recycling vesicles. Alternatively, ubiquitinated receptors are captured by the ESCRT machinery and internalized within ILVs,

forming multivesicular body (MVB). Fusion of MVB with lysosome leads to degradation of receptors. (Adapted from Scita *et al. Nature* 2010).

1.2.1. Internalization of cell surface receptors:

Receptor endocytosis is initiated by clustering and internalizing cell surface receptors at the PM. Clathrin coating protein mediates receptor internalization through a clathrin-mediated endocytosis (CME). On the other hand, receptor internalization is also mediated via "caveolae", orchestrated by the lipid binding protein caveolin, or by other clathrin-independent endocytic mechanisms. In CME, clathrin is recruited to the PM via AP2 adaptor molecule, which recognizes phosphatidylinositol biphosphate on the inner leaflet of the PM (Cocucci et al., 2012). Clathrin forms a triskelion and interacts with other clathrin triskelia to form the coat of a clathrin pit at the PM (Kirchhausen et al., 1981). Two clathrins recruited to four AP2 molecules are sufficient to nucleate the formation of a clathrin pit and to promote its stable assembly (Cocucci et al., 2012). As the clathrin pit matures, accessory adaptor molecules such as Eps15, Epsin and FCHo1/2 are recruited (Cocucci et al., 2012). Finally, the growing clathrin coat initiates the invagination of the PM to the inside of the cytosol (Stachowiak et al., 2013), and ubiquitinated receptors are incorporated in the clathrin pit following their recognition by Eps15 and Epsin (Barriere et al., 2007). Upon completion of clathrin assembly, the pit becomes a deeply invaginated bud, ready to be pinched off from the PM. Dynamin GTPase activity is required to drive the scission of the neck and to release the clathrin-coated vesicle into the cytosol (Macia et al., 2006). Next, Hsc70 and auxilin activity drive the uncoating of clathrin-coated vesicle (Böcking et al., 2011), so that clathrin and other adapter proteins are ready to be reused in the next rounds of CME.

Other clathrin-independent endocytosis pathways exist including caveolae, RhoA, Cdc42 and Arf6 mediated endocytosis, and other processes for large-scale engulfment of extracellular molecules such as phagocytosis and pinocytosis (Mayor et al., 2014).

1.2.2. Cargo sorting at early endosomes:

Early endosomes are composed of a vesicular body and tubular extensions (Gruenberg et al., 1989). The tubular extensions give rise to recycling endosomes (Maxfield et al., 2004), however the large vesicle transit into MVB through the formation of inside small vesicles called intraluminal vesicles (ILVs) (Piper et al., 2007).

Early endosomal cargo destined for recycling are rapidly sorted towards tubular compartments (Maxfield et al., 2004). Arf GTPase activity separates tubular extensions from early endosomes to form recycling endosomes. The cargo will be either rapidly recycled back to the PM through a Rab4-positive compartment (Sheff et al., 1999) or routed towards slow recycling through a Rab11-positive compartment (Sheff et al., 1999). For instance, transferrin and integrin receptors are recycled via Rab11 activity (Caswell et al., 2007, Sönnichsen et al., 2000). Sorting cargo on the surface of early endosomes towards recycling microdomains depends on specific sorting signals and adapter proteins such as sorting nexin family proteins (SNX). The recruitment of recycling sorting molecules is highly dynamic and depends on cytoplasmic tail motifs such as integrin NPxY-motif recycling by SNX17 (Böttcher et al., 2012).

On the other hand, ubiquitinated cargo of the early endosomes are incorporated within the lumen of early endosomes after the formation of ILVs, which is catalyzed by the endosomal sorting complexes required for transport (ESCRT) machinery (Henne et al., 2011) (Figure 2). Components of the ESCRT machinery bind to ubiquitinated cargo at the surface of early endosomes and trigger MVB biogenesis (Henne et al., 2011). Once MVBs are fully formed they fuse with lysosomes and

cargo is degraded by lysosomal proteases (Luzio et al., 2007). Therefore, ubiquitinated cell surface receptors are downregulated and receptor signaling is attenuated (Rodahl et al., 2009).

1.2.3. Cargo sorting and changes in endolysosomal pH:

The lumen of endosomes and lysosomes is characterized by low pH. Early endosomes start a rapid acidification process reaching pH values of 6.8 – 6.1. Upon MVB formation, pH drops further reaching 6.0 – 4.8 until they fuse with lysosomes where pH is ~ 4.5 (Yamashiro et al., 1987). Endosomal V-ATPase, which acts as a proton pump, mediates the progressive acidification of the endosomal lumen (Marshansky et al., 2008). Endosomal acidification is indispensable for ligand dissociation from its receptor, such as integrin α5β1 and fibronectin (Kharitidi et al., 2015). This process permits receptor recycling back to the PM and concentrating ligands in the vesicular portion of an endosome (Maxfield et al., 2004). Therefore, ligands will be degraded upon lysosome fusion and receptors are rapidly resensitized after returning to the PM for additional rounds of receptor activation and signaling (Luzio et al., 2007, Maxfield et al., 2004).

1.2.4. Ubiquitination and lysosomal degradation:

Ubiquitination of cell surface receptors is demonstrated as a signal for endocytosis and for their subsequent degradation through the formation of MVBs (Lauwers et al., 2009). Lysine ubiquitination of a protein is a covalent modification, and it is capable to form poly-ubiquitin chains which mediate different signaling pathways. A ubiquitin molecule contains seven lysines where the addition of another ubiquitin occurs to form poly-ubiquitin chains of different conformations (i.e., K11, K29, K48 and K63 poly-ubiquitin chains) with different signals (Trempe, 2011).

The ubiquitination process is conducted by a ubiquitin-conjugating system composed of E1-ubiquitin activating enzyme, E2-ubiquitin conjugation enzyme and E3-ubiquitin ligase

(Varshavsky, 2012). These enzymes catalyze the formation of a covalent bond between a ubiquitin moiety and the lysine residue of the target protein. However, ubiquitination is not a permanent posttranslational modification, since deubiquitinating enzymes (DUBs) can remove ubiquitin from its substrate via their protease activity (Clague et al., 2012). Hence, ubiquitin signaling and ubiquitin-dependent endocytic sorting are regulated by E3-ubiquitin ligases and DUBs activities.

An activated cell surface receptor is usually ubiquitinated by E3-ubiquitin ligase at the PM. A mono- or poly-ubiquitinated cell surface receptor is recognized by endocytic adaptor proteins such as Epsin and Eps15, which bind ubiquitin (Sigismund et al., 2005), followed by a rapid internalization of the receptor complex (Barriere et al., 2008, Barriere et al., 2007). K63-ploy-ubiquitinated cell surface receptors are sorted towards lysosomal degradation (Lauwers et al., 2009), since ESCRT proteins recognize poly-ubiquitinated cargo at the surface of early endosomes and sort them into the lumen of MVBs (Randles et al., 2012). This terminates receptor signaling and leads to the lysosomal degradation of MVB cargo (Rodahl et al., 2009).

1.3. The ESCRT machinery:

Endocytosis is a well-known membrane scission mechanism that enables the cell to internalize cell surface molecules, such as activated receptors, to regulate cell signaling. This process requires the participation of a complex network of protein–protein interactions resulting in the budding of a vesicle towards the cytosol (Sorkin et al., 2009). Reverse-topology membrane scission, on the other hand, is the formation of a vesicle budding away from the cytosol and is involved in numerous processes such as virus budding, cytokinesis, exosome formation, neuronal pruning, autophagy, and plasma membrane repair. All of these mechanisms require the participation of ESCRT proteins. ESCRT proteins are also well known for their role in the formation of ILVs within late endosomes to form MVBs. These ILVs can then continue their

progression to fuse with lysosomes for subsequent degradation (Christ et al., 2017, Schöneberg et al., 2017).

1.3.1. Canonical ESCRT components:

The ESCRT machinery is composed of several proteins classified into five different complexes, named ESCRT-0 to ESCRT-III and Vps4 (Christ et al., 2017, Schöneberg et al., 2017, Williams et al., 2007) (Figure 2). Altogether, the successive establishment of these protein complexes enables membrane scission events and the formation of ILVs. The ESCRT-0 complex mediates the first step of this process and is composed of Hrs and STAM1/2. Hrs is recruited to the membrane via its FYVE domain that binds phosphatidylinositol 3-phosphate. STAM1/2 interacts with Hrs and both of these proteins bind to clathrin. They also specifically recognize and bind ubiquitylated cargos through their UIM as well as bind to ESCRT-I components. TSG101, Vps28, Vps37, and MVB12 are classical ESCRT-I proteins that bind to ubiquitin and stabilize the cargo to be internalized. Along with ESCRT-II proteins EAP20, EAP30, and EAP45, they form an ESCRT-I/ESCRT-II supercomplex responsible for the recruitment of ESCRT-III proteins. In yeast, the ESCRT-I complex adopts a rod-shaped structure whereas the ESCRT-II is Y-shaped. The mammalian ESCRT machinery is conserved and is likely to adopt a similar architecture, although there is more diversity among mammalian ESCRT components, as there are four different Vps37 isoforms (Vps37A– Vps37D) and three UMA-containing isoforms (MVB12A, MVB12B, and UBAP1). The ESCRT-III complex is composed of CHMP1A, CHMP1B, CHMP2A, CHMP2B, CHMP3, CHMP4A–CHMP4C, CHMP5, CHMP6, CHMP7, and IST1. The ESCRT-III proteins undergo conformational changes and assemble on membranes as filamentous structures displaying various shapes. ESCRT-III proteins would thus play a major role in membrane remodeling and scission events taking place during ILV formation. The final step is

achieved by the Vps4 complex composed of the AAAs Vps4A, Vps4B (also known as SKD1), CHMP5, and LIP5. The Vps4 complex catalyzes the dissociation of ESCRT-III proteins to promote the disassembly of the ESCRT machinery. In addition, Vps4 proteins are also involved in membrane constriction and scission events in the final step of ILV formation (Christ et al., 2017, Schöneberg et al., 2017, Williams et al., 2007).

Likewise, clathrin is associated with ESCRTs playing a key role in both cargo concentration and ILV formation (Raiborg et al., 2001, Raiborg et al., 2006, Wenzel et al., 2018). It is recruited to early endosomes by the ESCRT-0 protein Hrs (Raiborg et al., 2001, Raiborg et al., 2006). Static and live-cell imaging of the prototype epidermal growth factor receptor (EGFR) indicated that the initial steps of ILV formation consist of a wave of ESCRT-0, ESCRT-I, clathrin and HD-PTP recruitment (Wenzel et al., 2018).

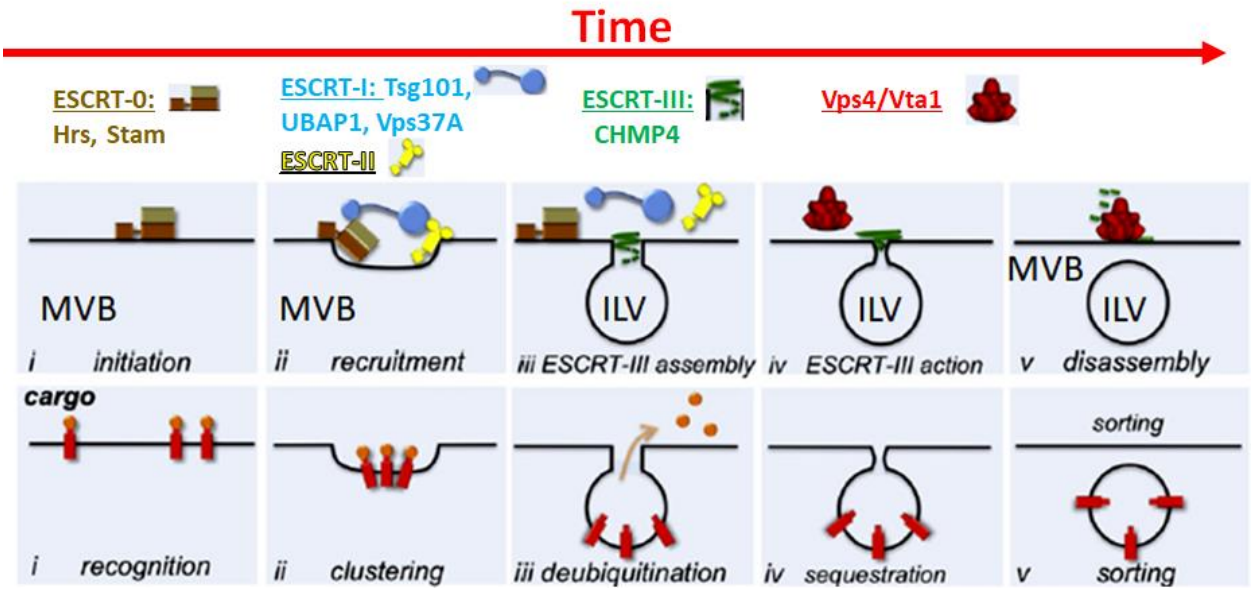

Figure 2: The ESCRT machinery mechanism:

Ubiquitinated cargo at endosomal surface is recognized and packaged within endosomal lumen by the ESCRT machinery. ESCRT-0 components Hrs/STAM recognize polyubiquitinated cargo via their UIM and VHS domains. Then, polyubiquitinated cargo is transferred to ESCRT-I complex, which recruits ESCRT-II. Recruitment of DUBs is responsible for cargo deubiquitination prior to its incorporation within ILVs. After ESCRT-II recruitment, CHMP4 filaments are polymerized driving the ILV neck constriction and scission. The activity of Vps4/Vta1 complex drives the depolymerization of CHMP4 filaments promoting the pinching of the ILV and CHMP4 monomer recycling. (Adapted from Henne *et al. Developmental Cell* 2011).

1.3.2. Alternative ESCRT-III recruitment:

In addition to the classical succession of ESCRT complexes just described, there is an alternative route that can also lead to the recruitment of ESCRT-III proteins and ILV formation. The Bro1- domain protein family thus constitutes an alternative for ESCRT-I/II to recruit CHMP4 and the ESCRT-III complex (Ali et al., 2013, Christ et al., 2016, Ichioka et al., 2007, McCullough et al., 2008, Parkinson et al., 2015, Tang et al., 2016, Tomas et al., 2015). Alix and HD-PTP are two Bro1 domain alternative ESCRT proteins involved in the early steps of MVB formation that bind to both clathrin and ubiquitin (Pashkova et al., 2013). Alix and HD-PTP contribute to the sorting of activated EGFRs to ILVs during MVB formation (Ali et al., 2013, Mercier et al., 2016, Sun et al., 2015a, Sun et al., 2015b, Tomas et al., 2015). Alix also displays partially redundant functions with ESCRT-I/ESCRT-II in the recruitment of ESCRT-III proteins for membrane scission events involved in viral budding and cytokinesis whereas the function of HD-PTP would be more specific for MVB formation (Carlton et al., 2008, Christ et al., 2016, Tang et al., 2016).

Interestingly, Alix and HD-PTP display some binding specificities, even though they share some interacting partners and have a similar overall architecture (Ichioka et al., 2007). For instance, HD-PTP, but not Alix, is able to bind UBAP1 (Stefani et al., 2011).

1.3.3. Proposed endosome-specific ESCRT complex:

UBAP1 has been proposed to be an endosome-specific ESCRT-I component involved in MVB sorting (Stefani et al., 2011). It contains a region conserved in the ESCRT-I protein MVB12 (De Souza et al., 2010) and a SOUBA domain enabling its interaction with ubiquitin (Agromayor et al., 2012). Its N terminus is composed of a UMA domain interacting with other ESCRT-I components. UBAP1 is thus part of an alternative ESCRT-I complex formed with Vps37 and TSG101 (Wunderley et al., 2014). This complex is required for the MVB sorting of ubiquitylated EGFRs and is dispensable for HIV-1 budding and cytokinesis (Agromayor et al., 2012, Stefani et al., 2011, Wunderley et al., 2014). UBAP1 selectively associates with the Vps37A isoform in endosome-specific ESCRT-I complexes. UBAP1 depletion, but not MVB12A or MVB12B, also impaired ubiquitin-dependent EGFR sorting. It is thus possible that the heterogeneity observed among ESCRT-I components in mammalian cells enables the formation of endosomal complexes specifically involved in lysosomal degradation. Interestingly, UBAP1 also interacts with another ESCRT protein called HD-PTP and both of these proteins are involved in EGFR trafficking (Gahloth et al., 2016). HD-PTP could therefore act as an accessory protein transiently recruited to this endosome-specific complex or even be an integral member of this complex, as it was demonstrated for UBAP1. In this model, HD-PTP could act as a scaffold to recruit many proteins for efficient sorting in the MVB (Ali et al., 2013, Stefani et al., 2011, Wunderley et al., 2014). In addition to its role in MVB sorting and degradation, HD-PTP is also involved in the recycling of internalized cargos back to the plasma membrane. Depletion of Myopic, the Drosophila ortholog

of HD-PTP, indeed resulted in the endosomal accumulation of the transmembrane protein Frizzled and decreased its colocalization with the recycling endosome marker Rab11 (Pradhan-Sundd et al., 2015). Similarly, HD-PTP was shown to impact recycling of the α5β1 integrin receptor in both Drosophila and human cells (Chen et al., 2012, Kharitidi et al., 2015).

1.3.4. Role of ESCRTs in diseases:

Consistent with its essential function in many cell signaling pathways, dysfunctional ESCRT machinery due to gene mutations has been linked to several diseases (Saksena et al., 2009). For instance, defects in the endosomal–lysosomal system are a major cause of several neurodegenerative diseases (Saksena et al., 2009). More specifically, endosomal abnormalities in neuronal cells have been associated with Alzheimer's disease and amyotrophic lateral sclerosis (Keating et al., 2006, Yang et al., 2001). In addition, the fact that Huntington's and Parkinson's diseases are characterized by the accumulation of intracellular ubiquitinated protein aggregates might be associated with MVB accumulation caused by the loss of ESCRT function (Saksena et al., 2009). ESCRT and MVB formation are the key players of lysosomal degradation of ion channels and are crucial for ion homeostasis in different tissues (Saksena et al., 2009). Therefore, chronic diseases caused by abnormalities in the levels of ion channels, such as the renal pseudohypoaldosteronism type I and hypertension leading to cardiovascular disease, have been associated with defective ESCRT-mediated endocytic function (Botero-Velez et al., 1994, Chang et al., 1996, Saksena et al., 2009, Stutts et al., 1995). Finally, several classes of enveloped viruses utilize the ESCRT machinery for budding out of host cells via an interaction between TSG101 and Gag proteins of HIV, Ebola and HTLV (Freed, 2002, Pornillos et al., 2002).

1.3.5. ESCRT functions in cancer:

Owing to their critical function in degradation of cell surface receptors, several reports have proposed a tumor suppressive gene (TSG) function of the ESCRT members (Jiang et al., 2013, Mattissek et al., 2014). However, both oncogenic and tumour suppressor functions of ESCRT components were suggested in various types of human cancer. As examples, Hrs is up-regulated in stomach, colon, liver, cervix and melanoma tumors (Toyoshima et al., 2007); TSG101 is up-regulated in breast cancer (Oh et al., 2007), papillary thyroid (Liu et al., 2002) and colorectal carcinomas (Ma et al., 2008); and CHMP4C is up-regulated in ovarian carcinoma tissues (Nikolova et al., 2009). In contrast, Vps37A is reduced in hepatocellular carcinoma (HCC) (Xu et al., 2003) and was reported as a growth inhibitory protein capable of decreasing the invasive potential of HCC cells (Xu et al., 2003). Moreover, reduced expression levels of UBAP1 in nasopharyngeal carcinomas (Xiao et al., 2006) and CHMP1A in pancreatic ductal adenocarcinomas (Li et al., 2008) were reported. Furthermore, Vps4B is reduced in high-grade breast tumors (Stage IV) (Liao et al., 2013) and correlates negatively with EGFR levels (Lin et al., 2012). Vps4B is overexpressed in non-small-cell lung cancer (NSCLC) and promotes cell proliferation and NSCLC progression (Liu et al., 2013). While correlative expression levels and in vitro functional experiments suggested both positive and negative roles in cancer, the bona fide function of the ESCRT components in tumorigenesis had not been systematically demonstrated, since homozygous gene deletion of ESCRT components is embryonic lethal in mice and most ESCRT members are involved in other essential functions described above (Hurley, 2015). Strikingly, HD-PTP was recently identified as the first ESCRT component with tumor suppressive function in mammals *in vivo*.

1.4. The ESCRT component HD-PTP:

1.4.1. Domain organization of HD-PTP:

HD-PTP is a large 1636 amino acid protein of 185 kDa composed of a N-terminal Bro1 domain followed by a V domain, PRR, phosphatase-like domain, and a C-terminal PEST sequence (Figure 3). HD-PTP is thus similar to Alix, which displays a similar Bro1-V-PRR domain organization (Zhai et al., 2011).

These Bro1-containing proteins are homologous to the yeast Bro1 and are associated with the ESCRT pathway through their capacity to bind the ESCRT-III protein CHMP4. This protein binds to a concave hydrophobic surface within the Bro1 domain of HD-PTP. This region, as well as an adjacent specificity pocket, also binds Endofin (Gahloth et al., 2017c), which is localized to the early endosomes via its FYVE domain and acts as a Smad1/5/8 anchor for receptor activation in BMP signaling (Goh et al., 2015, Shi et al., 2007). In addition, Endofin also binds to Smad4 to facilitate TGF-β signaling (Chen et al., 2007b). Immunofluorescence analysis revealed the colocalization of Endofin and HD-PTP in the endosomal compartments. In agreement with the broader region bound by Endofin, it has a significantly higher affinity compared to CHMP4 and both of these proteins compete to bind HD-PTP (Gahloth et al., 2017c). Interestingly, the Bro1 domain of HD-PTP also interacts with the deubiquitylating enzyme UBPY (also known as USP8) and the ESCRT-0 protein STAM2, although the binding of these proteins is more complex and does not solely rely on the Bro1 domain of HD-PTP. UBPY and STAM2 participate in the sorting of EGF receptors to the MVBs. HD-PTP is also important for sorting of activated EGFRs but was found to be dispensable for the ILV formation itself (Ali et al., 2013, Lee et al., 2016). Accordingly, reintroduction of HD-PTP Bro1-V in HeLa cells depleted for HD-PTP restored the efficient sorting and trafficking of receptors (Doyotte et al., 2008).

The V domain of HD-PTP is also involved in the establishment of protein–protein interactions. HD-PTP interacts with UBAP1 and these proteins were proposed to be part of an alternative ESCRT complex specific to endosomes. The V domain of HD-PTP adopts an elongated conformation and contains a FYX2L motif enabling its interaction with a short FPXL motif within UBAP1 (Gahloth et al., 2016). Such a binding mechanism is conserved within the yeast Bro1 protein and its mammalian homologs (Kimura et al., 2015). Interestingly, the V domain of the yeast Bro1 displays binding preferences similar to ESCRT-0 proteins, since it is able to bind to both clathrin and ubiquitin. Yeast Bro1 would thus act early in the ESCRT pathway, in parallel with ESCRT-0, to sort ubiquitylated cargos into ILVs. Alix and HD-PTP retain the capacity to bind ubiquitin chains and would play such role in mammalian cells (Pashkova et al., 2013). Despite these similarities, the V domain of Alix and HD-PTP are structurally different. The V domain of Alix is flexible and can adopt two conformations. The balance between the open and closed conformation of the V domain can be regulated by phosphorylation or via the binding of other proteins at the site of the intramolecular inhibition between the PRR and Bro1 domains of Alix. The closed conformation of Alix was shown to restrict its capacity to bind proteins through its V domain (Sun et al., 2016, Sun et al., 2015a, Sun et al., 2015b). HD-PTP does not appear to display such regulation, since hydrodynamic analyses revealed that its V domain only adopts an open conformation and would thus be constitutively available for protein–protein interactions (Gahloth et al., 2017a).

HD-PTP contains a PRR located between the V domain and the phosphatase-like domain. This region is well known for its capacity to interact with the ESCRT-I protein TSG101. The PRR of HD-PTP indeed contains two P(S/T)AP motifs that could bind TSG101 (Ichioka et al., 2007). The PRR of HD-PTP also contributes to interactions established by its Bro1 domain with UBPY

and STAM2, since the coimmunoprecipitation of these proteins was more efficient with the full-length HD-PTP compared to a Bro1-V construct (Ali et al., 2013). In addition to STAM2, other SH3 domain containing proteins such as Endophilin, Grb2, and Grap2 were shown to interact with the PRR of HD-PTP (Harkiolaki et al., 2009, Ichioka et al., 2007, Tanase, 2010). Interestingly, these proteins are all involved in EGFR trafficking (Jiang et al., 2003, Soubeyran et al., 2002). To date, the specific functions of these interactions with the PRR of HD-PTP remain poorly understood.

The catalytic activity of HD-PTP is controversial. It was initially classified as a classical phosphatase based on its amino acid sequence. However, *in vitro* phosphatase assays using the highly sensitive DiFMUP substrate, and a panel of phosphatidylinositol phosphates failed to identify a phosphatase activity for HD-PTP (Gingras et al., 2009). The PTP-like domain located near the C terminus of HD-PTP was also shown to be inactive against a panel of 38 phosphopeptides (Barr et al., 2009). These results are consistent with the divergence observed for three amino acids within the HD-PTP sequence (His1223, Glu1357, and Ser1394) that are usually conserved in active phosphatases (respectively, Tyr, Asp, and Ala residues). Reactivation of the HD-PTP phosphatase activity was achieved by back-mutation of one residue towards the PTP consensus sequence (S1394A) (Gingras et al., 2009). Mariotti et al. reported a phosphatase activity for HD-PTP towards Src, but in the absence of a negative control with an inactive mutant, this effect could be attributed to the presence of copurified contaminants (Mariotti et al., 2009). A recent study also showed phosphatase activity of HD-PTP towards FYN in vitro (Zhang et al., 2017). This activity was abolished by mutation of the catalytic cysteine critical for the dephosphorylation. Intriguingly, mutations of HD-PTP to create an artificial catalytic domain that would match the amino acid consensus of active phosphatases further increased its activity,

suggesting that HD-PTP only has a low activity. This activity might also be specific for a few proteins like FYN, as Src and Yes were not shown to bind to HD-PTP in substrate-trapping experiments (Gingras et al., 2009, Zhang et al., 2017). Whether or not HD-PTP is a fully active phosphatase, the deletion of the PTP domain was shown to impact colony growth formation, which suggests the functional significance of this domain (Gingras et al., 2009). On the other hand, studies in Drosophila revealed that ablation of HD-PTP inhibits photoreceptor differentiation regulated by EGFR, which can be rescued by reexpression of the wild type and an inactive C/S mutant pointing to the insignificance of an active phosphatase (Miura et al., 2008). Additional studies are required to shed light on the specific functions of the phosphatase domain of HD-PTP.

HD-PTP harbors a PEST-rich sequence located at its C terminus. Such a motif is believed to act as a proteolytic signal for short-lived proteins by inducing their proteasomal degradation (Rechsteiner et al., 1996). HD-PTP expression was indeed stabilized by proteasome inhibitors, although the role of the PEST sequence in this specific case is still unknown (Mariotti et al., 2009). Despite the presence of a PEST sequence within HDPTP, it does not appear to be a rapidly degraded protein.

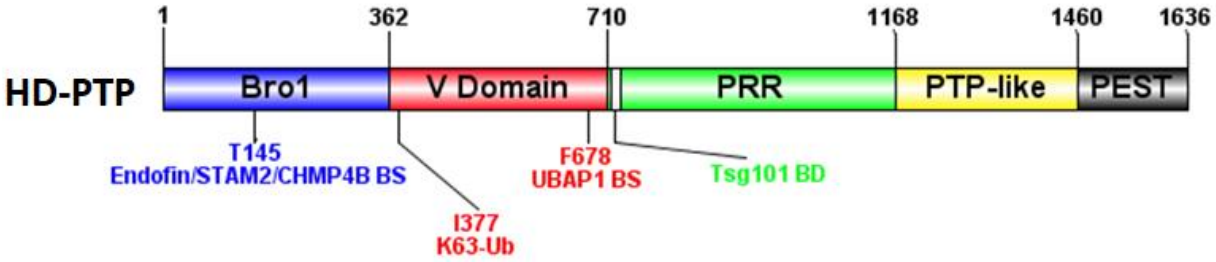

Figure 3: HD-PTP protein domains:

Domain organization of the HD-PTP protein. Numbers correspond to the amino acids of the human protein sequence. Regions involved in protein–protein interactions are highlighted below the schematic representation (Liu et al., 2015).

1.4.2. The role of HD-PTP in receptor trafficking and tumorigenesis:

The first study introducing HD-PTP showed that its overexpression in NIH-3T3 cells inhibits Ha-ras-mediated focus formation, a cell-based assay to determine the oncogenic potential of a gene, suggesting that HD-PTP may be involved in regulating cell growth (Cao et al., 1998). Another study investigating the role of Myopic, the Drosophila homolog of HD-PTP, reported that Myopic is localized to intracellular vesicles adjacent to Rab5-containing early endosomes (Miura et al., 2008). Moreover, the loss of Myopic prevented cleavage of the EGFR cytoplasmic domain, suggesting that it promotes EGFR signaling by mediating its progression through the endocytic pathway (Miura et al., 2008). It was also shown that HD-PTP is essential for the down-regulation of polyubiquitylated cell surface MHC class I (Parkinson et al., 2015). Ali et al. demonstrated that HD-PTP has a role in driving EGFR into ILVs (Ali et al., 2013). This was proposed through a model showing the recruitment of CHMP4B and the deubiquitylating enzyme UBPY, which is indirectly controlled by HD-PTP function (Ali et al., 2013). A similar mechanism is also present in yeast where Doa4, the yeast homolog of UBPY, interacts with Bro1 (HD-PTP in mammals) to promote deubiquitylation of the cargo prior to its sorting into MVBs (Richter et al., 2007). Hence, HD-PTP has an essential role in MVB formation, since its depletion reduced the transfer of EGFR to lysosomes, caused the accumulation of ubiquitylated proteins on endosomal compartments, and disrupted the formation of MVBs (Doyotte et al., 2008). The suppression of HD-PTP by RNAi

triggered cell invasion due to an increase in E-cadherin internalization, its accumulation in early endosomes, and the induction of mesenchymal protein expression (Lin et al., 2011). Since it was clearly demonstrated that HD-PTP has a major role in down-regulating cell surface receptors, it was also proposed that HD-PTP plays a role in cancer progression. For instance, silencing of HD-PTP in NIH-3T3 cells resulted in a reduced degradation of activated PDGFRβ (Ma et al., 2015). In addition, HD-PTP depletion increased migration, colony formation and tumorigenicity of NIH-3T3 cells stimulated by PDGF (Ma et al., 2015). Furthermore, Kharitidi et al. demonstrated that the loss of HD-PTP induces a proinvasive phenotype. Their depletion was shown to increase the cell surface stability of α5β1 integrin receptors, which in turn led to sustained signaling and cell migration (Kharitidi et al., 2015). The role of HD-PTP as a tumor suppressor was well established in several studies. For instance, Tanaka et al. presented HD-PTP as a tumor suppressor protein after showing that its expression in human TGCTs was lower than in normal testicular tissues (Tanaka et al., 2013). In addition, the expression of the *PTPN23* gene was shown to be regulated by miR-142-3p, which is highly expressed in TGCTs. Furthermore, overexpression of HD-PTP in NEC8, a human TGCT cell line, suppressed soft agar colony formation *in vitro* and tumor formation in nude mice *in vivo* (Tanaka et al., 2013). HD-PTP was further demonstrated as a haploinsufficient tumor suppressor (Manteghi et al., 2016). The heterozygous loss of the *PTPN23* gene predisposed mice to sporadic lung adenoma and B cell lymphoma and promoted Myc-driven lymphoma onset, dissemination, and aggressiveness. *PTPN23* deletion and down-regulation is frequent and concomitant in human tumors and is also correlated with poor survival (Manteghi et al., 2016). Moreover, Zhang et al. correlated the tumor suppressor function of HD-PTP in breast cancer cells with its role in regulating the activity of FYN, which belongs to the Src family kinases (Zhang et al., 2017).

1.5. Endofin protein:

1.5.1. Structure and function of Endofin:

Endofin, a FYVE domain protein, is 1539 amino acids and it is recruited to EEA1-positive early endosomes (Figure 4). A single cysteine mutation in the FYVE domain (C753S) is enough to abolish Endofin's endosomal localization. SARA protein is an another FYVE domain protein involved directly in the TGFβ signaling pathway. Endofin shares about 50% homology in its carboxyl-terminal region and other structure domains with SARA protein. Despite their colocalization on early endosomes, Endofin and SARA do not directly interact (Seet et al., 2001b).

Unlike SARA, Endofin does not interact with Smad2 neither does it influence the TGFβ signaling pathway (Seet et al., 2001b). However, Endofin interacts with BMP-specific R-smad Smad1 and regulates its phosphorylation and nuclear translocation. Since the overexpression of SARA did not show an effect on Smad1 phosphorylation, this indicates that Endofin plays the role of SARA in BMP signaling but there is no crossover in their roles (Seet et al., 2001b, Shi et al., 2007). Like SARA, Endofin binds PP1c phosphatase catalyzing the dephosphorylation of BMP receptor. F872A mutation in Endofin's PP1c binding domain inhibits their direct interaction and enhances BMP receptor phosphorylation (Shi et al., 2007). F872A-Endofin expression in mouse osteoblasts increases bone formation and density due to elevated levels of BMP signaling (Zhang et al., 2009a). Of note, the downregulation of SARA delayed the degradation of activated EGFR (Kostaras et al., 2013), and deletion of SARA gene in mice predispose skin tumorigenesis and malignant progression (Chang et al., 2014).

In controversy, Chen *et al.* found that Endofin does influence TGFβ signaling, since the expression of a FYVE-mutant Endofin in Hep3B cells suppresses transcriptional responses to

TGFβ. Moreover, it is shown that Endofin interacts with TGFβ receptor and Smad4, but not with Smad1 (Chen et al., 2007a).

Endofin is tyrosine phosphorylated (Y221 and Y515) within 5 to 15 minutes of EGF stimulation (Rush et al., 2005, Toy et al., 2010), and its overexpression in A431 cells trapped EGFR in large endosomal aggregates (Seet et al., 2001b). Endofin's C753S mutation and disrupting PI3K activity with Wortmannin triggered Endofin's redistribution to the cytoplasm and reduction in the levels of Y515 phosphorylation (Seet et al., 2001b, Toy et al., 2010). Of note, upon EGF stimulation Endofin is found in EEA1-negative compartments near the PM as well as in EEA1-positive perinuclear endosomes. However, upon treatment with EGFR-kinase inhibitor Iressa, Endofin presence in EEA1-negative compartments is abolished (Chen et al., 2007b). Moreover, C753S-Endofin expression in HeLa cells increased the phosphorylated levels of downstream EGFR effectors: Erk1 and Erk2 (Toy et al., 2010).

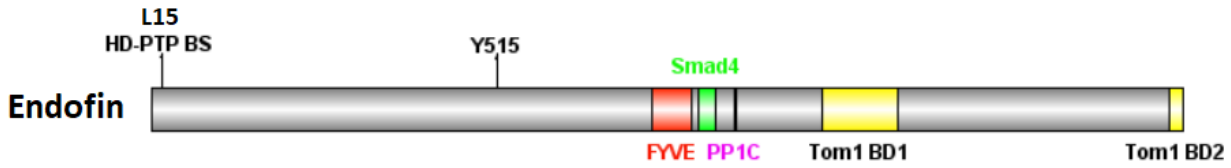

Figure 4: Endofin protein domains:

Domain organization of the Endofin protein. Numbers correspond to the amino acids of the human protein sequence. Domains and regions involved in protein–protein interactions are highlighted below the schematic representation (Liu et al., 2015).

1.5.2. Endofin interaction with Tom1:

The C-terminus of Tom1 protein, via two sites, directly interacts with Endofin (Seet et al., 2004). The overexpression of C753S-Endofin did not affect Tom1 binding indicating that Endofin's localization is not essential for this binding (Seet et al., 2004). However, overexpression of both Endofin and Tom1 showed a redistribution of Tom1 from cytosol to the endosomes (Seet et al., 2004). Of note, neither SARA nor Hrs, a FYVE-domain ESCRT-0 protein, can bind Tom1 C-terminus (Seet et al., 2004).

Tom1 protein contains a GGA domain, however it is shown that it does not have the same role as GGA proteins in transport from Golgi (Tumbarello et al., 2012). Tom1 is shown to play a role in autophagosome maturation and lysosome function through its interaction with Myosin VI (Tumbarello et al., 2012). In addition Tom1 contains VHS and GAT domains through which it interacts with ubiquitin (Katoh et al., 2004, Shiba et al., 2004). Moreover, Tom1 binds clathrin via its C-terminus, and through its binding to Endofin, clathrin is recruited to early endosomes (Seet et al., 2005). Of note, Hrs protein also directly interacts with ubiquitin and clathrin and recruits the latter to early endosomes (Raiborg et al., 2001, Shih et al., 2002).

DdTom1 is Tom1's ortholog and it is the only protein in *Dictyostelium discoideum* containing VHS and GAT domains, thus it interacts with ubiquitin and clathrin (Blanc et al., 2009). Therefore, it is proposed that in the absence of Hrs in *Dictyostelium discoideum*, ddTom1 is playing a role of an ancestral ESCRT-0 component (Blanc et al., 2009). In addition, Tom1 orthologs, but not for Hrs or STAM, are also found in the amoeboflagellate *Breviata anathema* (Herman et al., 2011). *S. cerevisiae* does not appear to have any Tom1 orthologs (Wang et al., 2010). Thus, it is proposed that an alternative ESCRT-0 complex is formed since Endofin is

recruited to early endosomes and it recruits clathrin through its direct interaction to Tom1 (Clague et al., 2012, Seet et al., 2005, Shi et al., 2007, Toy et al., 2010, Wang et al., 2010).

Tom1 also binds to Tollip through its GAT domain (Katoh et al., 2004), which is recruited to early endosomes through the interaction of its C2 domain with phosphatidylinositol 3-phosphate (Ankem et al., 2011). Moreover, Tollip also interacts with ubiquitin through its CUE domain (Brissoni et al., 2006). Therefore, both Endofin and Tollip are able to recruit Tom1 and clathrin to early endosomes (Katoh et al., 2006, Seet et al., 2005, Seet et al., 2004, Yamakami et al., 2003).

1.6. Integrin α5 receptor:

1.6.1. The role of integrin α5 in signaling and cell migration:

Integrins are cell surface transmembrane proteins which interact with their extracellular domains with the ECM thus launching a cascade of intracellular signaling from its cytoplasmic domain. Integrin α5β1 heterodimer activation occurs upon its interaction with fibronectin (outside-in signaling) or following binding of activating proteins to integrin cytoplasmic tail such as talin and kindlin (inside-out signaling) (Luo et al., 2006). In both cases, integrin α5β1 activation promotes the formation of focal adhesion, linkage between cytoskeleton and ECM and triggers intracellular pro-migratory signaling pathways (Byron et al., 2010).

Integrin α5β1 lacks intrinsic tyrosine kinase activity, hence integrins require activity of non-receptor tyrosine activity such as FAK to transduce extracellular cues into intracellular signaling pathways (Guo et al., 2004). Fibronectin-integrin α5β1 complex facilitates FAK autophosphorylation at Y379. Subsequently, the tyrosine kinase Src binds to activated FAK through its SH2 domain and induces the phosphorylation of FAK at Y925, which in turn promotes the formation of FAK-Grb2-SOS complex (Guo et al., 2004). In cancer, for instance, this complex

activates Ras GTPase and induces MAPK/Erk signaling thus contributing to tumorigenesis and metastasis (Lahlou et al., 2011).

Since integrin ligands are members of the ECM, it is not surprising that integrin cell surface dynamics regulate cell migration and invasion. Integrin recycling back to the PM is shown as a key requirement during cell migration (Powelka et al., 2004). In a 3D cell culture system, recycling of integrin α5β1 via Rab25 promotes invasion (Caswell et al., 2007). The constant circulation of integrins between the PM and Rab25 recycling vesicles maintains integrin at the tip of an invasive pseudopod. This is directly responsible for the formation of adhesions at the pseudopod to move the cell forward (Caswell et al., 2007). A portion of active integrins is recycled back to the trailing edge of an invading cell from CLIC3-positive lysosomal compartments (Dozynkiewicz et al., 2012). The rear recycling of integrins is likely to be associated with the release of lysosomal proteases to digest the ECM and to trigger cell rear release. Moreover, Rab-coupling protein (RCP) accelerates integrin α5β1 recycling and promotes invasion in fibronectin rich niche (Caswell et al., 2008). RCP is also shown to promote EGFR recycling along with integrins (Caswell et al., 2008). Together, EGFR and integrins activates Akt signaling and RhoA activation, which in turn enhance cell migration.

1.6.2. The role of integrin α5 in cancer:

Endocytic perturbation of β1 and β3 integrins contributes to cancer progression. Endocytic adaptors such as Dab2, Numb and HAX1 are shown to be involved in integrin endocytosis and their downregulation correlates with increased metastasis and poor patient's prognosis (Maiorano et al., 2007, Tong et al., 2010, Trebinska et al., 2010, Westhoff et al., 2009). In addition, it is shown that p53 mutations induces integrin α5β1 recycling and triggers downstream promigratory signaling (Muller et al., 2009). Of note, metastasis is promoted in p53 mutant mice, in line with

the aggressive tumor behavior in patients with p53 mutations (Muller et al., 2009). It is demonstrated that RCP promotes integrin α5β1 recycling to the PM (Caswell et al., 2008). RCP high expression in luminal B breast cancer subtype is shown to correlate with low survival and cancer aggressiveness (Zhang et al., 2009b). Therefore, RCP role in integrin recycling can be a critical factor in breast cancer progression (Mills et al., 2009). In addition, high expression of CLIC3, which catalyzes integrin recycling from lysosomes, correlates with poor prognosis of ovarian, breast and pancreatic cancer (Dozynkiewicz et al., 2012, Macpherson et al., 2014). These examples suggest that the mechanism of integrin recycling plays a critical role in cancer metastasis.

Cellular processes related to tumorigenesis and cancer progression such as proliferation and angiogenesis are also affected by the extensive crosstalk of integrin with other receptors. For instance, blocking integrin αvβ3 with Cilengitide triggers the rapid recycling of VEGFR2 (Reynolds et al., 2009). Thus, the high VEGFR2 density at the PM increases its downstream signaling leading to endothelial migration and tumor vascularization (Reynolds et al., 2009). Moreover, the crosstalk of integrin α5β1 with RTKs such as EGFR and Met receptor is initiated by RCP recruitment to integrin α5β1 (Caswell et al., 2008, Muller et al., 2013). This enhances recycling of integrin α5β1 and RTKs and increases MAPK downstream signaling promoting cancer cell survival and migration.

1.7. The role of EGFR signaling in cancer:

EGFR can be stimulated with eight different ligands. Upon ligand activation, EGFR undergoes dimerization and internalization (Ogiso et al., 2002). Unstimulated EGFR can also be internalized, but a 10-fold slower rate compared to stimulated EGFR (Wiley et al., 1991). Activated EGFR dimers undergo autophosphorylation at tyrosine residues in the receptor's cytoplasmic tail (Tomas et al., 2014). Next, phosphotyrosine-binding proteins are recruited

activating several downstream signaling pathways such as MAPK, PI3K which recruits Akt/PKB to the PM and the phospholipase Cγ pathway which interacts with EGFR and activates PKC (Lill et al., 2012). Although EGFR signaling occurs at the PM (Sousa et al., 2012), but activated EGFR-mediated signaling can proceed from endosomes (Teis et al., 2006). EGFR signaling cascades are well known to regulate cell proliferation and migration.

EGFR altered trafficking contributes to aberrant signaling and tumorigenesis. For instance, EGFR overexpression leads to an increase in its PM density, which in turn hyperactivates EGFR downstream signaling (Chung et al., 2010, Sawano et al., 2002). ESCRT perturbation through the disruption of Tsg101/Hrs interaction inhibits ligand-induced downregulation of EGFR and increases mitogenic signaling (Lu et al., 2003). It is also shown that the overexpression of EGFR in cancer cells saturates the endocytic/ubiquitination machinery and sustains EGFR signaling (Capuani et al., 2015). Moreover, the high number of activated EGFR saturates Cbl, an E3 ubiquitin ligase responsible for EGFR ubiquitination at the PM, this sustains receptor signaling and delays EGFR downregulation (Capuani et al., 2015). Certain types of cancers are characterized by the downregulation of the Rab5 effector, rabaptin-5, which causes an inefficient Rab5-mediated endosome fusion leading to the retention of activated EGFR in early endosomes and sustained receptor signaling (Wang et al., 2009). Furthermore, it is shown that in cancer patients with p53 mutations, tumor cells exhibit enhanced recycling of integrin β1/EGFR complex via RCP, resulting in continuous activation of integrin/EGFR signaling (Muller et al., 2009). Mutation in p53 favors tumor cell migration/invasion and metastatic dissemination (Muller et al., 2009).

1.8. Breast cancer:

1.8.1. Breast cancer subtypes:

Based on distinct intrinsic gene sets for cluster analysis, breast cancer is divided into four subtypes: luminal-A, luminal-B, HER2-positive and basal-like.

Luminal-A: 50-60% of breast cancer correspond to luminal-A subtype. It is characterized with estrogen receptor (ER)-positive and/or progesterone receptor (PR)-positive with negative HER2 and low Ki67 (proliferating cell nuclear antigen) index (Carey et al., 2006). Luminal-A breast cancer cells express cytokeratins (CK) 8 and 18 and other genes related to ER function. Hence, patients with luminal-A breast cancer have good prognosis and the relapse rate is significantly lower than other subtypes (Yersal et al., 2014). Treatment is mainly based on hormonal therapy and metastasis occurs in less than 10% of patients (Guarneri et al., 2009, Kennecke et al., 2010).

Luminal-B: 15-20% of breast cancer correspond to luminal-B subtype. Compared to luminal-A, luminal-B tumors are more aggressive, with higher proliferative index, worse prognosis, higher recurrence rate and lower survival rates after relapse (Creighton, 2012, Ellis et al., 2008). Immunohistochemistry defines luminal-B tumors as ER-positive, Her2-negative and Ki67 high or ER- and Her2-positive tumors (Nishimura et al., 2010). Of note, 6% of luminal-B tumors are negative for both ER and HER2 (Nishimura et al., 2010). Overall survival rates in untreated patients with luminal-B tumors is similar to patients with basal-like and HER2-positive, which are recognized as high-risk tumors (Hu et al., 2006). Luminal-B tumors have poorer outcomes with hormonal therapy compared to luminal-A. However, luminal-B tumors have better response to neoadjuvant chemotherapy than luminal-A tumors (Rouzier et al., 2005).

HER2-positive: Human epidermal growth factor receptor-2 is a cell surface receptor that forms heterodimers with another receptor from a different family of receptors or homodimers with itself when it is expressed at high levels. Receptor activation triggers downstream signaling pathways involved in cell proliferation, survival, differentiation, angiogenesis and invasion (Moasser, 2007). HER2-positive tumors are characterized by the high expression of HER2 gene and other genes related to the HER2 pathway and they account for 15-20% of breast cancer subtypes. HER2-positive tumors are highly proliferative and 40% have p53 mutations (Tsutsui et al., 2003). Approximately 50% of HER2-positive tumors are positive for ER, however ER is expressed at lower levels (Yersal et al., 2014). Untreated patients with HER2-positive tumors have poor prognosis with the propensity of tumor cells to metastasize to the brain and visceral organs. Moreover, they are resistant to hormonal therapy, but sensitive to the chemotherapeutic drug doxorubicin (Gabos et al., 2006).

Basal-like: The basal-like tumors represent 8-37% of all breast cancer and are characterized with high proliferative index, central necrotic or fibrotic zones, aggressive clinical behavior and high rate of brain and lung metastasis (Heitz et al., 2009). They express high levels of basal myoepithelial markers such as CK5, CK14, CK17 and laminin. Usually basal-like breast cancer subtype does not express ER, PR and HER2, hence they are referred as triple negative. It is important to mention that the terms triple negative and basal-like are not completely synonymous and there is 20-30% discordance across studies. Immunohistochemistry defines triple negative as tumors lacking the expression of ER, PR and HER2, however basal-like subtype is defined via gene expression microarray analysis (Kreike et al., 2007). Moreover, basal-like tumors overexpress EGFR, show P53 mutations and deregulated integrin expression which may contribute to the aggressive cell behavior and progression in this subtype (Heitz et al., 2009). In addition,

several signaling pathways are deregulated in basal-like tumors such as MAPK, PI3K, Akt and NF-κB pathways. It is also shown that cytoplasmic and nuclear accumulation of β-catenin occur in basal-like breast cancer subtype (Criscitiello et al., 2012).

1.8.2. Breast cancer metastasis:

The American Joint Committee on Cancer (AJCC) divided the stages of breast cancer into the TNM system. T: size of the tumor, N: extent of tumor spread to nearby lymph nodes and M: extent of metastasis to other organs of the body. The earliest stage of breast cancer is called stage 0 or carcinoma *in situ*. In stage I, the tumor is still small without being spread outside the patient's breast. In stage II, the tumor is less than 2 cm in diameter and may also be found in axillary lymph nodes. Stage III tumors can be of any size and usually it is spread to the chest wall and/or the skin of the breast. In stage IV, the cancer shows metastasis to distant organs such as the brain, lungs, liver or bones (Edge et al., 2010).

10-15% of breast cancer patients have an aggressive disease leading to metastasis within three years of developing primary tumors (Weigelt et al., 2005). Most patients do not die because of the primary tumor, but from the metastasis of breast cancer. Breast cancer metastasis, as any other solid tumor, consists of the following steps: 1) Metastasis starts when the cancer cell dissociates from the ECM and adjacent cells and starts invading the surrounding tissue through the secretion of proteolytic enzymes to degrade the surrounding ECM (Ha et al., 2013). 2) Intravasation: the cancer cell attaches to the endothelial wall, invades and moves through the walls of lymph or blood vessels (van Zijl et al., 2011). 3) Cancer cells spread through blood and lymph circulation to other organs and survive in an anchorage-independent manner (Valastyan et al., 2011). 4) Extravasation: cancer cells undergo cell cycle arrest, adhere to the capillary walls of the target organ and extravasate into the site of metastasis (Azevedo et al., 2015). 5) Finally, cancer

cells will proliferate to form small tumors in the metastatic site (Ben-Baruch, 2009). Disrupting any of these steps stops metastasis of cancer cells (Poste et al., 1980). Moreover, cancer cells should avoid immune reactions and apoptosis signals to survive (Friedl et al., 2008).

Integrins play an essential role in cell migration and survival. For instance, integrin α3β1 is shown to be associated with cancer cell invasion, metastasis and the activity of the matrix metalloproteinase MMP-9 (Morini et al., 2000). MMPs are a family of zinc-dependent endopeptidases which are secreted by the cell to degrade the ECM and invade the surrounding tissue (Reunanen et al., 2013). Moreover, the downregulation E-cadherin, involved in cell-cell interaction, is shown to be related to poor prognosis in triple negative breast cancer patients and to be associated with increased metastatic potential (Li et al., 2016, Wendt et al., 2011). Importantly, the downregulation of E-cadherin is an indicative of epithelial-to-mesenchymal transition (EMT), a cellular process playing a critical role in cancer progression and metastasis (Gotzmann et al., 2004). EMT increases the ability of cancer cells to invade and metastasize. Furthermore, breast cancer cells downregulating E-cadherin and overexpressing N-cadherin exhibit an increase in tumor cell invasion (Maret et al., 2010). In addition, specific transcription factors are involved in EMT such as TWIST, SNAIL, SLUG and ZEB1/2 which suppress E-cadherin expression in cancer cells (Cano et al., 2000). Consequently, these transcription factors regulate several signaling pathways such as TGFβ, β-catenin, PI3K/AKT which are all suggested to be associated with poor prognosis of breast cancer (Tungsukruthai et al., 2018).

The aggressiveness of triple negative breast cancer is shown to be associated with elevated levels of EGFR (Manupati et al., 2017). It is reported that 15-30% of breast carcinomas expressing high levels of EGFR exhibit poor prognosis (Gaedcke et al., 2007). In addition, 15-35% of invasive breast cancers expressing high levels of HER2 result in a decrease in patients' survival rates (Shao

et al., 2011). Studies show that EGFR and HER2 contribute to breast cancer metastasis to the brain (Lim et al., 2014).

Angiogenesis, the process of forming new blood vessels, is a critical step in mediating tumorigenesis and metastasis. Anti-angiogenesis therapeutic approaches gained much attention in the field of anti-cancer drug discovery. Clinical and experimental studies showed that breast cancer is an angiogenesis-dependent cancer (Schneider et al., 2005). The expression of vascular endothelial growth factor (VEGF) shows the most potent activity in triggering angiogenesis in several types of human cancers (Shibuya, 2011). VEGF stimulates VEGFR1 and VEGFR2 receptors on the surface of endothelial cells triggering endothelial cell motility, vascular permeability, cell survival and proliferation (Shibuya, 2001). Breast cancer patients with early tumor stage and with elevated levels of VEGF have higher rates of recurrence and lower survival rates (Niu et al., 2010). VEGF signaling facilitates metastasis in breast cancer patients (Valastyan et al., 2011). For instance, VEGF pathway in breast cancer enhances cell survival through AKT and ERK signaling pathways (Salameh et al., 2005), thus cancer cells avoid apoptosis and increase migration (Liang et al., 2006).

Hence, to understand more how activated cell surface receptors are sorted towards lysosomes and their signaling is regulated, the role of Endofin and the importance of its interaction with HD-PTP in receptor trafficking should be investigated. Moreover, Endofin might exert a tumor suppressor activity, similar to the role of HD-PTP.

1.9. References:

Agromayor, M., Soler, N., Caballe, A., Kueck, T., Freund, S. M., Allen, M. D., . . . McDonald, B. (2012). The UBAP1 subunit of ESCRT-I interacts with ubiquitin via a SOUBA domain. *Structure, 20*(3), 414-428.

Ali, N., Zhang, L., Taylor, S., Mironov, A., Urbé, S., & Woodman, P. (2013). Recruitment of UBPY and ESCRT exchange drive HD-PTP-dependent sorting of EGFR to the MVB. *Current biology, 23*(6), 453-461.

Ankem, G., Mitra, S., Sun, F., Moreno, A. C., Chutvirasakul, B., Azurmendi, H. F., . . . Capelluto, D. G. (2011). The C2 domain of Tollip, a Toll-like receptor signalling regulator, exhibits broad preference for phosphoinositides. *Biochemical Journal, 435*(3), 597-608.

Azevedo, A. S., Follain, G., Patthabhiraman, S., Harlepp, S., & Goetz, J. G. (2015). Metastasis of circulating tumor cells: favorable soil or suitable biomechanics, or both? *Cell adhesion & migration, 9*(5), 345-356.

Barr, A. J., Ugochukwu, E., Lee, W. H., King, O. N., Filippakopoulos, P., Alfano, I., . . . Knapp, S. (2009). Large-scale structural analysis of the classical human protein tyrosine phosphatome. *Cell, 136*(2), 352-363.

Barriere, H., & Lukacs, G. L. (2008). Analysis of Endocytic Trafficking by Single-Cell Fluorescence Ratio Imaging. *Current protocols in cell biology, 40*(1), 15.13. 11-15.13. 21.

Barriere, H., Nemes, C., Du, K., & Lukacs, G. L. (2007). Plasticity of polyubiquitin recognition as lysosomal targeting signals by the endosomal sorting machinery. *Molecular biology of the cell, 18*(10), 3952-3965.

Ben-Baruch, A. (2009). Site-specific metastasis formation: chemokines as regulators of tumor cell adhesion, motility and invasion. *Cell adhesion & migration, 3*(4), 328-333.

Blanc, C., Charette, S. J., Mattei, S., Aubry, L., Smith, E. W., Cosson, P., & Letourneur, F. (2009). Dictyostelium Tom1 participates to an ancestral ESCRT-0 complex. *Traffic, 10*(2), 161-171.

Böcking, T., Aguet, F., Harrison, S. C., & Kirchhausen, T. (2011). Single-molecule analysis of a molecular disassemblase reveals the mechanism of Hsc70-driven clathrin uncoating. *Nature structural & molecular biology, 18*(3), 295-301.

Botero-Velez, M., Curtis, J. J., & Warnock, D. G. (1994). Liddle's syndrome revisited--a disorder of sodium reabsorption in the distal tubule. *New England Journal of Medicine, 330*(3), 178-181.

Böttcher, R. T., Stremmel, C., Meves, A., Meyer, H., Widmaier, M., Tseng, H.-Y., & Fässler, R. (2012). Sorting nexin 17 prevents lysosomal degradation of β1 integrins by binding to the β1-integrin tail. *Nature cell biology, 14*(6), 584-592.

Brissoni, B., Agostini, L., Kropf, M., Martinon, F., Swoboda, V., Lippens, S., . . . Meylan, E. (2006). Intracellular trafficking of interleukin-1 receptor I requires Tollip. *Current biology, 16*(22), 2265-2270.

Byron, A., Morgan, M. R., & Humphries, M. J. (2010). Adhesion signalling complexes. *Current biology, 20*(24), R1063-R1067.

Cano, A., Pérez-Moreno, M. A., Rodrigo, I., Locascio, A., Blanco, M. J., del Barrio, M. G., . . . Nieto, M. A. (2000). The transcription factor snail controls epithelial–mesenchymal transitions by repressing E-cadherin expression. *Nature cell biology, 2*(2), 76-83.

Cao, L., Zhang, L., Ruiz-Lozano, P., Yang, Q., Chien, K. R., Graham, R. M., & Zhou, M. (1998). A novel putative protein-tyrosine phosphatase contains a BRO1-like domain and suppresses Ha-ras-mediated transformation. *Journal of Biological Chemistry, 273*(33), 21077-21083.

Capuani, F., Conte, A., Argenzio, E., Marchetti, L., Priami, C., Polo, S., . . . Ciliberto, A. (2015). Quantitative analysis reveals how EGFR activation and downregulation are coupled in normal but not in cancer cells. *Nature communications, 6*(1), 1-14.

Carey, L. A., Perou, C. M., Livasy, C. A., Dressler, L. G., Cowan, D., Conway, K., . . . Edmiston, S. (2006). Race, breast cancer subtypes, and survival in the Carolina Breast Cancer Study. *Jama, 295*(21), 2492-2502.

Carlton, J. G., Agromayor, M., & Martin-Serrano, J. (2008). Differential requirements for Alix and ESCRT-III in cytokinesis and HIV-1 release. *Proceedings of the National Academy of Sciences, 105*(30), 10541-10546.

Caswell, P. T., Chan, M., Lindsay, A. J., McCaffrey, M. W., Boettiger, D., & Norman, J. C. (2008). Rab-coupling protein coordinates recycling of α5β1 integrin and EGFR1 to promote cell migration in 3D microenvironments. *The Journal of cell biology, 183*(1), 143-155.

Caswell, P. T., Spence, H. J., Parsons, M., White, D. P., Clark, K., Cheng, K. W., . . . Anderson, K. I. (2007). Rab25 associates with α5β1 integrin to promote invasive migration in 3D microenvironments. *Developmental cell, 13*(4), 496-510.

Chang, H.-M., Lin, Y.-Y., Tsai, P.-C., Liang, C.-T., & Yan, Y.-T. (2014). The FYVE domain of Smad Anchor for Receptor Activation (SARA) is required to prevent skin carcinogenesis, but not in mouse development. *PLoS One, 9*(8), e105299.

Chang, S. S., Grunder, S., Hanukoglu, A., Rösler, A., Mathew, P., Hanukoglu, I., . . . Nelson-Williams, C. (1996). Mutations in subunits of the epithelial sodium channel cause salt wasting with hyperkalaemic acidosis, pseudohypoaldosteronism type 1. *Nature genetics, 12*(3), 248-253.

Chen, D. Y., Li, M. Y., Wu, S. Y., Lin, Y. L., Tsai, S. P., Lai, P. L., . . . Chen, G. C. (2012). The Bro1-domain-containing protein Myopic/HDPTP coordinates with Rab4 to regulate cell adhesion and migration. *J Cell Sci, 125*(Pt 20), 4841-4852. doi:10.1242/jcs.108597

Chen, Y.-G., Wang, Z., Ma, J., Zhang, L., & Lu, Z. (2007). Endofin, a FYVE domain protein, interacts with Smad4 and facilitates transforming growth factor-β signaling. *Journal of Biological Chemistry, 282*(13), 9688-9695.

Chen, Y., Low, T. Y., Choong, L. Y., Ray, R. S., Tan, Y. L., Toy, W., . . . Lim, S. (2007). Phosphoproteomics identified Endofin, DCBLD2, and KIAA0582 as novel tyrosine phosphorylation targets of EGF signaling and Iressa in human cancer cells. *Proteomics, 7*(14), 2384-2397.

Christ, L., Raiborg, C., Wenzel, E. M., Campsteijn, C., & Stenmark, H. (2017). Cellular functions and molecular mechanisms of the ESCRT membrane-scission machinery. *Trends in biochemical sciences, 42*(1), 42-56.

Christ, L., Wenzel, E. M., Liestøl, K., Raiborg, C., Campsteijn, C., & Stenmark, H. (2016). ALIX and ESCRT-I/II function as parallel ESCRT-III recruiters in cytokinetic abscission. *J Cell Biol, 212*(5), 499-513.

Chung, I., Akita, R., Vandlen, R., Toomre, D., Schlessinger, J., & Mellman, I. (2010). Spatial control of EGF receptor activation by reversible dimerization on living cells. *Nature, 464*(7289), 783-787.

Clague, M. J., Coulson, J. M., & Urbé, S. (2012). Cellular functions of the DUBs. *Journal of cell science, 125*(2), 277-286.
Cocucci, E., Aguet, F., Boulant, S., & Kirchhausen, T. (2012). The first five seconds in the life of a clathrin-coated pit. *Cell, 150*(3), 495-507.
Creighton, C. J. (2012). The molecular profile of luminal B breast cancer. *Biologics: targets & therapy, 6*, 289.
Criscitiello, C., Azim Jr, H., Schouten, P., Linn, S., & Sotiriou, C. (2012). Understanding the biology of triple-negative breast cancer. *Annals of oncology, 23*, vi13-vi18.
De Souza, R. F., & Aravind, L. (2010). UMA and MABP domains throw light on receptor endocytosis and selection of endosomal cargoes. *Bioinformatics, 26*(12), 1477-1480.
Doyotte, A., Mironov, A., McKenzie, E., & Woodman, P. (2008). The Bro1-related protein HD-PTP/PTPN23 is required for endosomal cargo sorting and multivesicular body morphogenesis. *Proceedings of the National Academy of Sciences, 105*(17), 6308-6313.
Dozynkiewicz, M. A., Jamieson, N. B., MacPherson, I., Grindlay, J., van den Berghe, P. V., von Thun, A., . . . Nixon, C. (2012). Rab25 and CLIC3 collaborate to promote integrin recycling from late endosomes/lysosomes and drive cancer progression. *Developmental cell, 22*(1), 131-145.
Edge, S. B., & Compton, C. C. (2010). The American Joint Committee on Cancer: the 7th edition of the AJCC cancer staging manual and the future of TNM. *Annals of surgical oncology, 17*(6), 1471-1474.
Ellis, M. J., Tao, Y., Luo, J., A'hern, R., Evans, D. B., Bhatnagar, A. S., . . . Smith, I. (2008). Outcome prediction for estrogen receptor–positive breast cancer based on postneoadjuvant endocrine therapy tumor characteristics. *Journal of the National Cancer Institute, 100*(19), 1380-1388.
Freed, E. O. (2002). Viral late domains. *Journal of virology, 76*(10), 4679-4687.
Friedl, P., & Wolf, K. (2008). Tube travel: the role of proteases in individual and collective cancer cell invasion. *Cancer research, 68*(18), 7247-7249.
Gabos, Z., Sinha, R., Hanson, J., Chauhan, N., Hugh, J., Mackey, J. R., & Abdulkarim, B. (2006). Prognostic significance of human epidermal growth factor receptor positivity for the development of brain metastasis after newly diagnosed breast cancer. *Journal of clinical oncology, 24*(36), 5658-5663.
Gaedcke, J., Traub, F., Milde, S., Wilkens, L., Stan, A., Ostertag, H., . . . Kreipe, H. H. (2007). Predominance of the basal type and HER-2/neu type in brain metastasis from breast cancer. *Modern pathology, 20*(8), 864-870.
Gahloth, D., Heaven, G., Jowitt, T. A., Mould, A. P., Bella, J., Baldock, C., . . . Tabernero, L. (2017). The open architecture of HD-PTP phosphatase provides new insights into the mechanism of regulation of ESCRT function. *Scientific Reports, 7*(1), 9151.
Gahloth, D., Levy, C., Heaven, G., Stefani, F., Wunderley, L., Mould, P., . . . Woodman, P. (2016). Structural basis for selective interaction between the ESCRT regulator HD-PTP and UBAP1. *Structure, 24*(12), 2115-2126.
Gahloth, D., Levy, C., Walker, L., Wunderley, L., Mould, A. P., Taylor, S., . . . Tabernero, L. (2017). Structural Basis for Specific Interaction of TGFβ Signaling Regulators SARA/Endofin with HD-PTP. *Structure*.
Gingras, M.-C., Zhang, Y. L., Kharitidi, D., Barr, A. J., Knapp, S., Tremblay, M. L., & Pause, A. (2009). HD-PTP is a catalytically inactive tyrosine phosphatase due to a conserved divergence in its phosphatase domain. *PLoS One, 4*(4), e5105.

Goh, J. B., Wallace, D. F., Hong, W., & Subramaniam, V. N. (2015). Endofin, a novel BMP-SMAD regulator of the iron-regulatory hormone, hepcidin. *Scientific Reports, 5*.

Gotzmann, J., Mikula, M., Eger, A., Schulte-Hermann, R., Foisner, R., Beug, H., & Mikulits, W. (2004). Molecular aspects of epithelial cell plasticity: implications for local tumor invasion and metastasis. *Mutation Research/Reviews in Mutation Research, 566*(1), 9-20.

Gruenberg, J., Griffiths, G., & Howell, K. E. (1989). Characterization of the early endosome and putative endocytic carrier vesicles in vivo and with an assay of vesicle fusion in vitro. *The Journal of cell biology, 108*(4), 1301-1316.

Guarneri, V., & Conte, P. (2009). Metastatic breast cancer: therapeutic options according to molecular subtypes and prior adjuvant therapy. *The oncologist, 14*(7), 645-656.

Guo, W., & Giancotti, F. G. (2004). Integrin signalling during tumour progression. *Nature Reviews Molecular Cell Biology, 5*(10), 816-826.

Ha, N.-H., Faraji, F., & Hunter, K. W. (2013). Mechanisms of metastasis. *Cancer Targeted Drug Delivery*, 435-458.

Harkiolaki, M., Tsirka, T., Lewitzky, M., Simister, P. C., Joshi, D., Bird, L. E., . . . Feller, S. M. (2009). Distinct binding modes of two epitopes in Gab2 that interact with the SH3C domain of Grb2. *Structure, 17*(6), 809-822.

Heitz, F., Harter, P., Lueck, H.-J., Fissler-Eckhoff, A., Lorenz-Salehi, F., Scheil-Bertram, S., . . . du Bois, A. (2009). Triple-negative and HER2-overexpressing breast cancers exhibit an elevated risk and an earlier occurrence of cerebral metastases. *European journal of cancer, 45*(16), 2792-2798.

Henne, W. M., Buchkovich, N. J., & Emr, S. D. (2011). The ESCRT pathway. *Developmental cell, 21*(1), 77-91.

Herman, E. K., Walker, G., van der Giezen, M., & Dacks, J. B. (2011). Multivesicular bodies in the enigmatic amoeboflagellate Breviata anathema and the evolution of ESCRT 0. *Journal of cell science, 124*(4), 613-621.

Hu, Z., Fan, C., Oh, D. S., Marron, J., He, X., Qaqish, B. F., . . . Dressler, L. (2006). The molecular portraits of breast tumors are conserved across microarray platforms. *BMC genomics, 7*(1), 1-12.

Hurley, J. H. (2015). ESCRT s are everywhere. *The EMBO journal, 34*(19), 2398-2407.

Ichioka, F., Takaya, E., Suzuki, H., Kajigaya, S., Buchman, V. L., Shibata, H., & Maki, M. (2007). HD-PTP and Alix share some membrane-traffic related proteins that interact with their Bro1 domains or proline-rich regions. *Archives of Biochemistry and Biophysics, 457*(2), 142-149.

Jiang, X., Huang, F., Marusyk, A., & Sorkin, A. (2003). Grb2 regulates internalization of EGF receptors through clathrin-coated pits. *Molecular biology of the cell, 14*(3), 858-870.

Jiang, Y., Ou, Y., & Cheng, X. (2013). Role of TSG101 in cancer. *Front Biosci (Landmark Ed), 18*, 279-288. Retrieved from https://www.ncbi.nlm.nih.gov/pubmed/23276921

Katoh, Y., Imakagura, H., Futatsumori, M., & Nakayama, K. (2006). Recruitment of clathrin onto endosomes by the Tom1–Tollip complex. *Biochemical and biophysical research communications, 341*(1), 143-149.

Katoh, Y., Shiba, Y., Mitsuhashi, H., Yanagida, Y., Takatsu, H., & Nakayama, K. (2004). Tollip and Tom1 form a complex and recruit ubiquitin-conjugated proteins onto early endosomes. *J Biol Chem, 279*(23), 24435-24443. doi:10.1074/jbc.M400059200

Keating, D. J., Chen, C., & Pritchard, M. A. (2006). Alzheimer's disease and endocytic dysfunction: clues from the Down syndrome-related proteins, DSCR1 and ITSN1. *Ageing research reviews, 5*(4), 388-401.

Kennecke, H., Yerushalmi, R., Woods, R., Cheang, M. C. U., Voduc, D., Speers, C. H., . . . Gelmon, K. (2010). Metastatic behavior of breast cancer subtypes. *Journal of clinical oncology, 28*(20), 3271-3277.

Kharitidi, D., Apaja, P. M., Manteghi, S., Suzuki, K., Malitskaya, E., Roldan, A., . . . Pause, A. (2015). Interplay of endosomal pH and ligand occupancy in integrin α5β1 ubiquitination, endocytic sorting, and cell migration. *Cell reports, 13*(3), 599-609.

Kimura, Y., Tanigawa, M., Kawawaki, J., Takagi, K., Mizushima, T., Maeda, T., & Tanaka, K. (2015). Conserved mode of interaction between yeast Bro1 family V domains and YP (X) nL motif-containing target proteins. *Eukaryotic cell, 14*(10), 976-982.

Kirchhausen, T., & Harrison, S. C. (1981). Protein organization in clathrin trimers. *Cell, 23*(3), 755-761.

Kostaras, E., Sflomos, G., Pedersen, N., Stenmark, H., Fotsis, T., & Murphy, C. (2013). SARA and RNF11 interact with each other and ESCRT-0 core proteins and regulate degradative EGFR trafficking. *Oncogene, 32*(44), 5220-5232.

Kreike, B., van Kouwenhove, M., Horlings, H., Weigelt, B., Peterse, H., Bartelink, H., & van de Vijver, M. J. (2007). Gene expression profiling and histopathological characterization of triple-negative/basal-like breast carcinomas. *Breast Cancer Research, 9*(5), 1-14.

Lahlou, H., & Muller, W. J. (2011). β1-integrins signaling and mammary tumor progression in transgenic mouse models: implications for human breast cancer. *Breast Cancer Research, 13*(6), 1-10.

Lauwers, E., Jacob, C., & André, B. (2009). K63-linked ubiquitin chains as a specific signal for protein sorting into the multivesicular body pathway. *Journal of Cell Biology, 185*(3), 493-502.

Lee, J., Oh, K.-J., Lee, D., Kim, B. Y., Choi, J. S., Ku, B., & Kim, S. J. (2016). Structural study of the HD-PTP Bro1 domain in a complex with the core region of STAM2, a subunit of ESCRT-0. *PLoS One, 11*(2), e0149113.

Li, J., Belogortseva, N., Porter, D., & Park, M. (2008). Chmp1A functions as a novel tumor suppressor gene in human embryonic kidney and ductal pancreatic tumor cells. *Cell Cycle, 7*(18), 2886-2893.

Li, P., Sun, T., Yuan, Q., Pan, G., Zhang, J., & Sun, D. (2016). The expressions of NEDD9 and E-cadherin correlate with metastasis and poor prognosis in triple-negative breast cancer patients. *OncoTargets and therapy, 9*, 5751.

Liang, Y., Brekken, R. A., & Hyder, S. M. (2006). Vascular endothelial growth factor induces proliferation of breast cancer cells and inhibits the anti-proliferative activity of anti-hormones. *Endocrine-related cancer, 13*(3), 905-919.

Liao, Z., Thomas, S. N., Wan, Y., Lin, H. H., Ann, D. K., & Yang, A. J. (2013). An internal standard-assisted synthesis and degradation proteomic approach reveals the potential linkage between VPS4B depletion and activation of fatty acid β-oxidation in breast cancer cells. *International journal of proteomics, 2013*.

Lill, N. L., & Sever, N. I. (2012). Where EGF receptors transmit their signals. *Science signaling, 5*(243), pe41-pe41.

Lim, E., & Lin, N. U. (2014). Updates on the management of breast cancer brain metastases. *Oncology, 28*(7), 572-572.

Lin, G., Aranda, V., Muthuswamy, S. K., & Tonks, N. K. (2011). Identification of PTPN23 as a novel regulator of cell invasion in mammary epithelial cells from a loss-of-function screen of the ‘PTP-ome'. *Genes & development, 25*(13), 1412-1425.

Lin, H. H., Li, X., Chen, J.-L., Sun, X., Cooper, F. N., Chen, Y.-R., . . . Cheng, C.-T. (2012). Identification of an AAA ATPase VPS4B-dependent pathway that modulates epidermal growth factor receptor abundance and signaling during hypoxia. *Molecular and Cellular Biology, 32*(6), 1124-1138.

Liu, R.-T., Huang, C.-C., You, H.-L., Chou, F.-F., Hu, C.-C. A., Chao, F.-P., . . . Cheng, J.-T. (2002). Overexpression of tumor susceptibility gene TSG101 in human papillary thyroid carcinomas. *Oncogene, 21*(31), 4830-4837.

Liu, W., Xie, Y., Ma, J., Luo, X., Nie, P., Zuo, Z., . . . Zhao, Y. (2015). IBS: an illustrator for the presentation and visualization of biological sequences. *Bioinformatics, 31*(20), 3359-3361.

Liu, Y., Lv, L., Xue, Q., Wan, C., Ni, T., Chen, B., . . . Mao, G. (2013). Vacuolar protein sorting 4B, an ATPase protein positively regulates the progression of NSCLC via promoting cell division. *Molecular and cellular biochemistry, 381*(1), 163-171.

Lu, Q., Hope, L. W., Brasch, M., Reinhard, C., & Cohen, S. N. (2003). TSG101 interaction with HRS mediates endosomal trafficking and receptor down-regulation. *Proceedings of the National Academy of Sciences, 100*(13), 7626-7631.

Luo, B.-H., & Springer, T. A. (2006). Integrin structures and conformational signaling. *Current opinion in cell biology, 18*(5), 579-586.

Luzio, J. P., Pryor, P. R., & Bright, N. A. (2007). Lysosomes: fusion and function. *Nature Reviews Molecular Cell Biology, 8*(8), 622-632.

Ma, H., Wardega, P., Mazaud, D., Klosowska-Wardega, A., Jurek, A., Engstrom, U., . . . Heldin, C. H. (2015). Histidine-domain-containing protein tyrosine phosphatase regulates platelet-derived growth factor receptor intracellular sorting and degradation. *Cell Signal, 27*(11), 2209-2219. doi:10.1016/j.cellsig.2015.07.020

Ma, X., Pauline, B., Patricia, L., & Rahman, J. (2008). Overexpression of WNT2 and TSG101 genes in colorectal carcinoma. *Tropical biomedicine, 25*(1), 46-57.

Macia, E., Ehrlich, M., Massol, R., Boucrot, E., Brunner, C., & Kirchhausen, T. (2006). Dynasore, a cell-permeable inhibitor of dynamin. *Developmental cell, 10*(6), 839-850.

Macpherson, I. R., Rainero, E., Mitchell, L. E., van den Berghe, P. V., Speirs, C., Dozynkiewicz, M. A., . . . Timpson, P. (2014). CLIC3 controls recycling of late endosomal MT1-MMP and dictates invasion and metastasis in breast cancer. *Journal of cell science, 127*(18), 3893-3901.

Maiorano, E., Favia, G., Pece, S., Resta, L., Maisonneuve, P., Di Fiore, P., . . . Viale, G. (2007). Prognostic implications of NUMB immunoreactivity in salivary gland carcinomas. *International journal of immunopathology and pharmacology, 20*(4), 779-789.

Manteghi, S., Gingras, M.-C., Kharitidi, D., Galarneau, L., Marques, M., Yan, M., . . . Witcher, M. (2016). Haploinsufficiency of the ESCRT component HD-PTP predisposes to cancer. *Cell reports, 15*(9), 1893-1900.

Manupati, K., Dhoke, N. R., Debnath, T., Yeeravalli, R., Guguloth, K., Saeidpour, S., . . . Das, A. (2017). Inhibiting epidermal growth factor receptor signalling potentiates mesenchymal–epithelial transition of breast cancer stem cells and their responsiveness to anticancer drugs. *The FEBS journal, 284*(12), 1830-1854.

Maret, D., Gruzglin, E., Sadr, M. S., Siu, V., Shan, W., Koch, A. W., . . . Colman, D. R. (2010). Surface expression of precursor N-cadherin promotes tumor cell invasion. *Neoplasia, 12*(12), 1066-IN1038.

Mariotti, M., Castiglioni, S., Garcia-Manteiga, J. M., Beguinot, L., & Maier, J. A. (2009). HD-PTP inhibits endothelial migration through its interaction with Src. *The international journal of biochemistry & cell biology, 41*(3), 687-693.

Marshansky, V., & Futai, M. (2008). The V-type H+-ATPase in vesicular trafficking: targeting, regulation and function. *Current opinion in cell biology, 20*(4), 415-426.

Mattissek, C., & Teis, D. (2014). The role of the endosomal sorting complexes required for transport (ESCRT) in tumorigenesis. *Molecular membrane biology, 31*(4), 111-119.

Maxfield, F. R., & McGraw, T. E. (2004). Endocytic recycling. *Nature Reviews Molecular Cell Biology, 5*(2), 121-132.

Mayor, S., Parton, R. G., & Donaldson, J. G. (2014). Clathrin-independent pathways of endocytosis. *Cold Spring Harbor Perspectives in Biology, 6*(6), a016758.

McCullough, J., Fisher, R. D., Whitby, F. G., Sundquist, W. I., & Hill, C. P. (2008). ALIX-CHMP4 interactions in the human ESCRT pathway. *Proceedings of the National Academy of Sciences, 105*(22), 7687-7691.

Mercier, V., Laporte, M. H., Destaing, O., Blot, B., Blouin, C. M., Pernet-Gallay, K., . . . Lamaze, C. (2016). ALG-2 interacting protein-X (Alix) is essential for clathrin-independent endocytosis and signaling. *Scientific Reports, 6*.

Mills, G. B., Jurisica, I., Yarden, Y., & Norman, J. C. (2009). Genomic amplicons target vesicle recycling in breast cancer. *The Journal of clinical investigation, 119*(8), 2123-2127.

Miura, G. I., Roignant, J.-Y., Wassef, M., & Treisman, J. E. (2008). Myopic acts in the endocytic pathway to enhance signaling by the Drosophila EGF receptor. *Development, 135*(11), 1913-1922.

Moasser, M. M. (2007). The oncogene HER2: its signaling and transforming functions and its role in human cancer pathogenesis. *Oncogene, 26*(45), 6469-6487.

Morini, M., Mottolese, M., Ferrari, N., Ghiorzo, F., Buglioni, S., Mortarini, R., . . . Albini, A. (2000). The α3β1 integrin is associated with mammary carcinoma cell metastasis, invasion, and gelatinase B (mmp-9) activity. *International journal of cancer, 87*(3), 336-342.

Muller, P., Trinidad, A., Timpson, P., Morton, J., Zanivan, S., Van Den Berghe, P., . . . Noll, J. (2013). Mutant p53 enhances MET trafficking and signalling to drive cell scattering and invasion. *Oncogene, 32*(10), 1252-1265.

Muller, P. A., Caswell, P. T., Doyle, B., Iwanicki, M. P., Tan, E. H., Karim, S., . . . Gosselin, P. (2009). Mutant p53 drives invasion by promoting integrin recycling. *Cell, 139*(7), 1327-1341.

Nikolova, D. N., Doganov, N., Dimitrov, R., Angelov, K., Low, S.-K., Dimova, I., . . . Zembutsu, H. (2009). Genome-wide gene expression profiles of ovarian carcinoma: Identification of molecular targets for the treatment of ovarian carcinoma. *Molecular medicine reports, 2*(3), 365-384.

Nishimura, R., Osako, T., Okumura, Y., Hayashi, M., Toyozumi, Y., & Arima, N. (2010). Ki-67 as a prognostic marker according to breast cancer subtype and a predictor of recurrence time in primary breast cancer. *Experimental and therapeutic medicine, 1*(5), 747-754.

Niu, G., & Chen, X. (2010). Vascular endothelial growth factor as an anti-angiogenic target for cancer therapy. *Current drug targets, 11*(8), 1000-1017.

Ogiso, H., Ishitani, R., Nureki, O., Fukai, S., Yamanaka, M., Kim, J.-H., . . . Shirouzu, M. (2002). Crystal structure of the complex of human epidermal growth factor and receptor extracellular domains. *Cell, 110*(6), 775-787.

Oh, K., Stanton, M., West, W., Todd, G., & Wagner, K. (2007). Tsg101 is upregulated in a subset of invasive human breast cancers and its targeted overexpression in transgenic mice reveals weak oncogenic properties for mammary cancer initiation. *Oncogene, 26*(40), 5950-5959.

Parkinson, M. D., Piper, S. C., Bright, N. A., Evans, J. L., Boname, J. M., Bowers, K., . . . Luzio, J. P. (2015). A non-canonical ESCRT pathway, including histidine domain phosphotyrosine phosphatase (HD-PTP), is used for down-regulation of virally ubiquitinated MHC class I. *Biochemical Journal, 471*(1), 79-88.

Pashkova, N., Gakhar, L., Winistorfer, S. C., Sunshine, A. B., Rich, M., Dunham, M. J., . . . Piper, R. C. (2013). The yeast Alix homolog Bro1 functions as a ubiquitin receptor for protein sorting into multivesicular endosomes. *Developmental cell, 25*(5), 520-533.

Piper, R. C., & Katzmann, D. J. (2007). Biogenesis and function of multivesicular bodies. *Annu. Rev. Cell Dev. Biol., 23*, 519-547.

Pornillos, O., Alam, S. L., Rich, R. L., Myszka, D. G., Davis, D. R., & Sundquist, W. I. (2002). Structure and functional interactions of the Tsg101 UEV domain. *The EMBO journal, 21*(10), 2397-2406.

Poste, G., & Fidler, I. J. (1980). The pathogenesis of cancer metastasis. *Nature, 283*(5743), 139-146.

Powelka, A. M., Sun, J., Li, J., Gao, M., Shaw, L. M., Sonnenberg, A., & Hsu, V. W. (2004). Stimulation-dependent recycling of integrin β1 regulated by ARF6 and Rab11. *Traffic, 5*(1), 20-36.

Pradhan-Sundd, T., & Verheyen, E. M. (2015). The Myopic-Ubpy-Hrs nexus enables endosomal recycling of Frizzled. *Mol Biol Cell, 26*(18), 3329-3342. doi:10.1091/mbc.E15-02-0086

Raiborg, C., Bache, K. G., Mehlum, A., Stang, E., & Stenmark, H. (2001). Hrs recruits clathrin to early endosomes. *EMBO J, 20*(17), 5008-5021. doi:10.1093/emboj/20.17.5008

Raiborg, C., Wesche, J., Malerod, L., & Stenmark, H. (2006). Flat clathrin coats on endosomes mediate degradative protein sorting by scaffolding Hrs in dynamic microdomains. *J Cell Sci, 119*(Pt 12), 2414-2424. doi:10.1242/jcs.02978

Randles, L., & Walters, K. J. (2012). Ubiquitin and its binding domains. *Frontiers in bioscience (Landmark edition), 17*, 2140.

Rechsteiner, M., & Rogers, S. W. (1996). PEST sequences and regulation by proteolysis. *Trends in biochemical sciences, 21*(7), 267-271.

Reunanen, N., & Kähäri, V. (2013). Matrix metalloproteinases in cancer cell invasion. In *Madame Curie Bioscience Database [Internet]*: Landes Bioscience.

Reynolds, A. R., Hart, I. R., Watson, A. R., Welti, J. C., Silva, R. G., Robinson, S. D., . . . Jones, M. C. (2009). Stimulation of tumor growth and angiogenesis by low concentrations of RGD-mimetic integrin inhibitors. *Nature medicine, 15*(4), 392-400.

Richter, C., West, M., & Odorizzi, G. (2007). Dual mechanisms specify Doa4-mediated deubiquitination at multivesicular bodies. *EMBO J, 26*(10), 2454-2464. doi:10.1038/sj.emboj.7601692

Rodahl, L. M., Stuffers, S., Lobert, V. H., & Stenmark, H. (2009). The role of ESCRT proteins in attenuation of cell signalling. *Biochem Soc Trans, 37*(Pt 1), 137-142. doi:10.1042/BST0370137

Rouzier, R., Perou, C. M., Symmans, W. F., Ibrahim, N., Cristofanilli, M., Anderson, K., . . . Wagner, P. (2005). Breast cancer molecular subtypes respond differently to preoperative chemotherapy. *Clinical Cancer Research, 11*(16), 5678-5685.

Rush, J., Moritz, A., Lee, K. A., Guo, A., Goss, V. L., Spek, E. J., . . . Comb, M. J. (2005). Immunoaffinity profiling of tyrosine phosphorylation in cancer cells. *Nature biotechnology, 23*(1), 94-101.

Saksena, S., & Emr, S. (2009). ESCRTs and human disease. *Biochemical Society Transactions, 37*(Pt 1), 167-172.

Salameh, A., Galvagni, F., Bardelli, M., Bussolino, F., & Oliviero, S. (2005). Direct recruitment of CRK and GRB2 to VEGFR-3 induces proliferation, migration, and survival of endothelial cells through the activation of ERK, AKT, and JNK pathways. *Blood, 106*(10), 3423-3431.

Sawano, A., Takayama, S., Matsuda, M., & Miyawaki, A. (2002). Lateral propagation of EGF signaling after local stimulation is dependent on receptor density. *Developmental cell, 3*(2), 245-257.

Schneider, B. P., & Miller, K. D. (2005). Angiogenesis of breast cancer. *Journal of clinical oncology, 23*(8), 1782-1790.

Schöneberg, J., Lee, I.-H., Iwasa, J. H., & Hurley, J. H. (2017). Reverse-topology membrane scission by the ESCRT proteins. *Nature Reviews Molecular Cell Biology, 18*(1), 5-17.

Seet, L.-F., & Hong, W. (2005). Endofin recruits clathrin to early endosomes via TOM1. *Journal of cell science, 118*(3), 575-587.

Seet, L.-F., Liu, N., Hanson, B. J., & Hong, W. (2004). Endofin recruits TOM1 to endosomes. *Journal of Biological Chemistry, 279*(6), 4670-4679.

Seet, L. F., & Hong, W. (2001). Endofin, an endosomal FYVE domain protein. *J Biol Chem, 276*(45), 42445-42454. doi:10.1074/jbc.M105917200

Shao, M.-m., Liu, J., Vong, J. S., Niu, Y., Germin, B., Tang, P., . . . Tan, P.-H. (2011). A subset of breast cancer predisposes to brain metastasis. *Medical molecular morphology, 44*(1), 15-20.

Sheff, D. R., Daro, E. A., Hull, M., & Mellman, I. (1999). The receptor recycling pathway contains two distinct populations of early endosomes with different sorting functions. *The Journal of cell biology, 145*(1), 123-139.

Shi, W., Chang, C., Nie, S., Xie, S., Wan, M., & Cao, X. (2007). Endofin acts as a Smad anchor for receptor activation in BMP signaling. *Journal of cell science, 120*(7), 1216-1224.

Shiba, Y., Katoh, Y., Shiba, T., Yoshino, K., Takatsu, H., Kobayashi, H., . . . Nakayama, K. (2004). GAT (GGA and Tom1) domain responsible for ubiquitin binding and ubiquitination. *Journal of Biological Chemistry, 279*(8), 7105-7111.

Shibuya, M. (2001). Structure and function of VEGF/VEGF-receptor system involved in angiogenesis. *Cell structure and function, 26*(1), 25-35.

Shibuya, M. (2011). Vascular endothelial growth factor (VEGF) and its receptor (VEGFR) signaling in angiogenesis: a crucial target for anti-and pro-angiogenic therapies. *Genes & cancer, 2*(12), 1097-1105.

Shih, S. C., Katzmann, D. J., Schnell, J. D., Sutanto, M., Emr, S. D., & Hicke, L. (2002). Epsins and Vps27p/Hrs contain ubiquitin-binding domains that function in receptor endocytosis. *Nature cell biology, 4*(5), 389-393.

Sigismund, S., Woelk, T., Puri, C., Maspero, E., Tacchetti, C., Transidico, P., . . . Polo, S. (2005). Clathrin-independent endocytosis of ubiquitinated cargos. *Proceedings of the National Academy of Sciences, 102*(8), 2760-2765.

Sönnichsen, B., De Renzis, S., Nielsen, E., Rietdorf, J., & Zerial, M. (2000). Distinct membrane domains on endosomes in the recycling pathway visualized by multicolor imaging of Rab4, Rab5, and Rab11. *The Journal of cell biology, 149*(4), 901-914.

Sorkin, A., & Von Zastrow, M. (2009). Endocytosis and signalling: intertwining molecular networks. *Nature Reviews Molecular Cell Biology, 10*(9), 609-622.

Soubeyran, P., Kowanetz, K., Szymkiewicz, I., Langdon, W. Y., & Dikic, I. (2002). Cbl–CIN85–endophilin complex mediates ligand-induced downregulation of EGF receptors. *Nature, 416*(6877), 183-187.

Sousa, L. P., Lax, I., Shen, H., Ferguson, S. M., De Camilli, P., & Schlessinger, J. (2012). Suppression of EGFR endocytosis by dynamin depletion reveals that EGFR signaling occurs primarily at the plasma membrane. *Proceedings of the National Academy of Sciences, 109*(12), 4419-4424.

Stachowiak, J. C., Brodsky, F. M., & Miller, E. A. (2013). A cost–benefit analysis of the physical mechanisms of membrane curvature. *Nature cell biology, 15*(9), 1019-1027.

Stefani, F., Zhang, L., Taylor, S., Donovan, J., Rollinson, S., Doyotte, A., . . . Woodman, P. (2011). UBAP1 is a component of an endosome-specific ESCRT-I complex that is essential for MVB sorting. *Current biology, 21*(14), 1245-1250.

Stutts, M. J., Canessa, C. M., Olsen, J. C., Hamrick, M., Cohn, J. A., Rossier, B. C., & Boucher, R. C. (1995). CFTR as a cAMP-dependent regulator of sodium channels. *Science, 269*(5225), 847-850.

Sun, S., Sun, L., Zhou, X., Wu, C., Wang, R., Lin, S.-H., & Kuang, J. (2016). Phosphorylation-dependent activation of the ESCRT function of ALIX in cytokinetic abscission and retroviral budding. *Developmental cell, 36*(3), 331-343.

Sun, S., Zhou, X., Corvera, J., Gallick, G. E., Lin, S.-H., & Kuang, J. (2015). ALG-2 activates the MVB sorting function of ALIX through relieving its intramolecular interaction. *Cell discovery, 1*, 15018.

Sun, S., Zhou, X., Zhang, W., Gallick, G. E., & Kuang, J. (2015). Unravelling the pivotal role of Alix in MVB sorting and silencing of the activated EGFR. *Biochemical Journal, 466*(3), 475-487.

Tanaka, K., Kondo, K., Kitajima, K., Muraoka, M., Nozawa, A., & Hara, T. (2013). Tumor-suppressive function of protein-tyrosine phosphatase non-receptor type 23 in testicular germ cell tumors is lost upon overexpression of miR142–3p microRNA. *Journal of Biological Chemistry, 288*(33), 23990-23999.

Tanase, C.-A. (2010). Histidine domain-protein tyrosine phosphatase interacts with Grb2 and GrpL. *PLoS One, 5*(12), e14339.

Tang, S., Buchkovich, N. J., Henne, W. M., Banjade, S., Kim, Y. J., & Emr, S. D. (2016). ESCRT-III activation by parallel action of ESCRT-I/II and ESCRT-0/Bro1 during MVB biogenesis. *Elife, 5*, e15507.

Teis, D., Kurzbauer, R., Taub, N., Hilber, D., Erlacher, M., Villunger, A., . . . Hess, M. (2006). The p14/MP1-MEK1-signalling complex links the late endosomal transport of the EGFR with mitogenic ERK signalling. In: Submitted.

Tomas, A., Futter, C. E., & Eden, E. R. (2014). EGF receptor trafficking: consequences for signaling and cancer. *Trends in cell biology, 24*(1), 26-34.

Tomas, A., Vaughan, S. O., Burgoyne, T., Sorkin, A., Hartley, J. A., Hochhauser, D., & Futter, C. E. (2015). WASH and Tsg101/ALIX-dependent diversion of stress-internalized EGFR from the canonical endocytic pathway. *Nature communications, 6*.

Tong, X., Zitserman, D., Serebriiskii, I., Andrake, M., Dunbrack, R., & Roegiers, F. (2010). Numb independently antagonizes Sanpodo membrane targeting and Notch signaling in Drosophila sensory organ precursor cells. *Molecular biology of the cell, 21*(5), 802-810.

Toy, W., Lim, S. K., Loh, M. C. S., & Lim, Y.-P. (2010). EGF-induced tyrosine phosphorylation of Endofin is dependent on PI3K activity and proper localization to endosomes. *Cellular signalling, 22*(3), 437-446.

Toyoshima, M., Tanaka, N., Aoki, J., Tanaka, Y., Murata, K., Kyuuma, M., . . . Sugamura, K. (2007). Inhibition of tumor growth and metastasis by depletion of vesicular sorting protein Hrs: its regulatory role on E-cadherin and beta-catenin. *Cancer Res, 67*(11), 5162-5171. doi:10.1158/0008-5472.CAN-06-2756

Trebinska, A., Rembiszewska, A., Ciosek, K., Ptaszynski, K., Rowinski, S., Kupryjanczyk, J., . . . Grzybowska, E. A. (2010). HAX-1 overexpression, splicing and cellular localization in tumors. *BMC cancer, 10*(1), 1-16.

Trempe, J.-F. (2011). Reading the ubiquitin postal code. *Current opinion in structural biology, 21*(6), 792-801.

Tsutsui, S., Ohno, S., Murakami, S., Kataoka, A., Kinoshita, J., & Hachitanda, Y. (2003). Prognostic significance of the coexpression of p53 protein and c-erbB2 in breast cancer. *The American journal of surgery, 185*(2), 165-167.

Tumbarello, D. A., Waxse, B. J., Arden, S. D., Bright, N. A., Kendrick-Jones, J., & Buss, F. (2012). Autophagy receptors link myosin VI to autophagosomes to mediate Tom1-dependent autophagosome maturation and fusion with the lysosome. *Nature cell biology, 14*(10), 1024-1035.

Tungsukruthai, S., Petpiroon, N., & Chanvorachote, P. (2018). Molecular mechanisms of breast cancer metastasis and potential anti-metastatic compounds. *Anticancer research, 38*(5), 2607-2618.

Valastyan, S., & Weinberg, R. A. (2011). Tumor metastasis: molecular insights and evolving paradigms. *Cell, 147*(2), 275-292.

van Zijl, F., Krupitza, G., & Mikulits, W. (2011). Initial steps of metastasis: cell invasion and endothelial transmigration. *Mutation Research/Reviews in Mutation Research, 728*(1-2), 23-34.

Varshavsky, A. (2012). The ubiquitin system, an immense realm. *Annual review of biochemistry, 81*, 167-176.

Wang, C.-Y., Wang, Y.-T., Tzeng, D.-W., & Yang, J.-L. (2009). Lead acetate induces EGFR activation upstream of SFK and PKCα linkage to the Ras/Raf-1/ERK signaling. *Toxicology and applied pharmacology, 235*(2), 244-252.

Wang, T., Liu, N. S., Seet, L. F., & Hong, W. (2010). The emerging role of VHS domain-containing Tom1, Tom1L1 and Tom1L2 in membrane trafficking. *Traffic, 11*(9), 1119-1128.

Weigelt, B., Peterse, J. L., & Van't Veer, L. J. (2005). Breast cancer metastasis: markers and models. *Nature Reviews Cancer, 5*(8), 591-602.

Wendt, M. K., Taylor, M. A., Schiemann, B. J., & Schiemann, W. P. (2011). Down-regulation of epithelial cadherin is required to initiate metastatic outgrowth of breast cancer. *Molecular biology of the cell, 22*(14), 2423-2435.

Wenzel, E. M., Schultz, S. W., Schink, K. O., Pedersen, N. M., Nähse, V., Carlson, A., . . . Raiborg, C. (2018). Concerted ESCRT and clathrin recruitment waves define the timing and morphology of intraluminal vesicle formation. *Nature communications, 9*(1), 1-18.

Westhoff, M.-A., & Fulda, S. (2009). Adhesion-mediated apoptosis resistance in cancer. *Drug Resistance Updates, 12*(4-5), 127-136.

Wiley, H. S., Herbst, J. J., Walsh, B. J., Lauffenburger, D., Rosenfeld, M., & Gill, G. (1991). The role of tyrosine kinase activity in endocytosis, compartmentation, and down-regulation of the epidermal growth factor receptor. *Journal of Biological Chemistry, 266*(17), 11083-11094.

Williams, R. L., & Urbé, S. (2007). The emerging shape of the ESCRT machinery. *Nature Reviews Molecular Cell Biology, 8*(5), 355-368.

Wunderley, L., Brownhill, K., Stefani, F., Tabernero, L., & Woodman, P. (2014). The molecular basis for selective assembly of the UBAP1-containing endosome-specific ESCRT-I complex. *J Cell Sci, 127*(3), 663-672.

Xiao, B., Fan, S., Zeng, Z., Xiong, W., Cao, L., Yang, Y., . . . Qian, J. (2006). Purification of novel UBAP1 protein and its decreased expression on nasopharyngeal carcinoma tissue microarray. *Protein expression and purification, 47*(1), 60-67.

Xu, Z., Liang, L., Wang, H., Li, T., & Zhao, M. (2003). HCRP1, a novel gene that is downregulated in hepatocellular carcinoma, encodes a growth-inhibitory protein. *Biochemical and biophysical research communications, 311*(4), 1057-1066.

Yamakami, M., Yoshimori, T., & Yokosawa, H. (2003). Tom1, a VHS domain-containing protein, interacts with tollip, ubiquitin, and clathrin. *J Biol Chem, 278*(52), 52865-52872. doi:10.1074/jbc.M306740200

Yamashiro, D. J., & Maxfield, F. R. (1987). Kinetics of endosome acidification in mutant and wild-type Chinese hamster ovary cells. *Journal of Cell Biology, 105*(6), 2713-2721.

Yang, Y., Hentati, A., Deng, H.-X., Dabbagh, O., Sasaki, T., Hirano, M., . . . Azim, A. C. (2001). The gene encoding alsin, a protein with three guanine-nucleotide exchange factor domains, is mutated in a form of recessive amyotrophic lateral sclerosis. *Nature genetics, 29*(2), 160-165.

Yersal, O., & Barutca, S. (2014). Biological subtypes of breast cancer: Prognostic and therapeutic implications. *World journal of clinical oncology, 5*(3), 412.

Zhai, Q., Landesman, M. B., Robinson, H., Sundquist, W. I., & Hill, C. P. (2011). Structure of the Bro1 domain protein BROX and functional analyses of the ALIX Bro1 domain in HIV-1 budding. *PLoS One, 6*(12), e27466.

Zhang, F., Qiu, T., Wu, X., Wan, C., Shi, W., Wang, Y., . . . Cao, X. (2009). Sustained BMP signaling in osteoblasts stimulates bone formation by promoting angiogenesis and osteoblast differentiation. *Journal of Bone and Mineral Research, 24*(7), 1224-1233.

Zhang, J., Liu, X., Datta, A., Govindarajan, K., Tam, W. L., Han, J., . . . Phua, T. Y. (2009). RCP is a human breast cancer–promoting gene with Ras-activating function. *The Journal of clinical investigation, 119*(8), 2171-2183.

Zhang, S., Fan, G., Hao, Y., Hammell, M., Wilkinson, J. E., & Tonks, N. K. (2017). Suppression of protein tyrosine phosphatase N23 predisposes to breast tumorigenesis via activation of FYN kinase. *Genes & development, 31*(19), 1939-1957.

Chapter 2 - Endofin is Required for HD-PTP and ESCRT-0 Interdependent Endosomal Sorting of Ubiquitinated Transmembrane Cargoes.

Endofin is Required for HD-PTP and ESCRT-0 Interdependent Endosomal Sorting of Ubiquitinated Transmembrane Cargoes.

Jalal M. Kazan[1,2,6], Guillaume Desrochers[1,2,6], Claire E. Martin[3], Hyeonju Jeong[1,2], Dmitri Kharitidi[1,2], Pirjo M. Apaja[5], Ariel Roldan[5], Nicole St. Denis[3], Anne-Claude Gingras[3,4], Gergely L. Lukacs[2,5,7]* and Arnim Pause[1,2,7,8]*.

1. Goodman Cancer Research Center, McGill University, Montreal, Quebec, H3A 1A3, Canada.

2. Biochemistry Department, McGill University, Montreal, Quebec, H3G 1Y6, Canada.

3. Lunenfeld-Tanenbaum Research Institute, Sinai Health System, Toronto, Ontario, M5G 1X5, Canada.

4. Department of Molecular Genetics, University of Toronto, Toronto, Ontario, M5S 1A8, Canada.

5. Physiology Department, McGill University, Montreal, Quebec, H3G 1Y6, Canada.

6. These authors contributed equally.

7. Senior author

8. Lead contact

* Correspondence: Arnim.pause@mcgill.ca (A.P) or Gergely.lukacs@mcgill.ca (G.L.L)

Key words: ESCRT, Endofin, HD-PTP, receptor trafficking, lysosomes, EGFR, migration, receptor signaling, ubiquitinated cargo sorting.

2.1. Abstract:

Internalized and ubiquitinated signaling receptors are silenced by their intraluminal budding into multivesicular bodies, aided by the Endosomal Sorting Complexes Required for Transport (ESCRT) machinery. HD-PTP, an ESCRT protein, forms complexes with ESCRT-0, -I and -III proteins, and binds to Endofin, a FYVE-domain protein confined to endosomes with poorly understood roles. Using proximity-biotinylation we show that Endofin forms a complex with ESCRT constituents and Endofin depletion increased integrin α5- and EGF-receptor plasma membrane density and stability by hampering their lysosomal delivery. This coincided with sustained receptor signaling and increased cell migration. Complementation of Endofin- or HD-PTP-depleted cells with wild-type Endofin or HD-PTP, but not with mutants harboring impaired Endofin/HD-PTP association or cytosolic Endofin, restored EGFR lysosomal delivery. Endofin also promoted Hrs indirect interaction with HD-PTP. Jointly, our results indicate that Endofin is required for HD-PTP and ESCRT-0 interdependent sorting of ubiquitinated transmembrane cargoes, ensuring efficient receptor desensitization and lysosomal delivery.

2.2. Introduction:

Receptor signaling is a tightly regulated cellular process. Ligand-activated receptors are endocytosed and internalized to the endosomal compartments where they remain an active signaling hub (Sorkin et al., 2009). At the endosomal surface, transmembrane cargo segregation into different microdomains by different machineries determines cargo fate; sorting towards tubulovesicular recycling or towards lysosomal degradation (Norris et al., 2017). Receptor resensitization takes place when receptors are recycled back to the plasma membrane (PM). Alternatively, signal termination occurs when receptors are targeted for lysosomal degradation. Receptor downregulation is initiated by their sorting and incorporation into intraluminal vesicles (ILVs) to form the multivesicular bodies (MVBs). This process is accomplished by the Endosomal Sorting Complexes Required for Transport (ESCRT) machinery.

The ESCRT machinery is composed of five protein complexes responsible for the formation of an ILV. ESCRT-0, -I and -II proteins are recruited to the endosomal membranes and directly interact with multi-mono- or poly-ubiquitinated receptors. ESCRT-III proteins mediate membrane deformation and scission, whereas the Vps4 complex is responsible for ESCRT-III disassembly and their recycling back to the cytoplasm (Christ et al., 2017, Vietri et al., 2020). The MVBs will then fuse to the lysosomes and their cargo will be degraded or exocytosed. By controlling the fate of numerous receptors, ESCRT proteins are crucial regulators of cell signaling events underlying key cellular processes such as cell migration and proliferation (Kharitidi et al., 2015, Miller et al., 2018, Szymanska et al., 2018, Toyoshima et al., 2007), as well as in the elimination of misfolded or damaged PM proteins (Okiyoneda et al., 2010).

Likewise, clathrin is associated with ESCRTs playing a key role in both cargo concentration and ILV formation (Wenzel et al., 2018, Raiborg et al., 2001, Raiborg et al., 2006).

It is recruited to early endosomes by the ESCRT-0 protein Hrs (Raiborg et al., 2001, Raiborg et al., 2006). Static and live-cell imaging of the prototype epidermal growth factor receptor (EGFR) indicated that the initial steps of ILV formation consist of a wave of ESCRT-0, ESCRT-I, clathrin and HD-PTP recruitment (Wenzel et al., 2018).

The ESCRT protein HD-PTP (*PTPN23*) was shown to affect the degradation of ubiquitinated receptors such as TGFβ/BMP receptors, PDGFRβ, EGFR, integrins, neurotrophin and EphB2 receptors (Ali et al., 2013, Doyotte et al., 2008, Kharitidi et al., 2015, Ma et al., 2015, Miller et al., 2018, Stefani et al., 2011, Budzinska et al., 2020, Lahaie et al., 2019). HD-PTP directly binds to ESCRT-0, -I and -III proteins and contributes to the endosomal sorting of ubiquitinated receptors towards MVBs and lysosomal degradation (Ali et al., 2013, Doyotte et al., 2008, Gahloth et al., 2016, Gahloth et al., 2017c, Ichioka et al., 2007, Kharitidi et al., 2015). During the early phase of ILV formation, recruitment of ESCRT-0, -I and HD-PTP increase until ESCRT-III is recruited, after which they begin dissociating from the endosomal membrane (Wenzel et al., 2018). HD-PTP also acts as a tumor suppressor and its haploinsufficiency was shown to increase cell migration and invasion (Manteghi et al., 2016). Rescue experiments further demonstrated that the N-terminus of HD-PTP, containing the Bro1 and V domain, was sufficient to restore most of the EGFR trafficking defects observed upon HD-PTP depletion (Doyotte et al., 2008). This minimal functional unit of HD-PTP indeed retains the capacity to bind ubiquitinated cargo, as well as several components of the ESCRT machinery such as STAM2 (ESCRT-0) and CHMP4B (ESCRT-III) (Desrochers et al., 2019, Gahloth et al., 2016, Gahloth et al., 2017c, Lee et al., 2016, Pashkova et al., 2013). Interestingly, the same region of HD-PTP, which binds STAM2 and CHMP4B, was also shown to bind Endofin (*ZFYVE16*) (Gahloth et al., 2017c).

Endofin is a large protein composed of a central FYVE domain enabling its proper localization to the membrane of early endosomes, where it can form a complex with receptors such as TGFβR1 (Chen et al., 2007a, Seet et al., 2001b). It also displays a Smad binding domain next to its FYVE domain and was found to impact TGFβ and BMP signaling (Chen et al., 2007a, Goh et al., 2015, Shi et al., 2007). Furthermore, the C-terminus of Endofin directly interacts with Tom1, a protein that binds to clathrin and ubiquitinated receptors (Seet et al., 2004, Yamakami et al., 2003). Endofin was shown to recruit clathrin to early endosomes *via* its direct interaction with Tom1 (Seet et al., 2005). However, the impact and significance of Endofin-mediated clathrin recruitment on ubiquitinated cargo trafficking is still poorly understood.

Endofin binds HD-PTP with higher affinity than STAM2 and CHMP4B (Gahloth et al., 2017a, Gahloth et al., 2017c). The competition between ESCRT proteins for HD-PTP binding was, therefore, proposed to interfere with the capacity of the receptor to engage with ESCRT components and to be efficiently delivered to the lysosomes (Gahloth et al., 2017a, Lee et al., 2016). The direct interaction between Endofin and HD-PTP also suggests a broader role for Endofin in ESCRT-dependent receptor trafficking and signaling, as well as in ubiquitinated membrane cargo sorting in general.

Here, we show that Endofin is required for the ESCRT-dependent lysosomal sorting of integrin α5, EGFR as well as other poly-ubiquitinated transmembrane model cargo. We propose that Endofin is permissive for HD-PTP interaction and colocalization with ESCRT-0 and facilitates clathrin recruitment to early endosomes. Thus, disruption of Endofin binding to HD-PTP is sufficient to severely compromise ESCRT-mediated lysosomal ubiquitinated-cargo sorting. Consequently, Endofin depletion caused sustained receptor signaling and increased cell migration.

Altogether, this study identifies Endofin as a key regulator of ESCRT-dependent receptor trafficking and cell signaling.

2.3. Results:

Endofin forms a complex with ESCRTs and EGF receptor:

Endofin directly binds Tom1 and HD-PTP, which both have direct roles in receptor trafficking (Doyotte et al., 2008, Gahloth et al., 2017a, Katoh et al., 2004, Kharitidi et al., 2015, Seet et al., 2004, Yamakami et al., 2003). Endofin's interactome is likely to reflect its function; however, it remains poorly characterized. To investigate the binding partners of HD-PTP and Endofin in further detail, two proteomic workflows were designed. In the first, we performed proximity-dependent biotin tagging (BioID), in which a biotin ligase (BirA*) fused to the N- or C-terminus of either HD-PTP and Endofin are used as 'baits' to covalently tag nearby proteins ('preys') with biotin, which can then be purified and identified by MS (Lambert et al., 2015). Subsequently, an affinity-purification mass spectrometry (AP-MS) approach was employed, with an inducible expression of Flag-tagged HD-PTP and Endofin as baits. Our findings reveal Endofin as a robust proximity interactor of HD-PTP by BioID and AP-MS (Figure 1A and Figure S1B), and that HD-PTP forms a complex with a variety of ESCRT proteins from different ESCRT complexes (ESCRT-0, -I and -III) (Figure 1A). Likewise, HD-PTP was identified as a proximity interactor of Endofin-BirA* (Figure 1A), and while interactions between Endofin and ESCRT proteins were not detected by BioID (Figure 1A), AP-MS revealed that various ESCRT proteins (HD-PTP, ESCRT-I and -III) complex with Endofin (Figure S1B). Further, our results demonstrate HD-PTP as a robust interactor of clathrin heavy chain 1 (CLTC) and, more broadly, endocytic and trafficking machinery within the cell (Figure S1B). Collectively, these proteomic assays

demonstrate that Endofin and HD-PTP complex with endocytic machinery and ESCRTs (further annotated in Figure S1A). To better understand the role of Endofin in relation to HD-PTP, BioID data were further analyzed using the STRING database, by which networks of interaction were designed and clustered into different cellular processes. In support of our observations, Endofin's network is linked to receptor trafficking, a finding that paralleled that of HD-PTP (Figures S2 and S3) (Doyotte et al., 2008).

To validate that Endofin, HD-PTP and ESCRTs are forming a complex on early endosomes, isopycnic sucrose gradient centrifugation was performed on 293T cell organelles. While Endofin and HD-PTP were absent in cellular fractions containing LAMP1 and Tom20, the lysosome and mitochondria markers, respectively (Figure S1C), they were present together within cellular fractions containing ESCRT proteins (Hrs, Tsg101 and UBAP1). Tom1 and the early endosomal marker EEA1 were also present in these fractions. In addition, subcellular fractionation followed by size-exclusion chromatography (HPLC) showed Endofin, HD-PTP and ESCRT-0 components (Hrs and STAM2) as part of large protein complexes ranging from 525 to 927 kDa, however the ESCRT-I component Tsg101 was found mostly within complexes of lower molecular weight (Figure S1D). As a further validation of complex formation with ESCRT proteins, co-immunoprecipitation was performed on transiently expressed myc-Endofin. Indeed, Endofin showed to form a complex with HD-PTP, ESCRT-0 (Hrs and STAM2) and ESCRT-I (Tsg101 and UBAP1) (Figure 1B), where STAM2, Tsg101 and UBAP1 directly interact with HD-PTP (Ali et al., 2013, Gahloth et al., 2016, Ichioka et al., 2007). This data further supports that Endofin is part of a complex containing HD-PTP and ESCRTs on early endosomes.

Finally, we probed whether EGFR activation elicits Endofin recruitment using MiniTurbo BioID, which allows for shortened labelling time as compared to the BirA* enzyme. Results

showed that, upon EGF stimulation, Endofin and HD-PTP are rapidly recruited to EGFR, along with common endocytic machineries (Figure 1C). Altogether, this data demonstrates that Endofin forms a complex with HD-PTP, ESCRTs and EGFR, suggesting that Endofin might have a role in regulating receptor trafficking.

Endofin regulates plasma membrane density, stability and lysosomal degradation of integrin α5 and EGFR:

HD-PTP is known to have a direct role in regulating EGFR, integrin α5 and PDGFRβ endo-lysosomal membrane trafficking (Belle et al., 2015, Doyotte et al., 2008, Kharitidi et al., 2015). Since Endofin directly interacts with HD-PTP and forms a complex with different ESCRTs (Gahloth et al., 2017c) and EGFR, we thought to investigate the role of Endofin in receptor trafficking. We used HD-PTP-depleted HeLa cells as a positive control to disrupt receptor trafficking (Figure S4A). HeLa cells were Endofin-depleted by shRNA and infected with a non-target shRNA (NT) as a negative control for depletion (Figure S4A). Western blotting of total cell lysates from Endofin- and HD-PTP-depleted cells revealed at least 2.5-fold increase in cellular expression levels of integrin α5 (Figure S4B), and ~ 1.2 – 1.6-fold increase in EGFR levels (Figure S4C).

Several studies have demonstrated that ligand-activation, ubiquitination and internalization of both integrin α5 and EGFR facilitate their sorting towards lysosomal degradation (Alwan et al., 2003, Kharitidi et al., 2015, Lobert et al., 2010). Next, we assessed the effect of Endofin depletion on integrin α5 and EGFR lysosomal degradation kinetics in comparison to HD-PTP depletion. Serum-starved cells were stimulated with fibronectin (3 and 6 h) or EGF (2 and 4 h) in the presence of cycloheximide (CHX) to inhibit protein synthesis. To inhibit lysosomal degradation, cells were

pretreated with Bafilomycin A1 (1 h) in the presence of CHX. Western blots revealed that upon Endofin and HD-PTP depletion, lysosomal degradation of integrin α5 and EGFR was delayed by >60% and ~ 40% after 6 and 2 h chase, respectively (Figure 2A), suggesting that Endofin plays a role in integrin α5 and EGFR lysosomal degradation.

Considering the crosstalk between ESCRT and ubiquitinated transmembrane proteins, which are preferentially targeted towards lysosomal degradation over recycling back to the PM, we asked whether Endofin depletion can delay the PM turnover of activated receptors. Cell surface stability of activated integrin α5 and EGFR were measured by cell surface-ELISA (cs-ELISA) upon fibronectin (4 h) and EGF (20 min) stimulation, respectively. Compared to NT cells, ~ 20% of integrin α5 was stabilized at the PM resembling the effect of an integrin α5β1 blocking antibody, which interferes with the activation and internalization of the receptor (Figure 2B). Similarly, ~ 20% of EGFR was stabilized at the PM upon Endofin depletion. A comparable effect was shown for Gefitinib, an EGFR inhibitor that blocks receptor activation, ubiquitination and internalization (Figure 2B). Notably, Endofin and HD-PTP depletion had no effect on the internalization rate of EGFR upon EGF stimulation (5 min) (Figure S4D). Moreover, using cs-ELISA we measured steady state PM receptor density upon Endofin and HD-PTP depletion. Integrin α5 and EGFR cell surface densities increased by at least 1.5-fold compared to NT cells (Figure 2C). Thus, Endofin depletion likely delays the lysosomal degradation of both integrin α5 and EGFR and increases their PM density and stability by facilitating recycling at the early endosome level.

Endofin is required for the efficient lysosomal delivery of integrin α5 and EGFR:

If the lysosomal degradation of integrin α5 and EGFR is delayed upon Endofin depletion, it is plausible that Endofin has a role in ESCRT-dependent receptor sorting from early endosomes

towards MVBs and lysosomes. Hence, to better understand the role of Endofin in the endo-lysosomal transfer kinetics, receptor delivery to lysosomes was determined by monitoring the pH of receptor-containing vesicles (pH_v) by fluorescent ratiometric image analysis (FRIA) (Figure 2D) (Barriere et al., 2008). HD-PTP- and Hrs-depleted HeLa cells (Figure S4A) were used as positive controls for the disruption of receptor trafficking (Kharitidi et al., 2015, Wenzel et al., 2018). First, serum-starved cells were labelled on ice with anti-EGFR or anti-integrin α5 followed by $F(ab')_2$ secondary antibody coupled to the pH-sensitive fluorescein isothiocyanate (FITC). Next, to induce synchronized receptor internalization, cells were stimulated with EGF (30- and 60-min chase, 37^{o}C) or with fibronectin (4 h chase, 37^{o}C) and pH_v was measured by FRIA. As expected, EGFR trafficking was delayed after 30- and 60-min chase in HD-PTP- and Hrs-depleted cells ($pH_v \sim 5.7 \pm 0.09$ and $pH_v \sim 5.7 \pm 0.1$, respectively) compared to NT cells ($pH_v \sim 5.2 \pm 0.07$) (Figure 2D and Figure S4E). Strikingly, after 30 min EGFR chase in Endofin-depleted cells, the receptor is confined to early endosomes ($pH_v \sim 6 \pm 0.17$), however in NT cells EGFR is delivered to late endosomes ($pH_v \sim 5.4 \pm 0.07$) (Figure 2D and Figure S4E). In addition, after 60 min chase, EGFR is delivered to late endosomes in Endofin-depleted cells ($pH_v \sim 5.4 \pm 0.23$), whereas in NT cells EGFR is delivered to lysosomes ($pH_v \sim 4.5 \pm 0.1$) (Figure 2D and Figure S4E). Endofin depletion also inhibited the egress of integrin α5 from early endosomes ($pH_v \sim 6.4 \pm 0.1$), while in control NT cells the receptor was delivered to late endosomes ($pH_v \sim 5.7 \pm 0.1$) (Figure 2D). The FRIA results clearly demonstrate that Endofin has a crucial role in the transport of receptors from early endosomes towards MVBs and lysosomes. This is exemplified by the identical effects of HD-PTP and Hrs depletion on EGFR trafficking.

Endofin is required for the efficient lysosomal delivery of poly-ubiquitinated model cargo:

The recognition of ubiquitinated receptors by ESCRTs is a key step in the sorting process of internalized receptors towards MVBs and lysosomes. To examine whether Endofin also contributes to the endo-lysosomal sorting of ubiquitinated cargoes incapable of receptor signaling, we used the established CD4-Ub chimera which undergoes constitutive poly-ubiquitination. For this, two different model receptors were used: truncated CD4 (CD4Tl), in which the cytoplasmic tail was deleted and replaced with a linker, thus lacking a ubiquitin acceptor site and sorting signal (Barriere et al., 2006). In addition, we used CD4Tl-Ub, a chimera where the linker has been fused to a ubiquitin (Ub) moiety. The fusion of a single Ub moiety to the linker is sufficient to induce constitutive poly-ubiquitination of the CD4Tl-Ub, which in turn accelerates its ESCRT-dependent lysosomal delivery (Apaja et al., 2010, Barriere et al., 2007).

Endofin- and HD-PTP-depleted cells were transiently transfected with CD4Tl and CD4Tl-Ub constructs to assess their degradation kinetics by CHX chase (2 h). Western blotting demonstrated that the lysosomal degradation of ~ 40% CD4Tl-Ub was delayed upon Endofin and HD-PTP depletion compared to NT cells (Figure 2E). As expected, Endofin and HD-PTP depletion had no significant effect on the levels of CD4Tl (Figure 2E). Furthermore, FRIA showed that Endofin depletion confined CD4Tl-Ub to recycling endosomes (pH_v ~ 6.4 ± 0.07) compared to NT cells where it is delivered to lysosomes (pH_v ~ 4.8 ± 0.07) after 2 h chase (Figure 2F). Hence, Endofin is required for the efficient lysosomal degradation of poly-ubiquitinated cargoes, even in the absence of second messenger signaling activity. To assess whether Endofin-dependent endo-lysosomal sorting has a preference towards specific ubiquitinated cargo, lysosomal delivery of the tetrameric mono-ubiquitinated cargo (CD4TCC-UbAllRΔG) was also determined by FRIA upon Endofin depletion. In CD4TCC-UbAllRΔG, a tetramerization signal was inserted before the Ub moiety and all seven Lys residues of the Ub moiety were replaced with Arg and the carboxy-

terminal Gly residues were deleted (Barriere et al., 2006). Consistent with the effect of HD-PTP depletion on CD4TCC-UbAllRΔG trafficking (Kharitidi et al., 2015), Endofin depletion did not affect the trafficking of the tetrameric mono-ubiquitinated cargo (Figure 2G), even though it was previously shown that the tetrameric mono-ubiquitin can serve as an efficient endocytic signal (Barriere et al., 2006). This data show that Endofin does not only play a role in EGFR and integrin α5 trafficking, but it regulates the specific sorting of poly-ubiquitinated cargo towards lysosomal degradation.

Endofin depletion decreases clathrin recruitment to early endosomes:

Endofin recruits clathrin *via* Tom1 to early endosomes (Seet et al., 2005), and Tom1 directly interacts with Endofin and with clathrin heavy chain (Seet et al., 2005, Seet et al., 2004) (Figure S5C). Our data demonstrates that clathrin colocalization with EGFR reached a peak (~ 0.65 ± 0.09) after 15 min EGFR chase (Figure S5A and B). To better understand why receptor trafficking is delayed upon Endofin depletion, we first assessed the effect of Endofin depletion on clathrin recruitment to early endosomes by immunofluorescence. Endofin-depleted HeLa cells were transiently transfected with Rab5Q79L, a GTPase deficient mutant, to induce the formation of enlarged endosomes (Raiborg et al., 2001, Wegener et al., 2010). Upon Endofin depletion, clathrin recruitment decreased by 33% ± 3% compared to NT cells (Figure S5D and E). In addition, we assessed Tom1 interaction with clathrin heavy chain in Endofin-depleted cells, and co-IP showed that clathrin interaction with Tom1 decreased upon Endofin depletion (Figure S5F). Since clathrin is indispensable for receptor clustering on the endosomal surface and their accumulation in ILVs during MVB biogenesis (Wenzel et al., 2018), this might contribute to the delay in EGFR lysosomal delivery. To mimic the recruitment of Tom1 protein to early endosomes *via* Endofin,

as previously described by Seet *et. al* we used a 2xFYVE-Tom1 chimera construct able to restore Tom1/clathrin interaction in Endofin-depleted cells (Seet et al., 2005). Of note, 2xFYVE-Tom1 chimera in Endofin-depleted cells lacks the ability to form a complex with Endofin binding partners once it is expressed, including HD-PTP. Our results showed that the complementation of Endofin-depleted HeLa cells with 2xFYVE-Tom1 chimera failed to restore EGFR lysosomal delivery (Figure S5G). Hence, although Endofin depletion reduced clathrin interaction with Tom1 and decreased clathrin recruitment to early endosomes, the delay in EGFR lysosomal delivery upon Endofin depletion is not directly linked to the loss of interaction between Endofin and Tom1 or to the role of Tom1 in receptor trafficking.

Endofin expression enhances HD-PTP colocalization with EGFR, Hrs and CHMP4B:

HD-PTP directly interacts with ESCRT-0, -I and -III proteins facilitating EGFR sorting towards MVBs and lysosomal degradation (Doyotte et al., 2008, Kharitidi et al., 2015). Endofin binds to the Bro1 domain of HD-PTP sharing the same binding site with STAM2 (ESCRT-0) and CHMP4B (ESCRT-III), however Endofin binds HD-PTP with a higher affinity than STAM2 and CHMP4B (Gahloth et al., 2017c). In addition, STAM2 also binds to a motif in the proline rich region of HD-PTP, which serves as a second site for STAM2 interaction (Ali et al., 2013). To investigate whether Endofin could regulate HD-PTP complex formation with ESCRTs, endogenous HD-PTP was immunoprecipitated in Endofin-depleted cells and the co-IP efficiency of the ESCRT-0 protein Hrs was assessed. The indirect interaction of HD-PTP with Hrs was reduced by ~ 80% upon Endofin depletion (Figure 3A).

Since HD-PTP interaction with ESCRT-0 and -III on early endosomes is essential for the sorting of activated EGFR towards MVBs and lysosomes (Ali et al., 2013) (Doyotte et al., 2008)

(Wenzel et al., 2018), we assessed in Endofin-depleted cells the colocalization of EGFR, red fluorescence protein-tagged Hrs (RFP-Hrs) and mCherry-tagged CHMP4B (mCherry-CHMP4B) with HD-PTP by pulse-chase experiments. EGFR colocalization with HD-PTP showed a significant decrease upon Endofin depletion (0.4 ± 0.03), after 5min EGF stimulation and 10 min EGFR chase, compared to NT cells (0.54 ± 0.03) (Figure 3B). Consistent with the co-IP result, Hrs colocalization with HD-PTP, after 5min EGF stimulation and 0 min EGFR chase, was significantly reduced upon Endofin depletion (0.44 ± 0.01) compared to NT cells (0.71 ± 0.03) (Figure 3C). Moreover, CHMP4B colocalization with HD-PTP also decreased upon Endofin depletion (0.44 ± 0.06) compared to NT cells (0.62 ± 0.05), after 5min EGF stimulation and 20min EGFR chase (Figure 3D). Therefore, this data suggests that EGFR, ESCRT-0 (Hrs) and ESCRT-III (CHMP4B) colocalizations and/or complex formation with HD-PTP are promoted by Endofin, which facilitates EGFR sorting towards MVBs and lysosomal degradation *via* ESCRT-dependent mechanisms.

Next, the colocalization of EGFR and RFP-Hrs with Endofin was also assessed in HD-PTP-depleted cells by pulse-chase experiments. We found that the colocalizations of EGFR and Hrs with Endofin are stabilized upon HD-PTP depletion after 5 min EGF stimulation and until 20 min EGFR chase. However, EGFR and Hrs showed dynamic colocalizations with Endofin in NT cells (Figure S6A and B). This infers that the dynamic colocalizations of EGFR and Hrs with Endofin are regulated by HD-PTP. This dynamic colocalization might reflect the egress of cargoes from early endosomes towards MVBs and lysosomes, which is indeed regulated by HD-PTP (Doyotte et al., 2008). On the other hand, the stabilized colocalizations of EGFR and Hrs with Endofin, upon HD-PTP depletion, might reflect the delay in cargo sorting from early endosomes towards MVBs and lysosomes.

Endofin/HD-PTP interaction is permissive for an efficient lysosomal delivery of activated EGFR:

Endofin directly binds and recruits HD-PTP to early endosomes (Gahloth et al., 2017c). The double L202D/I206D-HD-PTP mutation, which abrogates CHMP4B and Endofin binding to HD-PTP, prevented L202D/I206D-HD-PTP recruitment to early endosomes even upon its co-expression with myc-Endofin (Gahloth et al., 2017c). Our data showed that EGFR and ESCRT-0 colocalizations with HD-PTP are stabilized by Endofin. To assess the functional aspect of Endofin/HD-PTP interaction in regulating cargo sorting towards MVBs and lysosomes, we generated shRNA resistant wild-type (WT) and mutant Endofin constructs.

Transient overexpression of the FYVE-domain C753S-Endofin mutant displayed an impaired localization to early endosomes, a finding we reciprocated here (Figure S6C) (Seet et al., 2001a). To weaken Endofin's interaction with the Bro1 domain of HD-PTP (Gahloth et al., 2017a), we employed the L15P-Endofin mutant.

To investigate the effect of Endofin complementation on EGFR endo-lysosomal trafficking, pH_v of EGFR-containing vesicles was monitored by FRIA. Endofin-depleted HeLa cells were transiently transfected with WT- or mutated-Endofin (Figure S6D), and the mean pH_v was assessed after 30 min of EGF stimulation. WT-Endofin complementation restored EGFR lysosomal delivery (mean $pH_v \sim 5.1 \pm 0.03$) compared to mock transfected Endofin-depleted cells (mean $pH_v \sim 5.9 \pm 0.09$) and NT cells (mean $pH_v \sim 5.3 \pm 0.04$) (Figure 4A). L15P-Endofin complementation partially restored EGFR lysosomal delivery (mean $pH_v \sim 5.5 \pm 0.02$) compared to WT-Endofin (Figure 4A), in line with the partially disrupted biochemical interaction of L15P-

Endofin with HD-PTP (Figure S6E). Conversely, C753S-Endofin complementation completely failed to rescue EGFR lysosomal delivery (mean $pH_v \sim 5.9 \pm 0.05$) (Figure 4A), by profoundly reducing Endofin recruitment to early endosomes.

Importantly, complementing HD-PTP-depleted HeLa cells with WT-HD-PTP (Figure S6D) restored EGFR lysosomal delivery (mean $pH_v \sim 5.4 \pm 0.15$) (Figure 4B). T145K-HD-PTP, which partially disrupted HD-PTP/Endofin interaction (Figure S6F) (Gahloth et al., 2017b), failed to rescue EGFR lysosomal delivery (mean $pH_v \sim 5.9 \pm 0.05$) compared to mock transfected HD-PTP-depleted (mean $pH_v \sim 6.1 \pm 0.08$) and NT (mean $pH_v \sim 5.4 \pm 0.09$) cells (Figure 4B).

To better understand the mechanism by which Endofin's FYVE domain influences HD-PTP's recruitment to early endosomes, we extended our BioID investigation to C753S-Endofin N-terminally BirA* tagged baits. Consistent with our findings, disruption of the FYVE domain did not reduce Endofin's interaction with HD-PTP but did disrupt its proximity interaction with ubiquitin as well as several early endosome components, providing insight into a potential mechanism by which Endofin supports HD-PTP's recruitment to ubiquitinated cargoes on endocytic vesicles (Figure 4C). These results strongly suggest that both Endofin localization on early endosomes *via* its FYVE domain and its interaction with HD-PTP are necessary for an efficient endo-lysosomal transfer of activated EGFR.

Endofin depletion sustains integrin α5 and EGFR downstream signaling:

We previously showed that the heterozygous loss of *PTPN23* is frequent in several types of human cancers (Manteghi et al., 2016). Using the cBioPortal database, we show here that the heterozygous loss of *ZFYVE16* (Endofin gene) is also frequent in several types of human cancers

(Figure 5A). In addition, the PRECOG database, which measures associations between mRNA expression profiles and cancer prognosis by calculating a Z-score, revealed a negative Z-score of *ZFYVE16* mRNA in several types of human cancers (Figure 5B).

Cell surface receptors are competent of signaling from early endosomes or MVBs before the formation of ILVs (Mamińska et al., 2016, Rodahl et al., 2009, Wegner et al., 2011). Furthermore, HD-PTP depletion was shown to delay integrin α5 lysosomal delivery, thereby increasing its downstream signaling (Kharitidi et al., 2015). To investigate whether Endofin could also influence integrin α5 signaling, Endofin- and HD-PTP-depleted HeLa cells were stimulated with fibronectin (7 h) to assess levels of phosphorylated FAK, Src and Erk1/2 by Western blotting. In agreement with our previous study, HD-PTP depletion in serum-starved cells increased the levels of pFAK, pSrc and pErk1/2 compared to NT cells, both at steady-state and upon fibronectin stimulation (Figure 5C). Remarkably, the same effect was observed upon Endofin depletion (Figure 5C). This result clearly demonstrates that, in addition to receptor stabilization, Endofin depletion further increased integrin α5 signaling.

Next, the effect of Endofin and HD-PTP depletion on EGFR activation and the kinetics of its downstream signaling were evaluated. Interestingly, Endofin and HD-PTP depletion had no significant impact on steady-state EGFR phosphorylation and the activation of its downstream kinase MEK (Figure 5D). However, EGFR and MEK activation were both sustained after 30 min of EGF stimulation upon Endofin and HD-PTP depletion. The levels of pEGFR also remained higher in these cells, even after 60 min EGF stimulation (Figure 5D). Altogether, these results indicate that Endofin and HD-PTP do not only regulate EGFR and integrin α5 plasma membrane stability, but also control receptor activation and its downstream signaling.

Endofin depletion increases cell migration:

Integrin α5β1's central role in cell migration and its ESCRT-dependent lysosomal desensitization are well-established (Kharitidi et al., 2015, Lobert et al., 2010). Migration rate of Endofin-depleted HeLa cells was measured by real time cell analysis (RTCA), using fetal bovine serum as a chemoattractant. Endofin depletion revealed the same effect on cell migration rate as HD-PTP depletion with ~ 2-fold increase compared to NT cells. Migration of Endofin-depleted cells was suppressed by integrin α5β1 blocking antibody (Figure 5E). This shows that the increase in cell migration upon Endofin depletion is linked to the increase of PM and total integrin α5 levels (Figure 2C and Figure S4B).

Since Endofin/HD-PTP interaction is permissive for an efficient lysosomal delivery of activated EGFR (Figure 4B and C), we next addressed whether simultaneous depletion of Endofin and HD-PTP could further impair receptor trafficking. Thus, we compared total EGFR and integrin α5 levels between NT and Endofin-depleted cells, transiently transfected either with a non-targeting shRNA or an shRNA targeting HD-PTP. We found that depleting Endofin or HD-PTP increased total EGFR levels by ~ 2-fold and ~ 1.5-fold, respectively, whereas EGFR levels in double knock-down cells increased by ~ 2.7-fold in comparison to NT cells (Figure 5F). Interestingly, the impact was even more pronounced for integrin α5. Indeed, the individual depletion of Endofin or HD-PTP increased integrin α5 levels by ~ 3.4-fold and ~ 2.7-fold, respectively, whereas double knocked-down cells exhibited ~ 7.7-fold increase in comparison to NT cells (Figure 5F). To address the functional relevance of these findings, we also performed migration assays using fetal bovine serum as a chemoattractant. Results showed that the migration rate increased in double knock-down cells by ~ 1.5-fold in comparison to Endofin-depleted cells (Figure 5G). Altogether, these results indicate that the simultaneous depletion of Endofin and HD-

PTP has an additive effect on total receptor levels, which in turn increase their migration rate in comparison to Endofin-depleted cells.

In certain types of human cancers, integrin α5 and EGFR are well-known drivers of tumorigenesis. Here, we show that Endofin depletion increased integrin α5 and EGFR signaling and cell migration, which are two hallmarks of cancer progression. Hence, loss of Endofin expression delays receptor lysosomal degradation and increases receptor signaling and cell migration, which could ultimately contribute to tumorigenesis and cancer progression.

2.4. Discussion:

Here we unraveled the role of Endofin in promoting HD-PTP complex formation with ESCRT-0 on early endosomes to secure efficient ESCRT-dependent lysosomal degradation of internalized and ubiquitinated cell surface receptors and other transmembrane cargoes, a process which also desensitizes activated receptors (Wegner et al., 2011), controls cell migration (Kharitidi et al., 2015, Lobert et al., 2010, Lobert et al., 2012) and PM proteostasis (Apaja et al., 2014). Our findings can be summarized as follows: i) Endofin forms complexes with ESCRT and HD-PTP proteins, as well as EGFR on early endosomes. ii) The FYVE domain-dependent endosomal tether of Endofin and HD-PTP is required for the activated EGFR efficient lysosomal delivery, which is compromised by cytosolic relocation of Endofin or preventing its association with HD-PTP. iii) Endofin is also critical for poly-ubiquitinated but not multi-mono-ubiquitinated lysosomal delivery of model transmembrane cargoes which lack signaling capacity. iv) Endofin depletion, similar to HD-PTP haploinsufficiency, sustained EGF and integrin α5 receptor signaling and increased cell migration.

Segregation of internalized transmembrane cargoes into different microdomains on early endosomes is directed by specific sorting motifs towards the tubulovesicular recycling route, retrograde traffic to the Golgi complex or towards MVB/lysosomal degradation (Norris et al., 2017). Upon ligand stimulation, EGFR undergoes both K63 poly-ubiquitination and multi-mono-ubiquitination (Huang et al., 2006), while integrin α5β1 is poly-ubiquitinated (Kharitidi et al., 2015, Lobert et al., 2010), serving as both internalization and endo-lysosomal sorting signals (Piper et al., 2014). Ubiquitinated cargoes are recognized cooperatively by multiple low-affinity ubiquitin-binding domains of ESCRT-0 and -I proteins, including Hrs, STAM2, UBAP1 and Tsg101, which are concentrated at the double-layer clathrin coat (Agromayor et al., 2012, Bache et al., 2003, Raiborg et al., 2002, Sundquist et al., 2004). In addition, Tom1 and HD-PTP, binding partners of Endofin, can recognize the poly- and mono-ubiquitinated moieties *via* their GAT+VHS- and V-domain, respectively, fostering cargo concentration on the limiting membrane of early endosomes (Akutsu et al., 2005, Pashkova et al., 2013, Wang et al., 2010).

While the lysosomal sorting of activated receptors and MVB biogenesis require the dynamic interaction of HD-PTP with STAM2, Tsg101, UBAP1, and CHMP4B (Ali et al., 2013, Gahloth et al., 2016, Gahloth et al., 2017c, Ichioka et al., 2007), the functional significance of Endofin remained enigmatic in this process (Gahloth et al., 2017c, Seet et al., 2001b). As Endofin complex formation with Tom1 recruits clathrin and binds both directly and *via* Tollip to ubiquitin on early endosomes (Katoh et al., 2004, Seet et al., 2005, Seet et al., 2004), we assumed that Endofin may participate in endosomal sorting of ubiquitinated cargoes. This possibility was also supported by the role of Endofin in TGFβ/BMP signaling (Chen et al., 2007a, Shi et al., 2007), as well as Endofin complex formation with ESCRT-I (UBAP1, TSG101, Vps37A, Vps28) (Figure S1B). The functionality of the Endofin interaction networks was revealed by Endofin ablation that

stabilized the PM/endosomal pool of EGF and integrin α5 receptors (Figure 2), phenocopying the consequences of HD-PTP, Hrs or Tsg101 depletion (Ali et al., 2013, Bache et al., 2006, Doyotte et al., 2008, Kharitidi et al., 2015, Lu et al., 2003, Ma et al., 2015, Parkinson et al., 2015, Wenzel et al., 2018). Although EGFR internalization remained unaltered by Endofin depletion, it induced receptor accumulation in early endosomes and at the PM, presumably by fostering its recycling. Accelerated recycling of internalized integrin α5β1 was also observed upon HD-PTP depletion (Kharitidi et al., 2015).

Clathrin is known to be recruited to early endosomes *via* two different clathrin-binding proteins: Hrs and Tom1 (Raiborg et al., 2001, Seet et al., 2005). Dynamic assembly and disassembly of clathrin on early endosomes is essential for cargo and ESCRT-0 clustering into microdomains and subsequent ILV formation (Raiborg et al., 2001, Sachse et al., 2002, Wegner et al., 2011, Wenzel et al., 2018). A significant contribution of Endofin *via* Tom1 in the double-layer clathrin formation (Seet et al., 2005), however, could be excluded, as the 2xFYVE-Tom1 chimera failed to rescue EGFR lysosomal delivery in Endofin-depleted cells. We favor the model that Endofin binding to HD-PTP (Gahloth et al., 2017c) may also facilitate EGFR transfer from ESCRT-0 (Hrs and STAM2) to ESCRT-I and -III, as a prelude towards MVB/lysosomal delivery (Ali et al., 2013). In support, the yeast HD-PTP homolog Bro1 also binds to clathrin (Pashkova et al., 2013), consistent with our observation that HD-PTP top hit interactor was clathrin by AP-MS (Figure S1B). Thus Endofin/HD-PTP interaction on early endosomes might be a key event for sorting EGFR towards lysosomal degradation, which was demonstrated by our complementation with Endofin and HD-PTP variants, where the deletion of Endofin FYVE-domain also suppressed the recruitment of HD-PTP to early endosomes. In line, expression of the L202D/I206D-HD-PTP

variant, lacking both Endofin and CHMP4B bindings, prevented HD-PTP recruitment to early endosomes even upon its co-expression with myc-Endofin (Gahloth et al., 2017b).

Considering that ligand-stimulated poly-ubiquitination serves as a critical recognition signal for integrin α5 and EGFR engagement with the ESCRT machinery (Eden et al., 2012, Kharitidi et al., 2015, Lobert et al., 2010), we propose that dynamic Endofin-ESCRT association is a prerequisite for routing a panel of ubiquitinated cargo molecules from early endosomes towards MVB/lysosomes independently of the receptors downstream signaling. This inference is supported by Endofin-dependent lysosomal delivery of the poly-ubiquitinated (CD4Tl-Ub) model cargo, but not tetrameric mono-ubiquitinated (CD4TCC-UbAllRΔG) (Figure 2F and G), mono-ubiquitinated (CD4Tl-UbRΔG) or the CD4Tl model cargo, which lacks a ubiquitin acceptor site (Barriere et al., 2007, Barriere et al., 2006). These results also raise the possibility that the ESCRT machinery-driven ubiquitin-chain selectivity may be influenced by the ESCRT complex composition, including Endofin. This corollary is in line with Endofin-dependent regulation of TGFβ/BMP receptor that undergoes ligand-induced K63 poly-ubiquitination (Chen et al., 2007a, Iyengar, 2017). Thus, downregulation of Endofin in cancer cells may differentially alter the cell surface receptor proteome and signaling, pending on their ubiquitin-chain modification, which in turn could perturb downstream signaling cascades and transcriptional pathways.

The endosomal signaling of internalized receptors is terminated upon receptor budding into ILVs during MVB biogenesis (Platta et al., 2011, Wegner et al., 2011). Integrin α5β1 and EGFR uncontrolled signaling plays a major role in cell migration and cancer metastasis (Mierke et al., 2011, Yamaguchi et al., 2005). Sustained signaling of both integrin α5 and EGFR upon Endofin depletion, could be linked to the accumulation of EGFR at early endosomes and their delayed MVB/lysosome sorting (Figure 2D). Moreover, the blockage of integrin α5β1 activation and

coupled ubiquitination (Kharitidi et al., 2015) demonstrate that elevated PM level of integrin α5 is, at least partly, responsible for accelerated cell migration (Figure 5E). Augmented PM expression and downstream signaling of integrin α5 were also associated with accelerated cell migration upon HD-PTP depletion (Kharitidi et al., 2015), consistent with the importance of Endofin/HD-PTP interaction in regulating ESCRT-dependent receptor trafficking, receptor signaling and cell migration.

It has been shown that Hrs and STAM2, similar to Endofin, undergo phosphorylation upon EGF stimulation (Chen et al., 2007b, Pandey et al., 2000, Row et al., 2005). The sorting of internalized receptors triggers Hrs phosphorylation, promoting its dislocation from early endosomes (Urbé et al., 2000). Based on published data and our findings, we propose the following working model for Endofin role in the endo-lysosomal trafficking of ligand-activated and ubiquitinated cell surface receptors. Endofin, *via* its FYVE-dependent endosomal localization and binding to HD-PTP, facilitates HD-PTP recognition of ubiquitinated endosomal cargo in complex with STAM2 and Hrs (ESCRT-0), clathrin recruitment, and cargo clustering at endosomal microdomains. Subsequent dissociation of Endofin from HD-PTP (and STAM2) enables CHIMP4B/HD-PTP association by a presently poorly understood mechanism. We speculate that this process may be facilitated by the post-translational modification(s) favoring the dissociation of Endofin/HD-PTP, similar to that observed for the phosphorylation-induced Hrs dissociation from endosomes (Urbé et al., 2000). Furthermore, cargo loading and assembly of ESCRT-0/-I with HD-PTP may induce allosterically Endofin dissociation from the complex. Testing and refining this model will be accomplished by monitoring the kinetics of recruitment of fluorescent-tagged HD-PTP in relation to other ESCRTs in the presence of Endofin variants during cargo sorting by live-cell imaging and related to that described for concerted ESCRT and clathrin recruitment

waves to early endosomes by Wenzel *et al.* (Wenzel et al., 2018). Furthermore, SARA protein, Endofin's homologue, also directly binds to HD-PTP and its recruitment to early endosomes (Gahloth et al., 2017c) might serve as a compensatory mechanism in an Endofin-depleted context. In summary, we propose that Endofin is required for HD-PTP mediated cargo transfer from ESCRT-0/-I to ESCRT-III on early endosomes, a critical step in lysosomal delivery of poly-ubiquitinated cargoes (Figure 6).

Disruption of Endofin/HD-PTP interaction (e.g., by Endofin mutants or *PTPN23* haploinsufficiency) leads to sustained EGF and integrin α5 receptor signaling (Figure 5) (Kharitidi et al., 2015, Manteghi et al., 2016), including downstream transcriptional activation known to promote tumorigenesis and cancer progression (Hou et al., 2020, Sigismund et al., 2018). The heterozygous loss of *ZFYVE16* and downregulation of Endofin transcript in several types of human cancers (Figure 5) suggest that Endofin may exert a tumor suppressor activity, which requires further investigations.

2.5. Materials and Methods:

Constructs, reagents and cell culture:

Myc-tagged Endofin was a kind gift from Dr. H. Wang (Seet and Hong, 2001). pcDNA3-Flag-Endofin was generated by PCR amplification using myc-Endofin as a template and subcloning into the pcDNA3-Flag vector. pcDNA3-Flag-Endofin resistant to shRNA54 was generated by mutagenesis to introduce silent point mutations in the region targeted by the shRNA. This construct was used to create the C753S and L15P Endofin mutants obtained from BioBasic. Flag-tagged HD-PTP in pcDNA3.1 was described previously by Gingras *et al.* (Gingras et al.,

2009). pcDNA3-Flag-HD-PTP resistant to shRNA47 was generated by mutagenesis to introduce silent mutations in the shRNA targeted region. This construct was further mutated to obtain the T145K HD-PTP mutant (BioBasic). The FYVE-Tom1 chimera was generated in the pcDNA3-Flag vector by subcloning a tandem repeat of the coding region for Endofin FYVE domain followed by a linker and the coding sequence for Tom1 (Biomatik). pcDNA3-CD4 c-tail was replaced by a linker followed by either WT Ub (CD4Tl-Ub) or CC tetramerization domain with mutant Ub (all K to R and deletion of 76GG (CD4TCC-UbAllRΔG) as described by Barriere *et al.* (Barriere et al., 2006). pCS2-RFP-Hrs was a gift from Dr. E.M. De Robertis (Addgene plasmid #29685). pLNCX2-mCherry-CHMP4B was a gift from Dr. S. Simon (Addgene plasmid #116923). Complete list of primers is included in Table S1.

HeLa (ATCC® CCL-2™) and 293T (ATCC® CRL-3216™) cells were cultured in DMEM, 10% FBS (Wisent). MISSION® shRNA Lentiviral plasmids pLKO.1-puro for human Endofin (clone ID: NM_014733.2-4263s1c1 (sh54), NM_014733.3-3858s21c1 (sh75)), human HD-PTP (clone ID: NM_015466.x-571s1c1 (sh47), NM_015466.x-887s1c1 (sh51)), human Hrs (clone ID: NM_004712.3-494s1c1 (sh98)) and empty vector (MISSION® pLKO.1-puro Empty Vector Control Plasmid DNA, SHC001) were purchased from Sigma.

The complete list of antibodies used in this study are included in key resources table. Complementation experiments were performed *via* transient transfection using Lipofectamine 2000 (Invitrogen) according to manufacturer's instructions. Complete list of reagents used in this study are included in key resources table.

AP-MS cloning, stable cell line generation and sample collection:

The ORFs were transferred via Gateway cloning into N-terminal 3XFLAG mammalian expression vector for isogenic stable cell line generation and tetracycline-inducible expression. Flip-In T-REx 293T cells were transfected in a 6 well format with 0.2µg of tagged DNA (pcDNA5-FLAG-protein) and 2µg pOG44 (OpenFreezer V4134), using lipofectamine 2000 (Invitrogen), according to manufacturer's instructions. On day 2, cells were trypsinized, and passaged into 10 cm plates. On day 3, the medium is replaced by DMEM 10% Fetal bovine serum, 100 units/ml pen/strep, 200 ug/ml hygromycin. Medium was replaced every 2- 4 days until non-transfected cells die, and isolated clones were ~1-2 mm in diameter (13-15 days). Pools of cells were generated by trypsinization of the entire plate and replating in fresh selection medium (the size of the plate was dictated by the number and size of initial colonies). Cells at ~ 60-70% confluence were induced with 1 µg/ml tetracycline for 24 hours. Subconfluent cells (~85-95% confluent) were harvested for AP-MS analysis.

BioID cloning, stable cell line generation and sample collection:

Constructs for Endofin and HD-PTP were cloned into 5′ BirA* pcDNA5-FRT-TO or pcDNA5-FRT-TO 3′ BirA*. Constructs for EGFR were cloned into 5' (MiniTurbo pcDNA5-FRT-TO or pcDNA5-FRT-TO 3′ MiniTurbo. Flip-In T-REx 293T cells (Endofin-BirA* and HD-PTP-BirA*) or Flip-In T-Rex HeLa cells (EGFR-miniTurbo) were transfected in a 6 well format with 0.2µg of cloned constructs and 2µg pOG44 (OpenFreezer V4134), using lipofectamine 2000 (Invitrogen), according to manufacturer's instructions. On day 2, cells were trypsinized, and passaged into 10 cm plates. On day 3, the medium is replaced by DMEM 10% fetal bovine serum, 100 units/ml pen/strep, 200 ug/ml hygromycin. Medium was replaced every 2- 4 days until non-transfected cells die, and isolated clones were ~1-2 mm in diameter (13-15 days). Pools of cells were generated by

trypsinization of the entire plate and replating in fresh selection medium (the size of the plate was dictated by the number and size of initial colonies). For BirA* experiments, cells ~ 60-70% confluence were induced with 1ug/ml tetracycline for 24 hours. The next day, tetracycline-containing medium was supplemented with 50 µM biotin and cells were incubated for an additional 24 hours. For EGFR-miniTurbo experiments, cells ~ 60-70% confluence were induced with 1ug/ml tetracycline for 24 hours in biotin-depleted medium. On day 2, cells were switched to tetracycline-containing, serum-free medium. After 16 hours of serum starvation, the medium was supplemented with 50 µM biotin for 15 minutes in the presence or absence of 100ng/mL EGF. To harvest, cells were scraped off in ice-cold PBS, washed x2 in PBS, pelleted and frozen at −80°C until processing for MS.

AP-MS and BioID sample processing and Mass Spectrometry analysis:

For AP-MS studies, FLAG affinity purifications were performed as described previously by St-Denis *et al.* (St-Denis et al., 2016) and ¼ of each sample was analyzed by Velos Orbitrap mass spectrometry. A spray tip was formed on fused silica capillary column (0.75 µm ID, 350 µm OD) using a laser puller (program = 4; heat = 280, FIL = 0, VEL = 18, DEL = 200). 10 cm (+/- 1 cm) of C18 reversed-phase material (Reprosil-Pur 120 C18-AQ, 3 µm) was packed in the column by pressure bomb (in MeOH). The column was then pre-equilibrated in buffer A (6 µl) before being connected in-line to a NanoLC-Ultra 2D plus HPLC system (Eksigent) coupled to a LTQ-Orbitrap Velos (Thermo Electron) equipped with a nanoelectrospray ion source (Proxeon Biosystems). The LTQ-Orbitrap Velos instrument under Xcalibur 2.0 was operated in the data dependent mode to automatically switch between MS and up to 10 subsequent MS/MS acquisitions. Buffer A was 100% H2O, 0.1% formic acid; buffer B was 100 ACN, 0.1% formic acid. The HPLC gradient

program delivered an acetonitrile gradient over 125 min. For the first twenty minutes, the flow rate was 400 µL/min at 2% B. The flow rate was then reduced to 200 µL/min and the fraction of solvent B increased in a linear fashion to 35% until 95.5 min. Solvent B was then increased to 80% over 5 min and maintained at that level until 107 min. The mobile phase was then reduced to 2% B until the end of the run (125 min). The parameters for data dependent acquisition on the mass spectrometer were: 1 centroid MS (mass range 400–2000) followed by MS/MS on the 10 most abundant ions. General parameters were: activation type = CID, isolation width = 1 m/z, normalized collision energy = 35, activation Q = 0.25, activation time = 10 msec. For data dependent acquisition, the minimum threshold was 500, the repeat count = 1, repeat duration = 30 sec, exclusion size list = 500, exclusion duration = 30 sec, exclusion mass width (by mass) = low 0.03, high 0.03.

For BirA* BioID studies, streptavidin pulldowns were performed as described previously St-Denis *et al.* (St-Denis et al., 2016) and ¼ of each sample was run on a TripleTOF™ 5600 instrument (AB SCIEX, Concord, Ontario, Canada). Nano-spray emitters were generated from fused silica capillary tubing, with 75µm internal diameter, 365µm outer diameter and 5-8µm tip opening, using a laser puller (Sutter Instrument Co., model P-2000, with parameters set as heat: 280, FIL = 0, VEL = 18, DEL = 2000). Nano-spray emitters were packed with C18 reversed-phase material (Reprosil-Pur 120 C18-AQ, 3µm) resuspended in methanol using a pressure injection cell. Samples were directly loaded at 400nl/min for 14min onto a 75µmx10cm nano-spray emitter. Peptides were eluted from the column with an acetonitrile gradient generated by an Eksigent ekspert™ Nano Ultra 1D Plus and analyzed on the TripleTOF. The gradient was delivered at 200nl/min from 2% acetonitrile with 0.1% formic acid to 35% acetonitrile with 0.1% formic acid using a linear gradient of 90 min. This was followed by a 10 min wash with 80% acetonitrile with

0.1% formic acid, and equilibration for another 15min to 2% acetonitrile with 0.1% formic acid. The total DDA protocol was 140min. The first DDA scan had an accumulation time of 250ms within a mass range of 400-1250Da. This was followed by 20 MS/MS scans of the top 20 peptides identified in the first DDA scan, with accumulation time of 100 ms for each MS/MS scan. Each candidate ion was required to have a charge state from 2-4 and a minimum threshold of 250 counts per second, isolated using a window of 50mDa. Previously analyzed candidate ions were dynamically excluded for 15 seconds.

For MiniTurbo BioID studies, streptavidin pulldowns were performed as described previously by Hesketh *et al.* (Hesketh et al., 2020) and 1/6 of each sample was run on a TripleTOF™ 6600 instrument (AB SCIEX, Concord, Ontario, Canada). Samples were directly loaded at 800 nL/min onto an equilibrated HPLC column and LC-MS/MS was performed on a tripleTOF instrument as previously reported by Hesketh *et al.* (Hesketh et al., 2020). Samples were analyzed with two separate injections with instrument methods set to data dependent acquisition (DDA) and data independent acquisition (SWATH) modes, as reported previously by Hesketh *et al.* (Hesketh et al., 2020).

Data-dependent and independent acquisition data searches:

Data-dependent mass spectrometry data was stored, searched and analyzed using ProHits laboratory information management system (LIMS) platform. Within ProHits, WIFF files were converted to an MGF format using the WIFF2MGF converter and to an mzML format using ProteoWizard (V3.0.10702) and the AB SCIEX MS Data Converter (V1.3 beta). The data was then searched using Mascot (V2.3.02) and Comet (V2016.01 rev.2). The spectra were searched with the human and adenovirus sequences in the RefSeq database (version 57, January 30th, 2013)

acquired from NCBI, supplemented with "common contaminants" from the Max Planck Institute (http://maxquant.org/contaminants.zip) and the Global Proteome Machine (GPM; ftp://ftp.thegpm.org/fasta/cRAP/crap.fasta), forward and reverse sequences (labeled "gi|9999" or "DECOY"), sequence tags (BirA, GST26, mCherry and GFP) and streptavidin, for a total of 72,481 entries. Database parameters were set to search for tryptic cleavages, allowing up to 2 missed cleavages sites per peptide with a mass tolerance of 35ppm for precursors with charges of 2+ to 4+ and a tolerance of 0.15amu for fragment ions. Variable modifications were selected for deamidated asparagine and glutamine and oxidized methionine. Results from each search engine were analyzed through TPP (the Trans-Proteomic Pipeline, v.4.7 POLAR VORTEX rev 1) via the iProphet pipeline.

MSPLIT-DIA SWATH MS data were analyzed using MSPLIT-DIA (version 1.0 (Wang et al., 2015)) implemented in ProHits 4.0 (Liu et al., 2016). To generate a sample-specific spectral library, peptide-spectrum matches (PSMs) from matched DDA runs (BirA*) were pooled by retaining only the spectrum with the best MS-GFDB (Beta version 1.0072 (6/30/2014) (Kim et al., 2010)) probability for each unique peptide sequence and precursor charge state. The MS-GFDB parameters were set to search for tryptic cleavages with a precursor mass tolerance of 50 ppm and charges of 2+ – 4+. Peptide length was limited to 8–30 amino acids and oxidized methionine selected as a variable modification. For MiniTurbo searches, the Human SWATH Atlas (Rosenberger et al., 2014) served as the search library. A peptide-level false discovery rate (FDR) of 1% was enforced using a targetdecoy approach (Elias et al., 2007). The spectra were searched with the NCBI RefSeq database (version 57, January 30th, 2013) against a total of 7 36,241 human and adenovirus sequences supplemented with common contaminants from the Max Planck Institute (http://141.61.102.106:8080/share.cgi?ssid=0f2gfuB) and the Global Proteome Machine

(GPM; http://www.thegpm.org/crap/index.html). The spectral library was then used for peptide spectral matching to proteins by MSPLIT with peptides identified by MSPLIT-DIA passing a 1% FDR subsequently matched to genes using ProHits 4.0 (Liu et al., 2016).

SAINT analysis by SAINTexpress (version 3.6.1 (Teo et al., 2014)) was used to score interactions for all data. For AP-MS results, bait runs (two biological replicates each) were compared against 8 negative controls (GFP-FLAG). For BirA*-MSPLIT results, bait runs (two biological replicates each) were compared against four negative control runs (BirA*-FLAG and BirA*FLAG-GFP). For MiniTurbo-MSPLIT results, bait runs (two biological replicates each) were compared against five negative control runs (GFP-FLAG-miniTurbo and FLAG-miniTurbo). Preys with a false discovery rate (FDR) ≤ 1% (Bayesian estimation based on distribution of the Averaged SAINT scores across biological replicates) were considered high-confidence proximity interactions and were presented using dot plots generated using ProHits-viz (Knight et al., 2017)) (prohitsviz.lunenfeld.ca). In ProHits-viz, once a prey passes the selected FDR threshold (here 1%) with at least one bait, all its quantitative values across the dataset are retrieved for all baits. Bait-prey proximity interactions falling below the 5% FDR threshold are indicated by the color of the edge.

Proteomics data deposition:

AP-MS data has been deposited as a complete submission to the MassIVE repository (https://massive.ucsd.edu/ProteoSAFe/static/massive.jsp) and assigned the accession number MSV00087704. The ProteomeXchange accession is PXD026937. The dataset is currently available to the public at ftp://massive.ucsd.edu/MSV000087704/.

BirA BioID MSPLIT data has been deposited as an incomplete submission to the MassIVE repository (https://massive.ucsd.edu/ProteoSAFe/static/massive.jsp) and assigned the accession number MSV00087705. The dataset is currently available to the public at ftp://massive.ucsd.edu/MSV000087705/.

MiniTurbo BioID MSPLIT data has been deposited as an incomplete submission to the MassIVE repository (https://massive.ucsd.edu/ProteoSAFe/static/massive.jsp) and assigned the accession number MSV00087706. The dataset is currently available to the public at ftp://massive.ucsd.edu/MSV000087706/.

STRING analysis:

Protein-protein interaction networks were generated using the STRING database (Szklarczyk et al., 2019). Colored nodes represent the first shell of interactors identified from the BioID screen using a BFDR cutoff of 0.01 and SAINT score above 0.85. White nodes represent the second shell of interactors extracted from the STRING database. The edges represent protein-protein interactions collected from STRING experiments and databases. The thickness of the edge reflects its confidence score. A maximum of 50 proteins is represented in the second shell of interactors and unique interactors were removed from the network.

Immunoprecipitation:

Cells were lysed on ice in buffer A (50 mM Tris pH 7.5, 50 mM NaCl, 1,5 mM $MgCl_2$, 1 mM EDTA, 0.2% triton x-100, 5% glycerol, 1 mM DTT and cOmplete (Roche) protease inhibitors). Protein extracts were spun at 16,000g for 10 min at 4^o C. A fraction of the supernatant

was kept for SDS-PAGE and Western blots. The remaining fraction was pre-cleared then incubated with the primary antibody under agitation for 1h at 4° C. Protein-antigen complexes were retrieved with sepharose (Millipore) or magnetic beads (BioRad) coupled to an equal amount of protein A/G. Protein extracts were incubated with the beads under agitation for 1h at 4° C. Beads were then washed 3 times and eluted with Laemmli buffer followed by boiling the samples for 10 min. The immunoprecipitated fractions and the lysates were analyzed by SDS-PAGE followed by Western blotting.

Size-Exclusion Chromatography fractionation:

Cells were lysed in buffer (150mM NaCl, 0.1% NP40, 6.25mM TrisHCl ph8, 2mM EDTA, 0.1mM MgCl2, 1mM EGTA, Protease inhibitor cocktail) on ice. The lysate was centrifuged first at 16,000g for 10min, and then the supernatant was centrifuged at 100,000g for 1h. The supernatant was loaded on Superdex200 HPLC column and 0.3ml fractions were collected. Protein analysis was performed on collected fraction by SDS-PAGE followed by Western blot.

Isopycnic sucrose gradient cellular fractionation:

293T cells were washed with PBS on ice, scraped in low volume of ice-cold PBS on ice. The cell pellet was resuspended in isotonic buffer (20mM Hepes pH7.5; 150mM NaCl; 1mM DTT and protease inhibitor cocktail) and the cells were progressively broken down by needle strokes (10 strokes with 25-gauge needle, followed by 20 strokes with 27-gauge needle). The lysate was spun at 400g to eliminate nuclei, and the cytosolic supernatant was loaded on 10-40% sucrose gradient, centrifuged 16 h at 100,000g in Beckman Ti-55 rotor. The fractions were collected (0.25 ml) and analysed by Western blotting using the indicated markers.

Cycloheximide chase:

Cells were starved for 2 h in serum-free DMEM media and pretreated for 1 h with cycloheximide (CHX, Sigma) (10 µg/ml for HeLa cells, 100 µg/ml for 293T cells). As a negative control, cells were pretreated for 1 h in the presence of CHX with Bafilomycin A1 (Sigma) to block lysosomal acidification and thus suppressing receptor lysosomal degradation. Next, cells were stimulated with EGF (50 ng/ml, 2 and 4 h) or with fibronectin (10 µg/ml, 3 and 6 h) in the presence of CHX in 0.5% FBS DMEM media at 37^{o}C. After chasing the receptors for the indicated time points, cells were lysed on ice and receptor levels were analyzed by Western blotting.

Cell surface measurements using cs-ELISA:

Cell-surface ELISA-based assays were performed in live cells as described by Apaja *et al.* (Apaja et al., 2010). Briefly, cells were starved for 2 h in serum-free DMEM media, labeled with integrin α5 or EGFR antibodies on ice, and detected with horseradish peroxidase (HRP)-conjugated secondary antibody (Jackson ImmunoResearch) and Amplex Red (Life Technologies). In HeLa cells, internalization was measured after 5 min of EGF stimulation (50 ng/ml) at 37^{o} C. For receptor stability experiments at the plasma membrane, integrin α5 and EGFR were stimulated with fibronectin (10 µg/ml, 4 h) and EGF (50 ng/ml, 20 min), respectively.

Pulse chase experiments and immunofluorescence:

HeLa cells were seeded on glass coverslips and starved for 2 h in 0.5% FBS DMEM. For EGFR internalization, cells were stimulated with EGF (50 ng/ml, 5 min, 37^{o}C) in 0.5% FBS

DMEM. Next, EGF was washed with PBS and fresh 0.5% FBS DMEM media was added to chase EGFR for the indicated time points at 37^{o}C. HeLa cells were fixed with 4% paraformaldehyde for 15 min and permeabilized with 0.1% Triton X-100 for 10 min at room temperature. Cells were labeled with primary antibodies for 1 h at room temperature followed by labelling with fluorescent secondary antibodies (Molecular probes, Invitrogen) and mounted for imaging. Sequential image acquisition was done on LSM780 confocal microscope (Carl Zeiss MicroImaging, Inc), using the Plan-Apochromat 63x/NA 1.4 objective.

Complementation experiments and vesicular cargo tracking using FRIA:

Methodology for cargo labelled vesicular pH determination in live cells using FRIA has been described in Kazan *et al.* and Barriere *et al.* (Barriere et al., 2008, Kazan et al., 2019). Integrin α5 and EGFR were labelled with primary antibody and fluorescein isothiocyanate (FITC)-conjugated secondary Fab (Jackson ImmunoResearch) on ice and chased for indicated times. Transiently expressed CD4-Ub or CD4tCC-UbAllRΔG were used as before by Apaja *et al.* (Apaja et al., 2010). For complementation experiments, HeLa cells, seeded in 6 well plates, were transiently co-transfected by Lipofectamine 2000 (Invitrogen) with 0.5 µg of Endofin or HD-PTP constructs along with 100 ng of mcherry construct. 24 h post-transfection cells were seeded on glass coverslips (1.5 mm thickness, Fisher Scientific) to perform FRIA. FITC-dextran (10 kDa, 50 µg/ml, Molecular Probes) was used as control for lysosomal delivery. Dextran was endocytosed for 1 h and chased for 2 h at 37°C. Zeiss Observer Z1 (Carl Zeiss MicroImaging) equipped with X-Cite 120Q system (Lumen Dynamics Group Inc.) and MetaFluor software (Molecular Devices) were used to measure fluorescence intensities.

HeLa cell migration assay:

Migration assays were performed using xCELLigence system (ACEA Biosciences). 30,000 HeLa cells in serum-free DMEM media were allowed to migrate for 24 h towards 10% FBS medium serving as a chemoattractant. As a negative control, cells were treated with α5β1 integrin blocking antibody (10 µg/ml). Rate of cellular migration was analyzed by plotting for the slope of the real-time migration curve of each cell line tested.

Signaling experiment:

HeLa cells were starved for 2 h before treatment with EGF (5 ng/ml) or fibronectin (10 µg/ml) for the indicated time points at 37°C. Cells were collected and lysed on ice in buffer B (50 mM Tris pH 7.5, 150 mM NaCl, 1,5 mM $MgCl_2$, 1 mM EDTA, 1% triton x-100, 5% glycerol, 20 mM NaF, 5 mM NaPPi, 1 mM Na_3VO_4, 2 mM imidazole, 175 µg/ml PMSF and cOmplete (Roche) protease inhibitors). Protein extracts were separated by SDS-PAGE and analyzed by Western blotting.

Quantification and Statistical Analysis:

Western blots and immunofluorescence images were quantified using imageJ software. FRIA data was quantified using MetaFluor software, and pHv peaks were drawn and further analyzed using Origin software. Statistical analysis was performed using Microsoft Excel software. Significance was determined by paired two-tailed Student's t test, and data with p values: *<0.05, **<0.01 and ***<0.001 are considered to be significant.

Limitations of the study:

In this study we have characterized the role of Endofin in targeting integrin α5 and EGFR towards lysosomal degradation, whereby regulating receptor signaling and cell migration. We have also shown that Endofin is required for HD-PTP association with ESCRT-0/-III for an efficient EGFR lysosomal delivery. However, the exact mechanism of Endofin association/dissociation with/from HD-PTP, ESCRTs and clathrin complex on early endosomes is still unknown. This will be an interesting direction for future research requiring advanced imaging techniques and protein structural analysis.

Furthermore, it is not fully known whether Endofin regulates the endo/lysosomal delivery of all cell surface receptors undergoing poly-ubiquitination upon activation. Further investigation would be required to address the effect of Endofin depletion on the global cell surface proteome, which might further influence downstream transcriptional pathways.

Acknowledgements:

We would like to thank Dr. Paola Blanchette for her help and advice. J.M.K holds Fonds de Recherche Sante (FRQS) doctoral award. G.D holds Fonds de Recherche Sante (FRQS) post-doctoral award. This work was supported by the Canadian Institutes for Health Research (CIHR) grant 245969 and the Canadian Cancer Society Research Institute (CCSRI) grant 245095. Figure 6 was created using BioRender.com.

Author Contributions:

J.M.K., G.D., G.L.L. and A.P. carried out the study conceptualization and experimental design. J.M.K., G.D., C.E.M. performed experiments and analysis. H.J., D.K., P.M.A., A.R. and N.S.D. performed experiments. J.M.K., G.D., A.C.G., G.L.L., and A.P. wrote and edited the manuscript.

Declarations of Interest:

The authors declare no competing financial interests.

Resource Availability:

Lead contact:

Further information and requests for resources and reagents should be directed to and will be fulfilled by the Lead Contact, Arnim Pause (arnim.pause@mcgill.ca).

Materials availability:

Plasmids and cell lines generated in this study are available from the lead contact.

Data and code availability:

- All proteomics data in this study have been deposited at https://massive.ucsd.edu/ProteoSAFe/static/massive.jsp and are publicly available as of the date of publication. Accession numbers are listed in the key resources table.
- This paper does not report original code.
- Any additional information required to reanalyze the data reported in this paper is available from the lead contact upon request.

Experimental Model and Subject Details:

Cell lines:

Endofin- and HD-PTP-depleted HeLa and 293T cells were generated from wild-type cells purchased from ATCC. All cell lines generated in this study are listed in the key resources table and available from the lead contact upon request.

Key Resources Table

REAGENT or RESOURCE	SOURCE	IDENTIFIER
Antibodies		
Endofin	Proteintech	13118-2-AP
HD-PTP	Proteintech	10472-1-AP
Myc-Tag	Cell Signaling	2276
Hrs	Proteintech	10390-1-AP
STAM	Proteintech	12434-1-AP
Tsg101	Proteintech	14497-1-AP
UBAP1	Proteintech	12385-1-AP
Vps37A	Proteintech	11870-1-AP
CHMP4B	Proteintech	13683-1-AP
EGFR (A-10) used for WB and IP	Santa Cruz	Sc-373746
EGFR (ICR10) used for cs-ELISA, IF and FRIA	Abcam	Ab231
Integrin α5 used for WB	Proteintech	10569-1-AP
Integrin α5 used for cs-ELISA and FRIA	BD Pharmingen	555651
Anti-Human integrin $\alpha5\beta1$	Millipore	MAB1969
CD4 (H370) used for WB	Santa Cruz	Sc-7219
CD4 (OKT4) used for FRIA	Invitrogen	14-0048-82
Flag-Tag (M2)	Sigma	F1804
eEF2	Cell Signaling	2332
α-Tubulin	Sigma	T6074
Clathrin (X22)	Abcam	Ab2731
EEA1	Invitrogen	14-9114-82
anti-Rat HRP F(ab')2	Jackson ImmunoResearch	712-036-153
anti-Mouse HRP F(ab')2	Jackson ImmunoResearch	115-036-003
anti-Rat FITC F(ab')2	Jackson ImmunoResearch	712-096-150
anti-Mouse AF488	Invitrogen	A-28175
anti-Mouse AF594	Invitrogen	A-11032
anti-Rabbit AF488	Invitrogen	A-27034
anti-Rabbit AF594	Invitrogen	A-11012
anti-Rat AF647	Invitrogen	A-21247

Chemicals, peptides, and recombinant proteins		
Recombinant Human EGF	Gibco	PHG0311
Human Plasma Fibronectin	Gibco	33016-015
Cycloheximide	Sigma	66-81-9
Bafilomycin A1	Sigma	B1793
CCCP	Sigma	C2759
Monensin sodium	Sigma	M5273
Nigericin sodium salt	Sigma	N7143
Amplex Red	Invitrogen	A12222
Deposited data		
AP-MS Data	https://massive.ucsd.edu/ProteoSAFe/static/massive.jsp	MSV00087704
BirA BioID MSPLIT Data	https://massive.ucsd.edu/ProteoSAFe/static/massive.jsp	MSV00087705
MiniTurbo BioID MSPLIT Data	https://massive.ucsd.edu/ProteoSAFe/static/massive.jsp	MSV00087706
Experimental models: Cell lines		
HeLa NT	Pause Lab	
HeLa sh54Endofin	Pause Lab	
HeLa sh75Endofin	Pause Lab	
HeLa sh47HD-PTP	Pause Lab	
HeLa sh51HD-PTP	Pause Lab	
HeLa sh98Hrs	Pause Lab	
293T NT	Pause Lab	
293T sh54Endofin	Pause Lab	
293T sh75Endofin	Pause Lab	
293T sh47HD-PTP	Pause Lab	
Oligonucleotides		
Details of cloning and mutagenesis primers are in Table S1		
Recombinant DNA		
pcDNA3-Flag-Endofin	Pause Lab	
pcDNA3-Flag-Endofin resistant to shRNA54	Pause Lab	
pcDNA3-Flag-L15P-Endofin resistant to shRNA54	Pause Lab	
pcDNA3-Flag-C753S-Endofin resistant to shRNA54	Pause Lab	
pcDNA3-Flag-HD-PTP	Pause Lab	
pcDNA3-Flag-HD-PTP resistant to shRNA47	Pause Lab	
pcDNA3-Flag-T145K-HD-PTP resistant to shRNA47	Pause lab	
pcDNA3-CD4Tl	Lukacs Lab	
pcDNA3-CD4Tl-Ub	Lukacs Lab	
pcDNA3-CD4TCC-UbAllRΔG	Lukacs Lab	
Software and algorithms		
MetaMorph/MetaFluor Software	Molecular Devices	
Origin Software	OriginLab	https://www.originlab.com/

ImageJ Software	Schneider et al., 2012	https://imagej.nih.gov/ij/

2.6. Figures and Figure Legends:

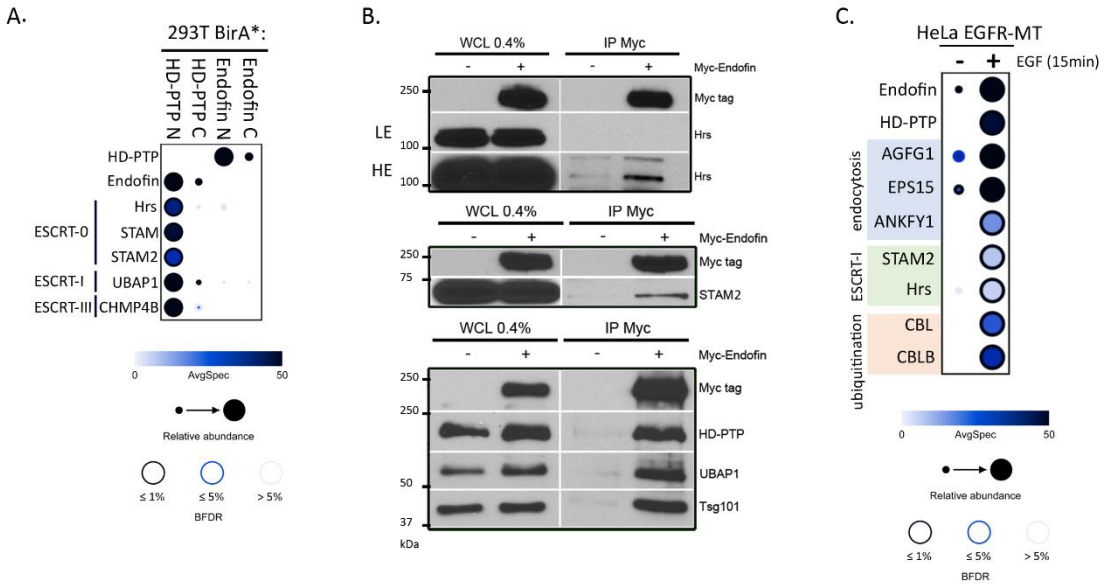

Figure 1: Endofin forms a complex with ESCRTs and EGF receptor.

(A) Dot plot of BioID screen showing ESCRT proteins in close proximity to HD-PTP and Endofin. Flag-tagged biotin ligase (BirA*) was fused to the N- or C-terminus of HD-PTP and Endofin and were used as baits. Constructs were transfected into Flp-In T-REx 293T cells. Fill shades in the dot plot indicate the average spectral counts (Avg Spec), the size of the dot represents its relative abundance across all preys and the outer circle color represents the BFDR value. (B) Co-immunoprecipitation (co-IP) performed on 293T cells transiently transfected with myc-Endofin compared to mock transfected cells. Myc-Endofin was immunoprecipitated (myc antibody) and co-IP of HD-PTP, ESCRT-0 (Hrs and STAM2) and ESCRT-I (Tsg101 and UBAP1) were assessed by Western blots. Whole cell lysate (WCL) is loaded to reveal protein content. Low exposure (LE) and high exposure (HE) immunoblots are shown for Hrs. Data are from n=3 independent

experiments. (C) Dot plot of TurboID screen showing ESCRT proteins and other proteins related to endocytosis and EGFR activation in close proximity to EGFR in the presence or absence of EGF stimulation (100 ng/ml, 15 min). Fast-acting miniTurbo biotin ligase (MT) was fused to the C-terminus of EGFR (EGFR-MT) and transfected into Flp-In T-REx HeLa cells and used as a bait.

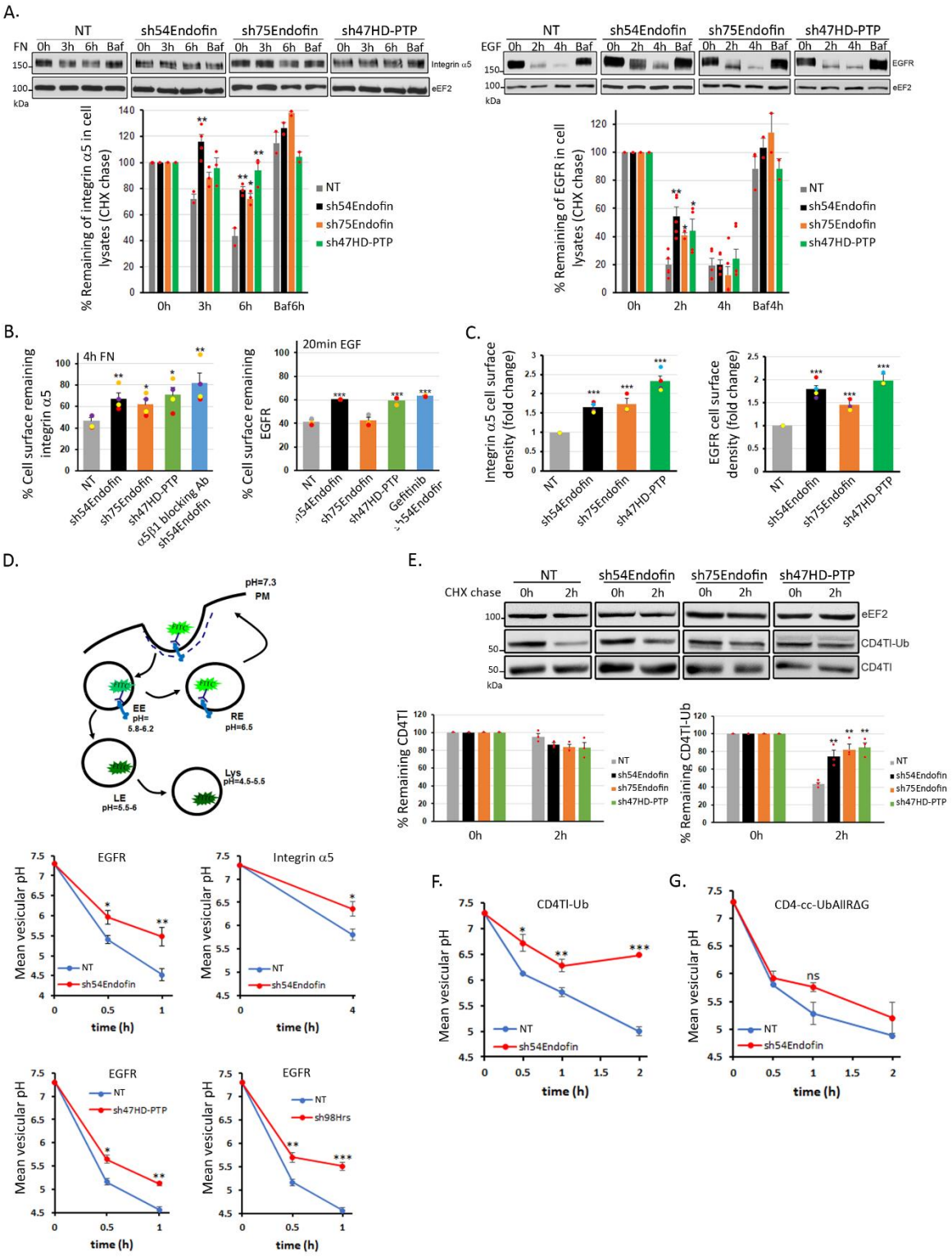
A.
NT
sh54Endofin
sh75Endofin
sh47HD-PTP
FN
0h 3h 6h Baf
Integrin α5
eEF2
kDa
% Remaining of integrin α5 in cell lysates (CHX chase)
NT
sh54Endofin
sh75Endofin
sh47HD-PTP
0h 3h 6h Baf6h
EGF
0h 2h 4h Baf
EGFR
% Remaining of EGFR in cell lysates (CHX chase)
0h 2h 4h Baf4h
B.
4h FN
% Cell surface remaining integrin α5
α5β1 blocking Ab
20min EGF
% Cell surface remaining EGFR
Gefitinib
C.
Integrin α5 cell surface density (fold change)
EGFR cell surface density (fold change)
D.
pH=7.3
PM
EE
pH= 5.8-6.2
RE
pH=6.5
Lys
pH=4.5-5.5
LE
pH=5.5-6
EGFR
Integrin α5
Mean vesicular pH
time (h)
sh47HD-PTP
sh98Hrs
E.
CHX chase
CD4TI-Ub
CD4TI
% Remaining CD4TI
% Remaining CD4TI-Ub
F.
CD4TI-Ub
G.
CD4-cc-UbAllRΔG
ns

Figure 2: Endofin mediates the efficient sorting of integrin α5, EGFR and CD4 poly ubiquitinated cargo model towards lysosomal degradation.

(A) Integrin α5 (left panel) and EGFR (right panel) cycloheximide chase (10 μg/ml CHX) of total receptor levels in Endofin- and HD-PTP-depleted HeLa cells. Cells were serum-starved (2 h), pre-treated with CHX (1 h) and then receptors were activated either with fibronectin (10 μg/ml FN, 37°C) or with EGF (50 ng/ml, 37°C). Integrin α5 was chased for 0, 3 and 6 h, whereas EGFR was chased for 0, 2 and 4 h in the presence of CHX. Control cells were also pre-treated with Bafilomycin A1 (200 nM Baf + CHX, 1 h) to inhibit lysosomal acidification and hence lysosomal degradation (6 h FN + Baf or 4 h EGF + Baf). Western blots were performed on cell extracts to measure degradation kinetics by densitometric analysis using ImageJ software. Integrin α5 and EGFR levels were normalized to eEF2. (B) Integrin α5 (left panel) and EGFR (right panel) plasma membrane (PM) stability in HeLa cells measured by cell surface-ELISA (cs-ELISA). After serum starvation, receptors were activated either with fibronectin (10 μg/ml FN, 4 h, 37°C) or with EGF (50 ng/ml, 20 min, 37°C). α5β1 integrin blocking antibody (10 μg/ml) and Gefitinib (2 μM) were used as negative controls to block receptor internalization in Endofin-depleted cells. For each cell line, levels of integrin α5 and EGFR are plotted as percentage remaining at the cell surface compared to unstimulated cells. (C) cs-ELISA was performed on serum-starved HeLa cells to quantify integrin α5 (left panel) and EGFR (right panel) PM receptor density at steady states. Endofin- and HD-PTP-depleted cells are compared to control NT cells. (D) (upper panel) Schematic representation of changes in vesicular pH during receptor trafficking (EE: early endosomes, RE: recycling endosomes, LE: late endosomes, Lys: lysosomes). (Lower panel) FRIA analysis of EGFR and integrin α5 endocytosis kinetics in serum-starved HeLa cells. Mean vesicular pH of FITC-labeled EGFR- or integrin α5-containing endocytic vesicles determined by

FRIA in Endofin-, HD-PTP- and Hrs-depleted HeLa cells compared to NT cells. After serum starvation, cells were either stimulated with EGF (50 ng/ml, 30 or 60 min, 37ºC) or with FN (10 µg/ml, 4 h, 37ºC). (E) Endofin- and HD-PTP-depleted 293T cells were transiently transfected with CD4Tl (negative control for receptor sorting towards lysosomal degradation) or with CD4Tl-Ubiquitin chimera (CD4Tl-Ub, which serves as a model for poly-ubiquitinated cargo). Serum-starved 293T cells were pre-treated with CHX (100 µg/ml) to chase total protein levels of CD4Tl and CD4Tl-Ub for 2 h. Western blots (CD4 antibody) were performed on cell extracts to measure degradation kinetics by densitometric analysis using ImageJ software. CD4Tl and CD4Tl-Ub levels were normalized to eEF2. (F) Mean vesicular pH of CD4Tl-Ub- and (G) CD4TCC-UbAllRΔG-containing endocytic vesicles determined by FRIA in Endofin-depleted HeLa cells compared to NT cells after 15-, 30-, 60- and 120-min chase (37ºC). CD4TCC-UbAllRΔG serves as a model for tetrameric mono-ubiquitinated cargo. Data are mean ± SEM of n≥3 independent experiments. Unpaired student t-test: * $p<0.05$, ** $p<0.01$, *** $p<0.001$.

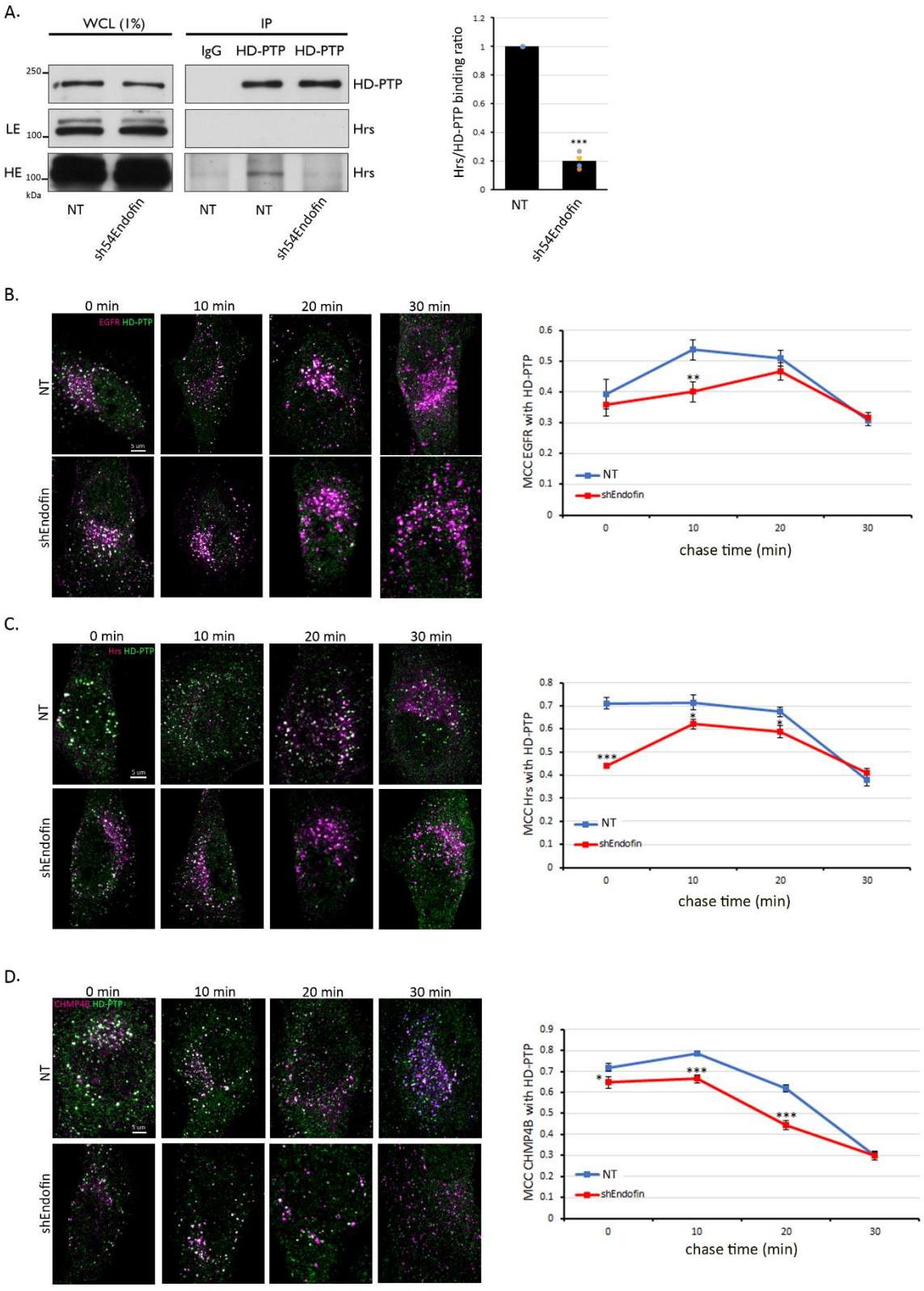
A.
WCL (1%)
IP
IgG
HD-PTP
HD-PTP
250
LE
100
HE
100
kDa
HD-PTP
Hrs
Hrs
NT
sh54Endofin
NT
NT
sh54Endofin
Hrs/HD-PTP binding ratio
1.2
1
0.8
0.6
0.4
0.2
0
***
NT
sh54Endofin
B.
0 min
10 min
20 min
30 min
EGFR HD-PTP
NT
shEndofin
5 um
MCC EGFR with HD-PTP
0.6
0.5
0.4
0.3
0.2
0.1
0
**
NT
shEndofin
0
10
20
30
chase time (min)
C.
0 min
10 min
20 min
30 min
Hrs HD-PTP
NT
shEndofin
5 um
MCC Hrs with HD-PTP
0.8
0.7
0.6
0.5
0.4
0.3
0.2
0.1
0
***
*
*
NT
shEndofin
0
10
20
30
chase time (min)
D.
0 min
10 min
20 min
30 min
CHMP4B HD-PTP
NT
shEndofin
5 um
MCC CHMP4B with HD-PTP
0.9
0.8
0.7
0.6
0.5
0.4
0.3
0.2
0.1
0
*
***
***
NT
shEndofin
0
10
20
30
chase time (min)

Figure 3: Endofin promotes HD-PTP colocalization with EGFR, Hrs and CHMP4B.

(A) Co-IP performed on control and Endofin-depleted 293T cells upon EGF stimulation (50 ng/ml, 15 min, 37ºC). Endogenous HD-PTP was immunoprecipitated and co-IP of Hrs was assessed by Western blotting. Whole cell lysate (WCL 1%) is loaded to reveal protein content. (B and C) Colocalization analysis of EGFR (B), Hrs (C) and CHMP4B (D) with HD-PTP in Endofin-depleted HeLa cells. Serum-starved cells were stimulated with EGF (50 ng/ml, 5 min, 37ºC) then EGFR was chased for 0, 10, 20 and 30 min at 37º C. Mander's Colocalization Coefficient (MCC) was quantified using ImageJ software (n=30). Representative immunofluorescence images are shown for each time point. Data are mean ± SEM of n≥3 independent experiments. Unpaired student t-test: * $p<0.05$, ** $p<0.01$, *** $p<0.001$.

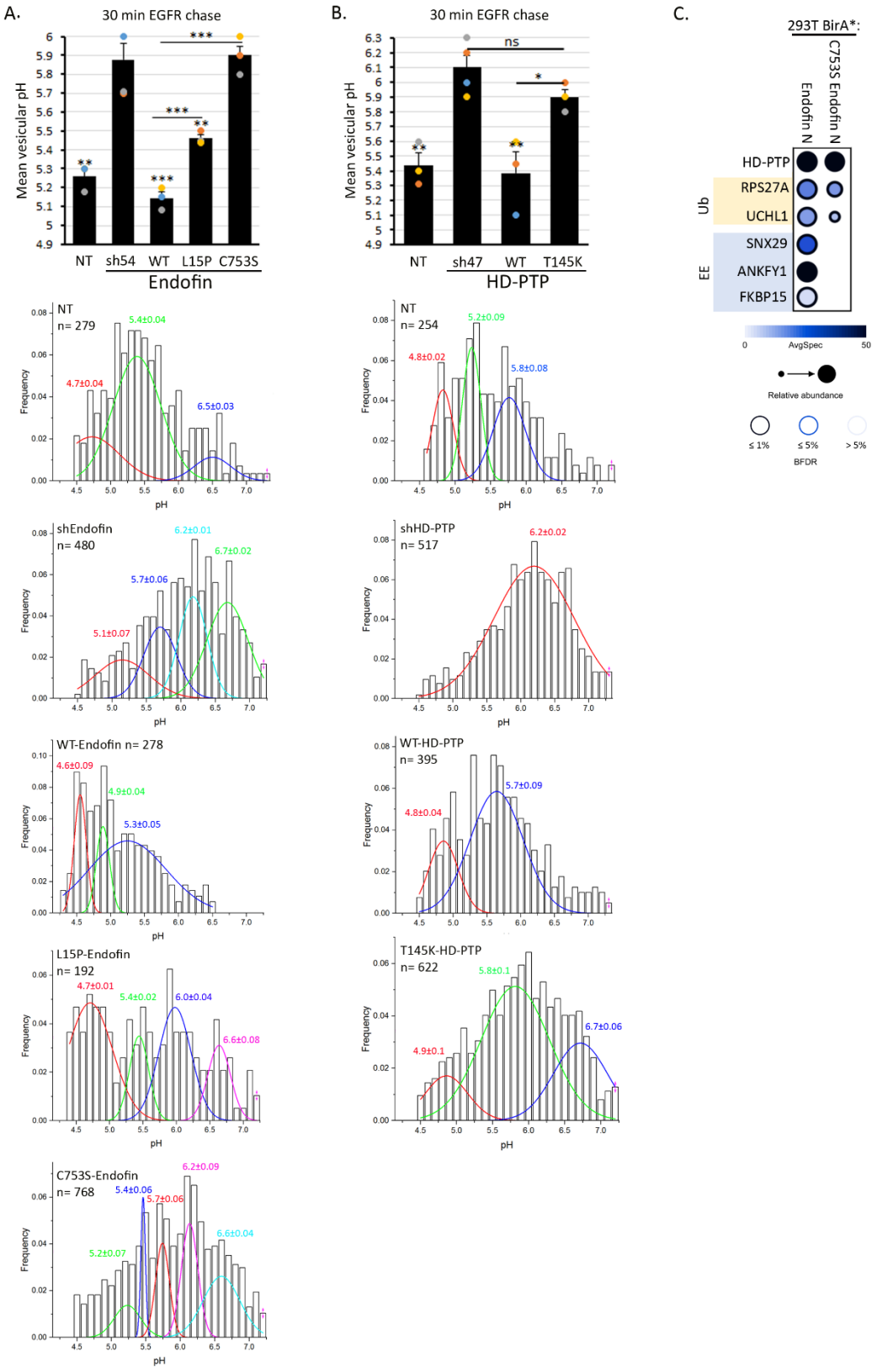
A.
30 min EGFR chase
Mean vesicular pH
NT
sh54
WT
L15P
C753S
Endofin
B.
30 min EGFR chase
Mean vesicular pH
ns
NT
sh47
WT
T145K
HD-PTP
C.
293T BirA*:
Endofin N
C753S Endofin N
HD-PTP
RPS27A
UCHL1
SNX29
ANKFY1
FKBP15
Ub
EE
AvgSpec
Relative abundance
≤ 1%
≤ 5%
> 5%
BFDR
NT
n= 279
5.4±0.04
4.7±0.04
6.5±0.03
NT
n= 254
5.2±0.09
4.8±0.02
5.8±0.08
shEndofin
n= 480
6.2±0.01
6.7±0.02
5.7±0.06
5.1±0.07
shHD-PTP
n= 517
6.2±0.02
WT-Endofin n= 278
4.6±0.09
4.9±0.04
5.3±0.05
WT-HD-PTP
n= 395
5.7±0.09
4.8±0.04
L15P-Endofin
n= 192
4.7±0.01
5.4±0.02
6.0±0.04
6.6±0.08
T145K-HD-PTP
n= 622
5.8±0.1
6.7±0.06
4.9±0.1
C753S-Endofin
n= 768
6.2±0.09
5.4±0.06
5.7±0.06
6.6±0.04
5.2±0.07
Frequency
pH

Figure 4: Endofin/HD-PTP interaction is permissive for an efficient lysosomal delivery of activated EGFR.

(A and B) Mean vesicular pH of FITC-labeled EGFR-containing endocytic vesicles determined by FRIA, after 30 min of EGFR chase (50 ng/ml EGF, 37^{o}C), in (A) Endofin-depleted HeLa cells transiently co-transfected with mCherry plasmid and Flag-tagged WT-, L15P- or C753S-Endofin constructs, or (B) HD-PTP-depleted HeLa cells transiently co-transfected with mCherry plasmid, WT- or T145K-HD-PTP (disrupts HD-PTP interaction with Endofin) constructs. Single cell FRIA analysis was performed on cells expressing mCherry (vesicles: n>190, microscopic fields: n>10). Vesicular pH distribution of internalized EGFR after 30 min of EGFR chase is plotted. The mean vesicular pH of the distinct peaks and the number of vesicles in NT, shEndofin, WT-Endofin, L15P-Endofin, C753S-Endofin, shHD-PTP- and T145K-HD-PTP HeLa cells are indicated. (C) Dot plot of BioID screen showing proteins related to ubiquitination (Ub) and early endosomes (EE) in close proximity to WT-Endofin and C753S-Endofin. Flag-tagged biotin ligase (BirA*) was fused to the N-terminus of WT-Endofin and C753S-Endofin and were used as baits. Constructs were transfected into Flp-In T-REx 293T cells. Fill shades in the dot plot indicate the average spectral counts (Avg Spec), the size of the dot represents its relative abundance across all preys and the outer circle color represents the BFDR value. Data are mean ± SEM of n≥3 independent experiments. Unpaired student t-test: * $p<0.05$, ** $p<0.01$, *** $p<0.001$.

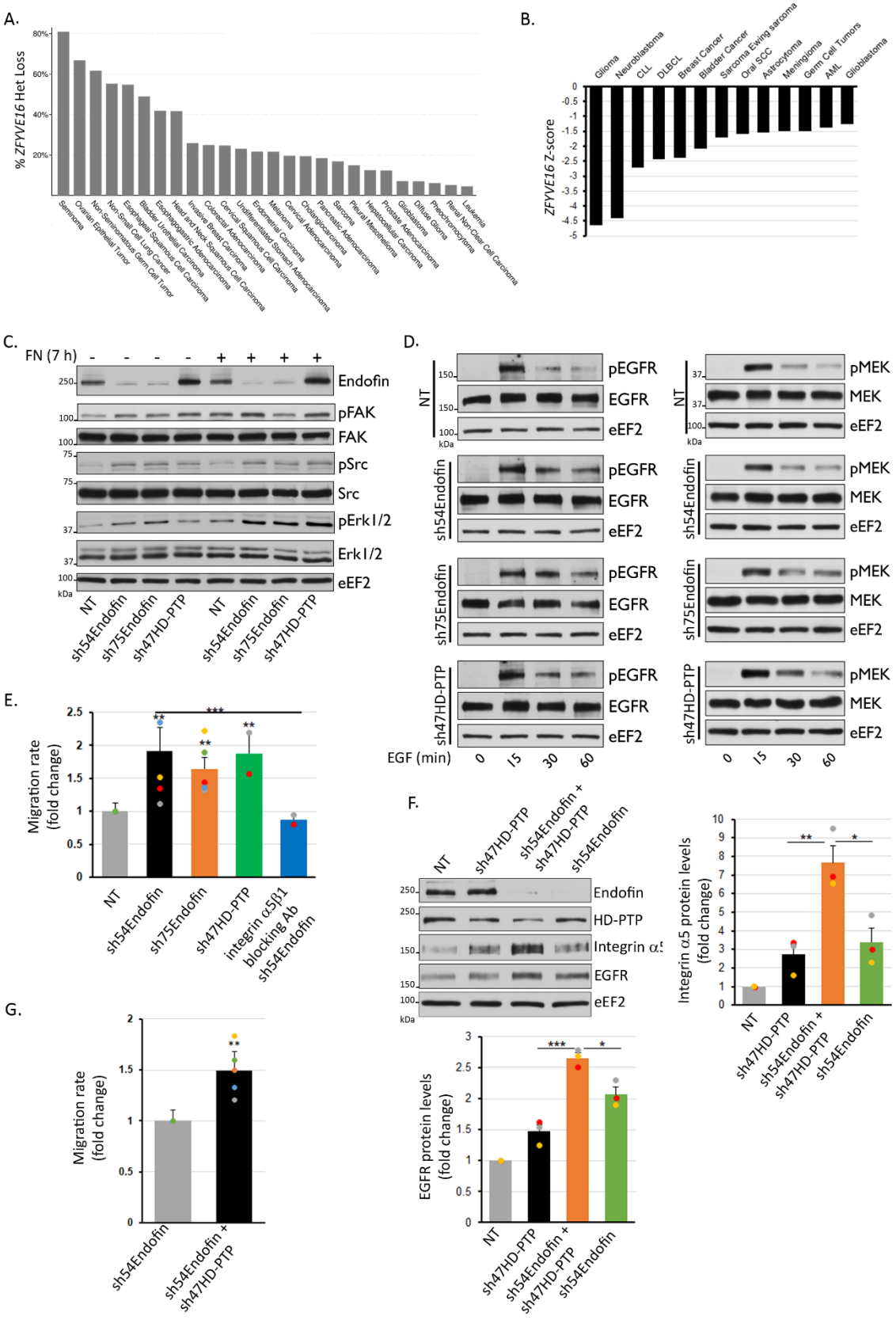
A.
% ZFYVE16 Het Loss
80%
60%
40%
20%
Seminoma
Ovarian Epithelial Tumor
Non-Seminomatous Germ Cell Tumor
Non-Small Cell Lung Cancer
Esophageal Squamous Cell Carcinoma
Bladder Urothelial Carcinoma
Esophagogastric Adenocarcinoma
Head and Neck Squamous Cell Carcinoma
Invasive Breast Carcinoma
Colorectal Adenocarcinoma
Cervical Squamous Cell Carcinoma
Undifferentiated Carcinoma
Endometrioid Carcinoma
Melanoma
Stomach Adenocarcinoma
Cervical Adenocarcinoma
Cholangiocarcinoma
Pancreatic Adenocarcinoma
Sarcoma
Pleural Mesothelioma
Hepatocellular Carcinoma
Prostate Adenocarcinoma
Glioblastoma
Diffuse Glioma
Pheochromocytoma
Renal Non-Clear Cell Carcinoma
Leukemia
B.
ZFYVE16 Z-score
0
-0.5
-1
-1.5
-2
-2.5
-3
-3.5
-4
-4.5
-5
Glioma
Neuroblastoma
CLL
DLBCL
Breast Cancer
Bladder Cancer
Sarcoma Ewing sarcoma
Oral SCC
Astrocytoma
Meningioma
Germ Cell Tumors
AML
Glioblastoma
C.
FN (7 h)
- - - - + + + +
Endofin
pFAK
FAK
pSrc
Src
pErk1/2
Erk1/2
eEF2
kDa
NT
sh54Endofin
sh75Endofin
sh47HD-PTP
D.
NT
sh54Endofin
sh75Endofin
sh47HD-PTP
pEGFR
EGFR
eEF2
pMEK
MEK
EGF (min)
0
15
30
60
E.
Migration rate (fold change)
NT
sh54Endofin
sh75Endofin
sh47HD-PTP
integrin α5β1 blocking Ab sh54Endofin
F.
NT
sh47HD-PTP
sh54Endofin + sh47HD-PTP
sh54Endofin
Endofin
HD-PTP
Integrin α5
EGFR
eEF2
kDa
Integrin α5 protein levels (fold change)
EGFR protein levels (fold change)
G.
Migration rate (fold change)
sh54Endofin
sh54Endofin + sh47HD-PTP

Figure 5: Endofin depletion sustains integrin α5 and EGFR downstream signaling and increases cell migration.

(A) Frequency of heterozygous loss of *ZFYVE16* (Endofin gene) in human patients with different types of cancers. Data extracted from cBioPortal database and plotted as the percentage of patients with *ZFYVE16* heterozygous loss. (B) Z-score analysis of Endofin in human patients with different types of cancers. Endofin Z-score for each cancer type was extracted from PRECOG database and plotted. (C) Western blots showing the phosphorylation levels of integrin α5 receptor downstream effectors: FAK, Src and Erk1/2 in Endofin- and HD-PTP-depleted HeLa cells compared to NT cells after fibronectin stimulation (10 μg/ml FN, 7 h, 37^{o}C). eEF2 blots serve as a loading control. (D) Endofin- and HD-PTP-depleted HeLa cells compared to NT cells were stimulated with EGF (5 ng/ml, 37^{o}C) for 0-, 15-, 30- and 60-min. Western blots were performed to reveal the phosphorylation state of EGFR (left panel) and its downstream effector MEK (right panel). eEF2 blots serve as a loading control. (E) Real time cell analysis (RTCA) measuring cell migration in Endofin- and HD-PTP-depleted HeLa cells compared to NT cells. Cell culture media supplemented with 10% FBS was used as a chemoattractant to trigger cell migration. Serum-free media (absence of chemoattractant) was used as a negative control. Integrin α5β1 blocking antibody (10 μg/ml) was used as a negative control to inhibit cell migration in Endofin-depleted cells. (F) Endofin-depleted or control HeLa cells were transiently transfected with a non-targeting (NT) shRNA or with HD-PTP shRNA. Receptor levels were assessed by Western blotting and quantified by densitometric analysis using ImageJ software. (G) Real time cell analysis was performed as in (E) to compare the migration rate of Endofin-depleted cells transiently transfected with either HD-PTP shRNA or NT control. Data are mean ±

SEM of n≥3 independent experiments. Unpaired student t-test: * p<0.05, ** p<0.01, *** p<0.001.

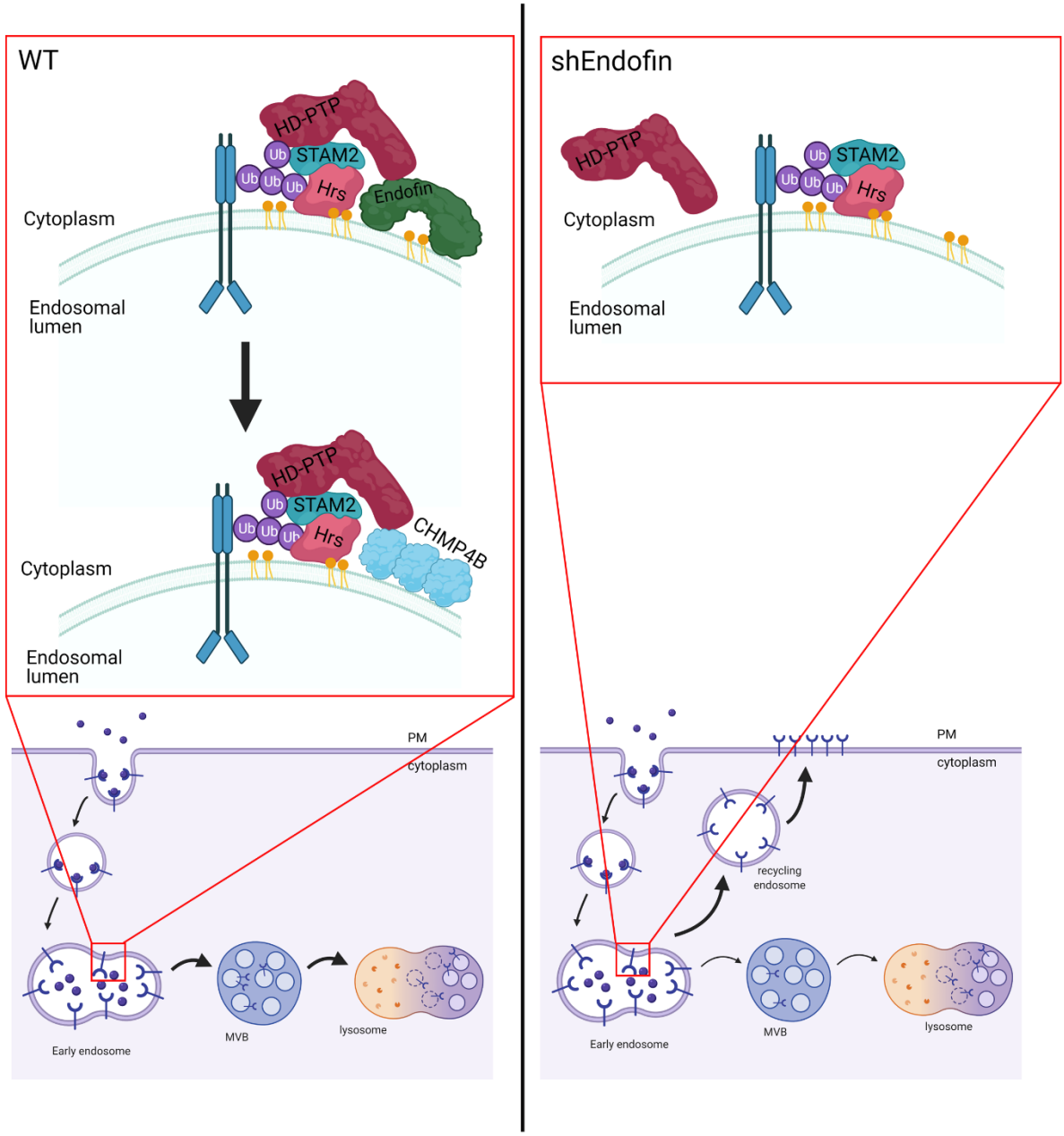

Figure 6: Schematic model of Endofin's role in receptor trafficking.

After internalized receptors are targeted towards early endosomes in wild-type cells (WT), Endofin recruits HD-PTP to early endosomes *via* its FYVE-domain and their direct interaction. Endofin promotes HD-PTP interaction with ESCRT-0 on early endosomes, through STAM2 binding to the proline rich region of HD-PTP. Next, Endofin may undergo allosteric conformational modifications (probably by post-translational modifications), which weakens Endofin/HD-PTP association and facilitates HD-PTP/CHMP4B interaction. Eventually, this leads to an efficient ESCRT-dependent sorting of EGFR towards MVBs and lysosomal degradation. On the other hand, in Endofin-depleted cells (shEndofin), HD-PTP interaction with ESCRT-0 decreases, which favors receptor recycling back to the plasma membrane and delays ESCRT-dependent EGFR sorting towards MVBs and lysosomal degradation.

2.7. Supplemental Figures:

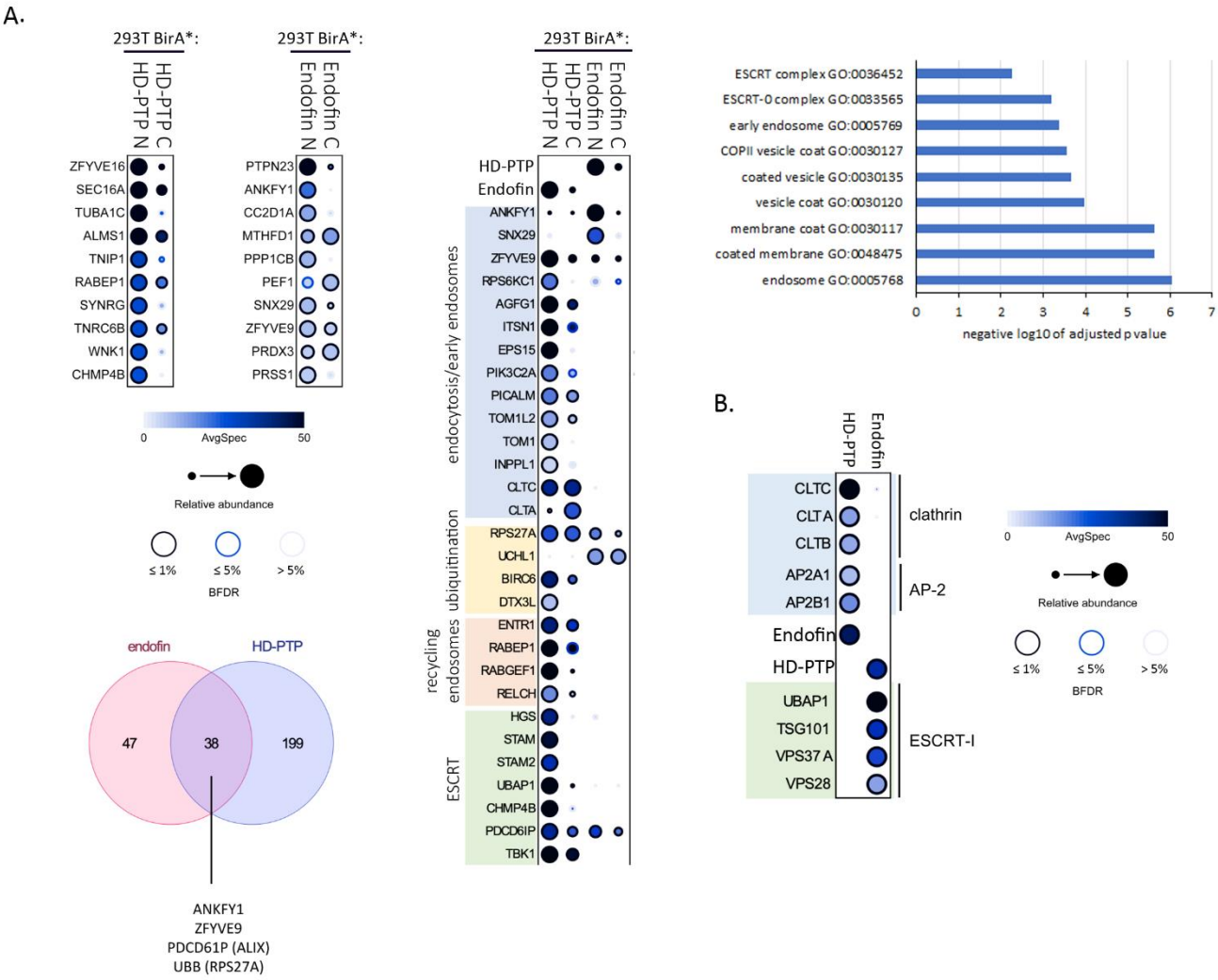

Figure S1. Potential role of Endofin in receptor trafficking, Related to Figure 1.

(A) Dot plot of BioID screen showing proteins in close proximity to HD-PTP and Endofin. Flag-tagged biotin ligase (BirA*) was fused to the N- or C-terminus of either HD-PTP or Endofin and were used as baits. Constructs were transfected into Flp-In T-REx 293T cells. Fill shades in the dot plot indicate the average spectral counts (Avg Spec), the size of the dot represents its relative abundance across all preys and the outer circle color represents the BFDR value. Dot plots of the BioID screen showing the top 10 hits for Endofin and HD-PTP (left and middle panels), as well as a list of hits involved in vesicle-mediated transport (GO:0016192, right panel). Gene ontology (GO) enrichment bar graph of preys recovered by HD-PTP-N-BirA* revealed an over-representation of cellular component terms related to vesicular traffic (top 9 terms displayed, based on adjusted p-value; search limited to terms <1000 genes, no electronic annotations). The Venn diagram illustrates the number of common and specific interactors for Endofin and HD-PTP in the BioID screen. (B) Dot plot of an Affinity Purification-Mass Spectrometry performed using Flp-In T-REx 293T cells expressing Flag-tagged HD-PTP or Endofin as baits. SAINT analysis was performed. (C) Cellular fractionation by isopycnic sucrose gradient centrifugation using 293T cell organelles. Dead cells and nuclei were removed before fractionation and post-nuclear supernatant (PNS) is loaded along with fractions to reveal protein content by Western blotting. Fraction number 1 is the lightest fraction. EEA1, LAMP1 and Tom20 are, respectively, used as markers of early endosomes, lysosomes and mitochondria. (D) Subcellular fractionation by size-exclusion chromatography (HPLC) of soluble protein complexes extracted from 293T cells. The elution profile of molecular mass standards was determined in parallel, and their positions are indicated. Whole cell lysate (WCL) is loaded to reveal protein content.

Endofin

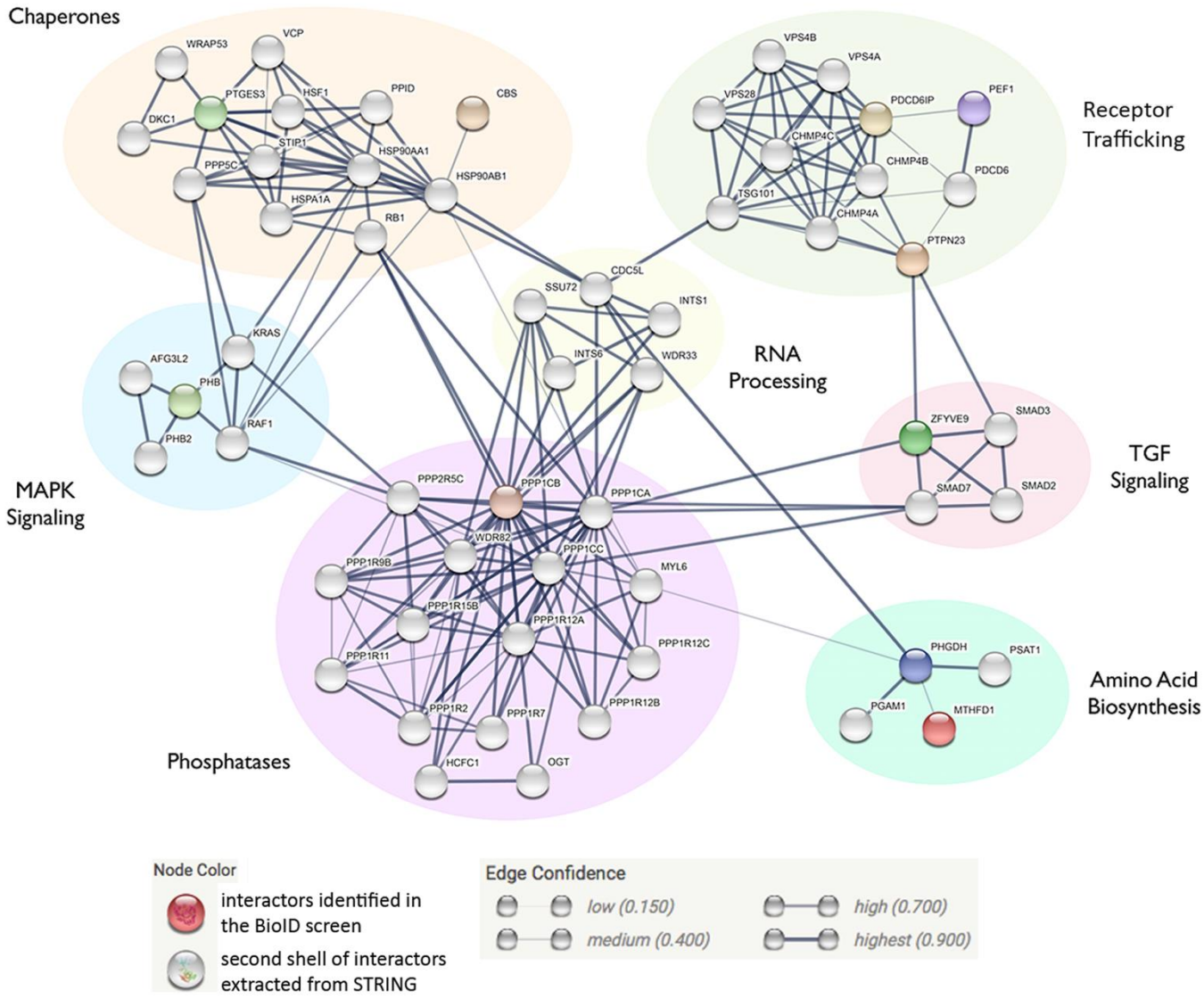
Chaperones
WRAP53
VCP
PTGES3
HSF1
PPID
CBS
DKC1
STIP1
HSP90AA1
PPP5C
HSP90AB1
HSPA1A
RB1
Receptor Trafficking
VPS4B
VPS4A
VPS28
PDCD6IP
PEF1
CHMP4C
CHMP4B
PDCD6
TSG101
CHMP4A
PTPN23
RNA Processing
CDC5L
SSU72
INTS1
INTS6
WDR33
MAPK Signaling
KRAS
AFG3L2
PHB
PHB2
RAF1
TGF Signaling
ZFYVE9
SMAD3
SMAD7
SMAD2
Phosphatases
PPP2R5C
PPP1CB
PPP1CA
WDR82
PPP1CC
PPP1R9B
MYL6
PPP1R15B
PPP1R12A
PPP1R12C
PPP1R11
PPP1R2
PPP1R7
PPP1R12B
HCFC1
OGT
Amino Acid Biosynthesis
PHGDH
PSAT1
PGAM1
MTHFD1
Node Color
interactors identified in the BioID screen
second shell of interactors extracted from STRING
Edge Confidence
low (0.150)
medium (0.400)
high (0.700)
highest (0.900)

Figure S2. Endofin contributes to receptor trafficking among different cellular processes. Related to Figure1.

Endofin protein-protein interaction network showing cellular processes potentially accomplished by these interactors. Colored nodes represent interactors identified in the BioID screen, whereas white nodes represent second shell of interactors extracted from the STRING database. The edges represent protein-protein interactions, and the thickness of the line reflects the edge confidence score.

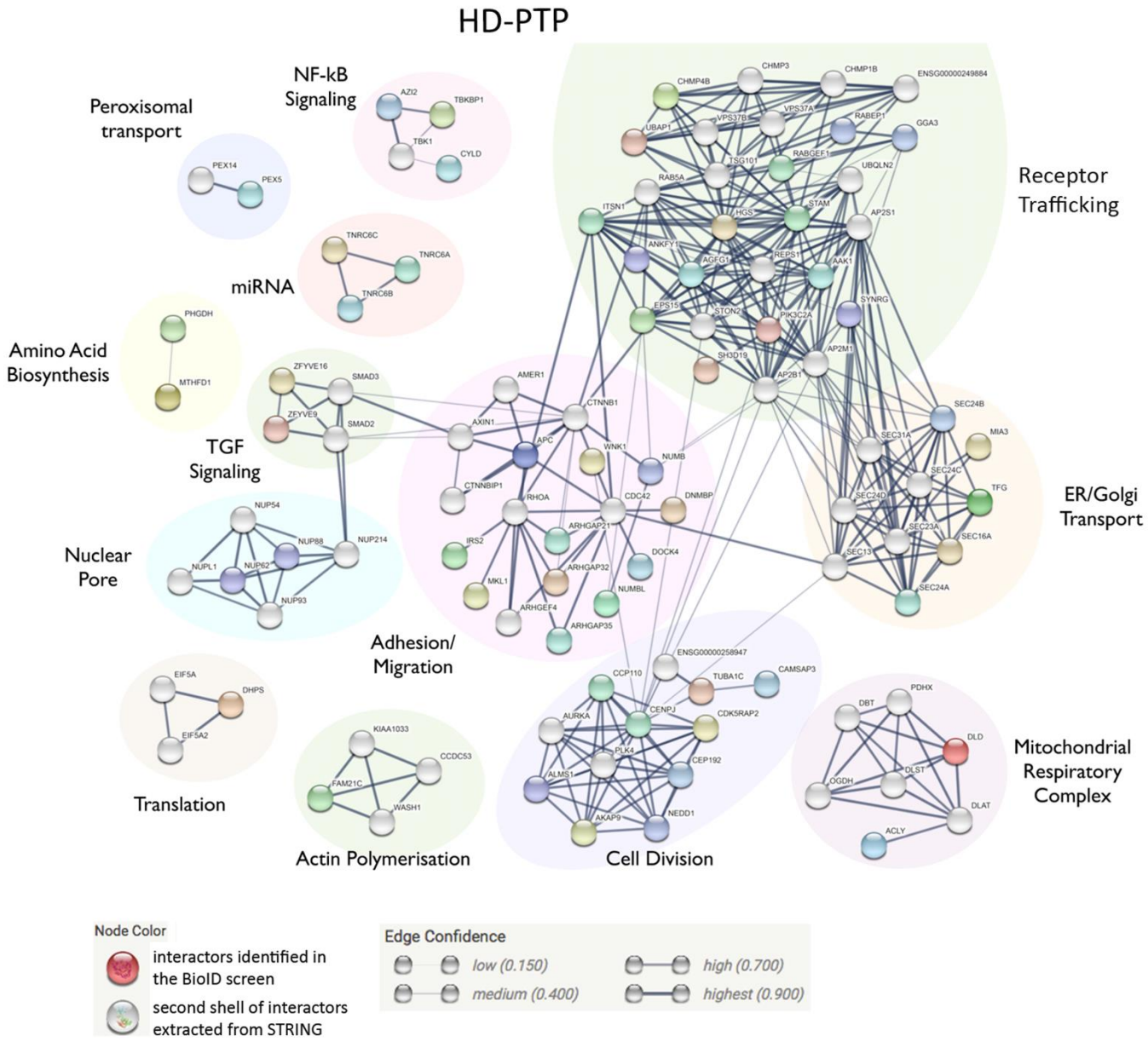

Figure S3. HD-PTP contributes to receptor trafficking among different cellular processes. Related to Figure 1.

HD-PTP protein-protein interaction networks showing cellular processes potentially accomplished by these interactors. Colored nodes represent interactors identified in the BioID screen, whereas

white nodes represent second shell of interactors extracted from the STRING database. The edges represent protein-protein interactions, and the thickness of the line reflects the edge confidence score.

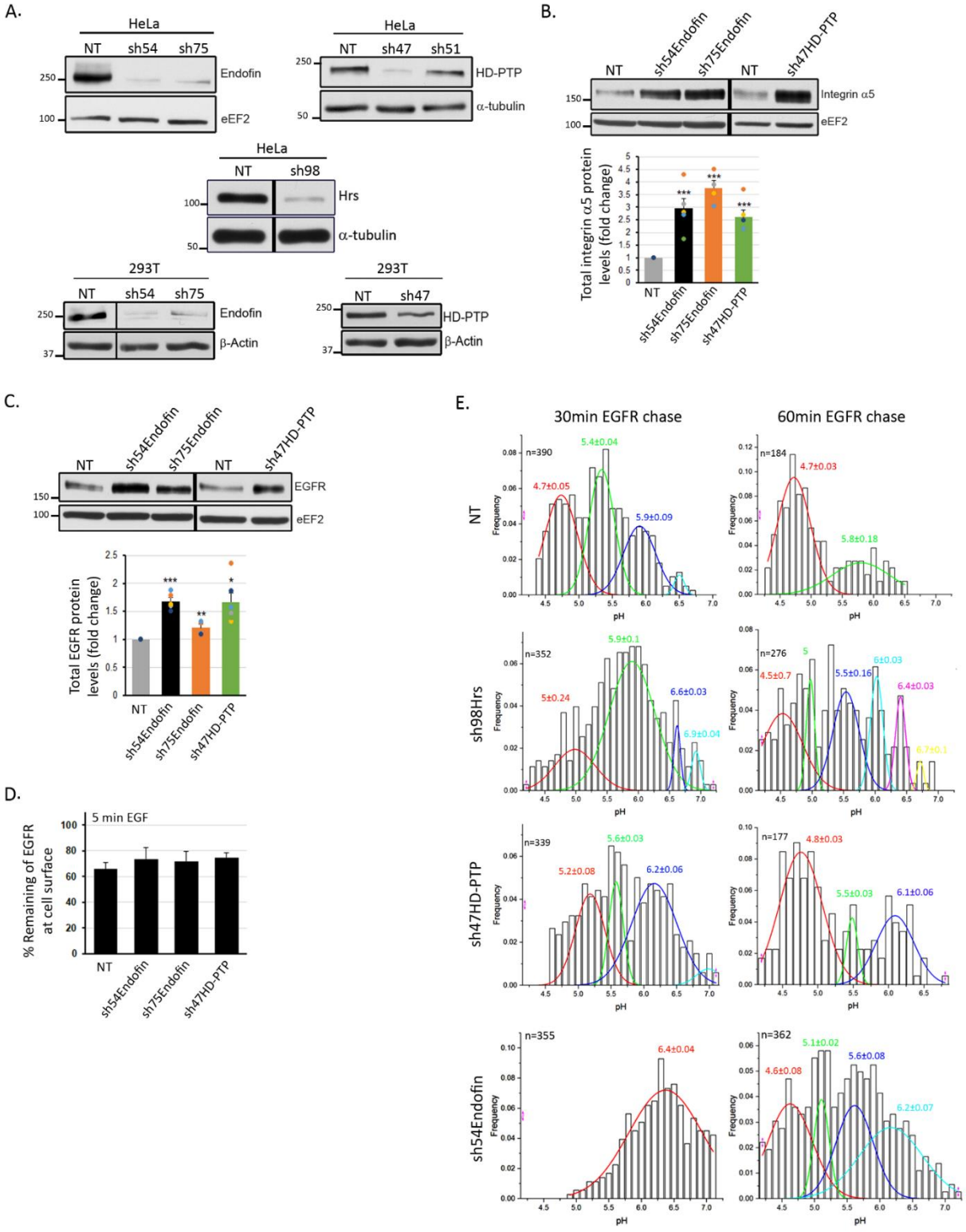
A.
HeLa
NT
sh54
sh75
Endofin
eEF2
HeLa
NT
sh47
sh51
HD-PTP
α-tubulin
HeLa
NT
sh98
Hrs
α-tubulin
293T
NT
sh54
sh75
Endofin
β-Actin
293T
NT
sh47
HD-PTP
β-Actin
B.
NT
sh54Endofin
sh75Endofin
NT
sh47HD-PTP
Integrin α5
eEF2
Total integrin α5 protein levels (fold change)
C.
NT
sh54Endofin
sh75Endofin
NT
sh47HD-PTP
EGFR
eEF2
Total EGFR protein levels (fold change)
D.
5 min EGF
% Remaining of EGFR at cell surface
E.
30min EGFR chase
60min EGFR chase
NT
sh98Hrs
sh47HD-PTP
sh54Endofin
Frequency
pH

Figure S4. Endofin depletion has the same impact on receptor trafficking as Hrs and HD-PTP depletion. Related to Figure 2.

(A) Western blots showing Endofin, HD-PTP and Hrs depletion in HeLa cells and Endofin and HD-PTP depletion in 293T cells using different shRNAs. (B) Western blots showing total protein levels of integrin α5 and (C) EGFR in Endofin- and HD-PTP-depleted HeLa cells compared to NT cells with densitometric analysis using ImageJ software. Integrin α5 and EGFR levels were normalized to eEF2. (D) cs-ELISA assay to detect levels of internalized EGFR upon EGF stimulation (50 ng/ml, 5 min, 37^{o}C) in serum-starved Endofin- and HD-PTP-depleted HeLa cells. For each cell line, levels of EGFR are plotted as percentage remaining at the cell surface compared to unstimulated cells. (E) FRIA representative analysis of FITC-labeled EGFR endocytosis kinetics in serum-starved HeLa cells. Vesicular pH distribution of internalized EGFR after 30 and 60 min of EGF stimulation (50 ng/ml, 37^{o}C) is plotted. The mean vesicular pH of the distinct peaks and the number of vesicles in NT, Endofin-, HD-PTP- and Hrs-depleted HeLa cells are indicated. Data are mean ± SEM of n≥3 independent experiments. Unpaired student t-test: * $p<0.05$, ** $p<0.01$, *** $p<0.001$.

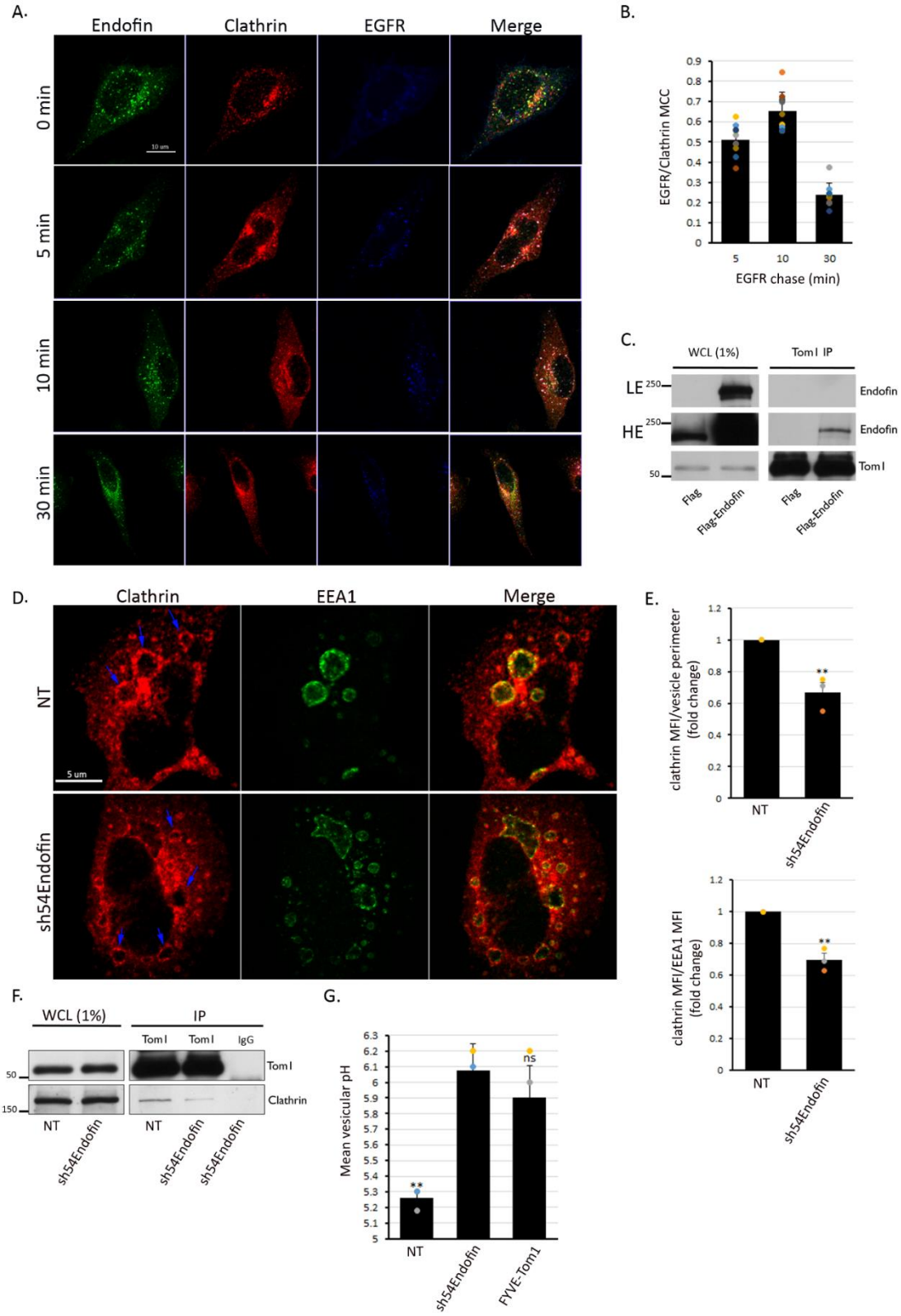
A.
Endofin
Clathrin
EGFR
Merge
0 min
5 min
10 min
30 min
10 um
B.
EGFR/Clathrin MCC
0.9
0.8
0.7
0.6
0.5
0.4
0.3
0.2
0.1
0
5
10
30
EGFR chase (min)
C.
WCL (1%)
Tom1 IP
LE
HE
250
50
Endofin
Endofin
Tom1
Flag
Flag-Endofin
Flag
Flag-Endofin
D.
Clathrin
EEA1
Merge
NT
sh54Endofin
5 um
E.
clathrin MFI/vesicle perimeter (fold change)
1.2
1
0.8
0.6
0.4
0.2
0
**
NT
sh54Endofin
clathrin MFI/EEA1 MFI (fold change)
1.2
1
0.8
0.6
0.4
0.2
0
**
NT
sh54Endofin
F.
WCL (1%)
IP
Tom1
Tom1
IgG
50
150
Tom1
Clathrin
NT
sh54Endofin
NT
sh54Endofin
sh54Endofin
G.
Mean vesicular pH
6.3
6.2
6.1
6
5.9
5.8
5.7
5.6
5.5
5.4
5.3
5.2
5.1
5
**
ns
NT
sh54Endofin
FYVE-Tom1

Figure S5. Endofin depletion decreases clathrin recruitment to early endosomes. Related to Figure 3.

(A) Colocalization analysis of Endofin (green), clathrin (red) and EGFR (blue) in serum-starved HeLa cells. EGFR was stimulated (50 ng/ml EGF, 5 min, 37ºC) and then chased for 0, 5, 10 and 30 min at 37ºC. (B) EGFR and clathrin colocalization was quantified by Mander's colocalization coefficient (MCC) using ImageJ software (experiments n=2, cells n=30). (C) Co-IP experiment performed on 293T cells transiently transfected with Flag-Endofin and stimulated with EGF (50 ng/ml, 15 minutes, 37ºC). Endogenous Tom1 was immunoprecipitated and Endofin co-IP was assessed (Endofin antibody). Cells transfected with Flag-only plasmid were used as an immunoprecipitation control and a fraction of the whole cell lysate (WCL 1%) was loaded to reveal protein content by Western blotting. Low exposure (LE) and high exposure (HE) are shown for Endofin immunoblots. (D) Immunofluorescence to assess clathrin (red) recruitment to early endosomes (EEA1, green) in Endofin-depleted HeLa cells compared to NT cells transiently transfected with Rab5Q79L to induce the formation of enlarged vesicles. Serum-starved cells were stimulated with EGF (50 ng/ml, 5 min, 37ºC) and then EGFR was chased for 10 min at 37ºC before fixation. (E) Clathrin recruitment was quantified by normalizing clathrin Mean Fluorescent Intensity (MFI) to the vesicle perimeter or to EEA1 MFI using ImageJ software (experiments n=3, vesicles n=121). (F) Co-IP experiment performed on Endofin-depleted 293T cells stimulated with EGF (50 ng/ml, 15 minutes, 37ºC). Endogenous Tom1 was immunoprecipitated and clathrin co-IP was assessed compared to NT cells. Rabbit IgG was used as an immunoprecipitation control and a fraction of the whole cell lysate (WCL 1%) was loaded to reveal protein content. (G) Mean vesicular pH of FITC-labeled EGFR-containing endocytic vesicles determined by FRIA in Endofin-depleted HeLa cells complemented with 2xFYVE-Tom1 chimera construct, after 30 min

of EGFR chase (50 ng/ml EGF, 37ºC). Data are mean ± SEM of n=3 independent experiments. Unpaired student t-test: ** $p<0.01$, *** $p<0.001$.

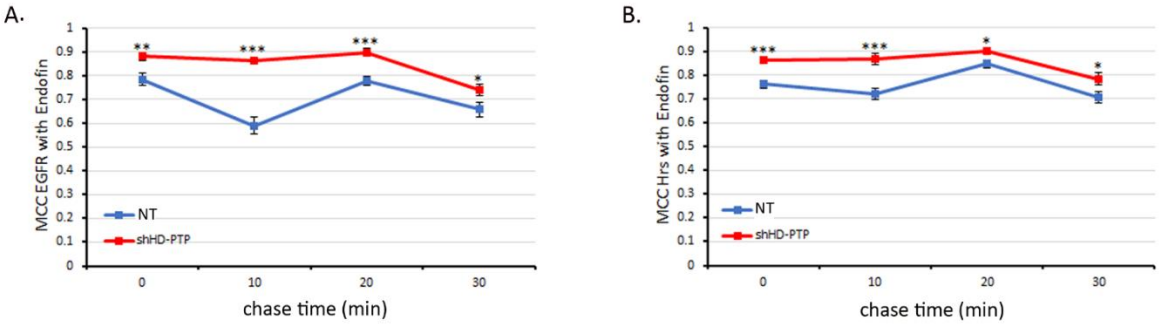
A.
MCC EGFR with Endofin
NT
shHD-PTP
chase time (min)
B.
MCC Hrs with Endofin
NT
shHD-PTP
chase time (min)

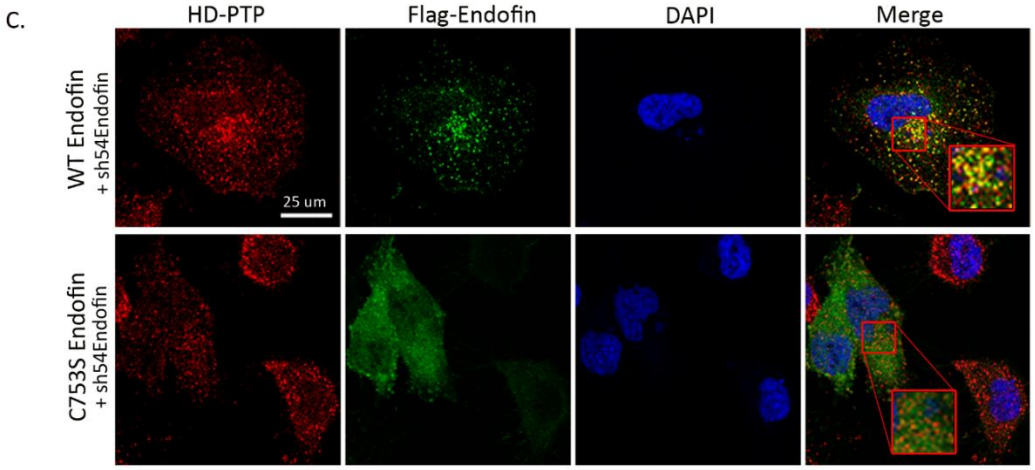
C.
HD-PTP
Flag-Endofin
DAPI
Merge
WT Endofin
+ sh54Endofin
25 um
C753S Endofin
+ sh54Endofin

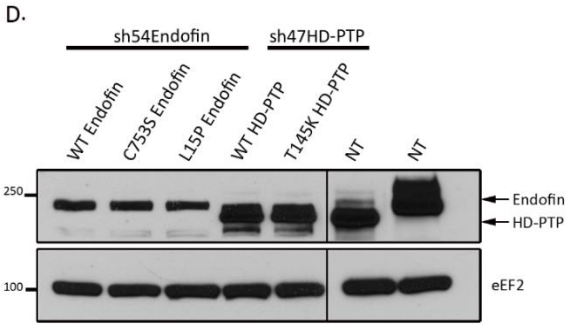
D.
sh54Endofin
sh47HD-PTP
WT Endofin
C753S Endofin
L15P Endofin
WT HD-PTP
T145K HD-PTP
NT
NT
Endofin
HD-PTP
eEF2

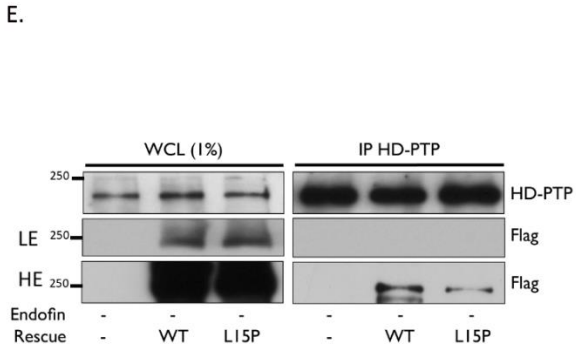
E.
WCL (1%)
IP HD-PTP
HD-PTP
LE
HE
Flag
Flag
Endofin
Rescue
WT
L15P
WT
L15P

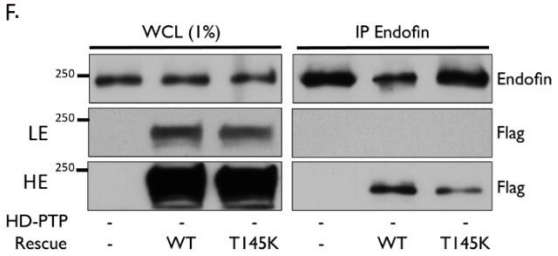
F.
WCL (1%)
IP Endofin
Endofin
LE
HE
Flag
Flag
HD-PTP
Rescue
WT
T145K
WT
T145K

Figure S6. HD-PTP depletion disrupts the dynamic colocalization of EGFR and Hrs with Endofin. Related to Figure 3 and 4.

(A and B) Colocalization analysis of (A) EGFR and (B) Hrs with Endofin in HD-PTP-depleted HeLa cells. Serum-starved cells were stimulated with EGF (50 ng/ml, 5 min, 37^{o}C) then EGFR was chased for 0, 10, 20 and 30 min at 37^{o} C. Mander's Colocalization Coefficient (MCC) was quantified using ImageJ software (n=30). (C) Immunofluorescence staining of endogenous HD-PTP (red) and overexpressed Flag-Endofin (Flag antibody, green) in transiently transfected Endofin-depleted HeLa cells with shRNA resistant Flag-tagged WT-Endofin and C753S-Endofin (FYVE-domain Endofin mutant). (D) Western blotting showing the expression levels of WT- or mutated-Endofin and -HD-PTP in Endofin- and HD-PTP-depleted HeLa cells, respectively, transiently co-transfected with mCherry plasmid. (E) Endofin- and (F) HD-PTP-depleted 293T cells were transiently transfected with WT- and L15P-Endofin or WT- and T145K-HD-PTP, respectively. Serum-starved cells were stimulated with EGF (50 ng/ml, 15 min, 37^{o}C) and after cell lysis endogenous (E) HD-PTP or endogenous (F) Endofin were immunoprecipitated and co-IP of either (E) Flag-Endofin or (F) Flag-HD-PTP were analyzed by Western blotting. WCL is loaded to reveal protein content. LH: Low exposure, HE: High Exposure. Data are mean ± SEM of n=3 independent experiments. Unpaired student t-test: * $p<0.05$, ** $p<0.01$, *** $p<0.001$.

Table S1. List of primers used to clone wild-type and mutant Endofin and HD-PTP. Related to STAR Methods.

Primer Name	Primer Sequence 5'-3'
HD-PTP BirA-N cloning Forward	ATTGGCGCGCCTGAGGCCGTGCCCCGC
HD-PTP BirA-N cloning Reverse	CCGCTCGAGTCAGGTCTTGTTGAGTGTC
HD-PTP BirA-C cloning Forward	CCCAAGCTTGGATGGAGGCCGTGCCCC
HD-PTP BirA-C cloning Reverse	AATGGCGCGCCTGGTCTTGTTGAGTGTCCAG
Endofin BirA-N cloning Forward	CGCGGCGCGCCTGACAGTTATTTTAAAGCAGC
Endofin BirA-N cloning Reverse	CGCGCGGCCGCCTAAAAAAGATGTTCTATAATG
Endofin BirA-C cloning Forward	CGCGGATCCATGGACAGTTATTTTAAAGCAG
Endofin BirA-C cloning Reverse	CGCGGCGCGCCAAAAAAGATGTTCTATAATGAAAAAC
Endofin-pcDNA3-Flag cloning Forward	TATAGGATCCATGGACAGTTATTTTAAAGCAG
Endofin-pcDNA3-Flag cloning Reverse	TATAGCGGCCGCCTAAAAAAGATGTTCTATAATGAAA
Endofin-sh54-mutagenesis Forward	TCTAAGGGAATACGTGGATATCTGCTGG
Endofin-sh54-mutagenesis Reverse	TCTACTGCATCAACTTTCCCACATGTAATTTTAAAGT
HD-PTP-sh47-mutagenesis Forward	ACAAATCCTTACGCTCAACGTCAAC
HD-PTP-sh47-mutagenesis Reverse	CGACTCATGTCGACGCTGTAGG

2.8. References:

AGROMAYOR, M., SOLER, N., CABALLE, A., KUECK, T., FREUND, S. M., ALLEN, M. D., BYCROFT, M., PERISIC, O., YE, Y. & MCDONALD, B. 2012. The UBAP1 subunit of ESCRT-I interacts with ubiquitin via a SOUBA domain. *Structure,* 20**,** 414-428.

AKUTSU, M., KAWASAKI, M., KATOH, Y., SHIBA, T., YAMAGUCHI, Y., KATO, R., KATO, K., NAKAYAMA, K. & WAKATSUKI, S. 2005. Structural basis for recognition of ubiquitinated cargo by Tom1-GAT domain. *FEBS letters,* 579**,** 5385-5391.

ALI, N., ZHANG, L., TAYLOR, S., MIRONOV, A., URBÉ, S. & WOODMAN, P. 2013. Recruitment of UBPY and ESCRT exchange drive HD-PTP-dependent sorting of EGFR to the MVB. *Current biology,* 23**,** 453-461.

ALWAN, H. A., VAN ZOELEN, E. J. & VAN LEEUWEN, J. E. 2003. Ligand-induced lysosomal epidermal growth factor receptor (EGFR) degradation is preceded by proteasome-dependent EGFR de-ubiquitination. *Journal of Biological Chemistry,* 278**,** 35781-35790.

APAJA, P. M. & LUKACS, G. L. 2014. Protein homeostasis at the plasma membrane. *Physiology,* 29**,** 265-277.

APAJA, P. M., XU, H. & LUKACS, G. L. 2010. Quality control for unfolded proteins at the plasma membrane. *Journal of Cell Biology,* 191**,** 553-570.

BACHE, K. G., RAIBORG, C., MEHLUM, A. & STENMARK, H. 2003. STAM and Hrs are subunits of a multivalent ubiquitin-binding complex on early endosomes. *Journal of Biological Chemistry,* 278**,** 12513-12521.

BACHE, K. G., STUFFERS, S., MALERØD, L., SLAGSVOLD, T., RAIBORG, C., LECHARDEUR, D., WÄLCHLI, S., LUKACS, G. L., BRECH, A. & STENMARK, H. 2006. The ESCRT-III subunit hVps24 is required for degradation but not silencing of the epidermal growth factor receptor. *Molecular biology of the cell,* 17**,** 2513-2523.

BARRIERE, H. & LUKACS, G. L. 2008. Analysis of Endocytic Trafficking by Single-Cell Fluorescence Ratio Imaging. *Current protocols in cell biology,* 40**,** 15.13. 1-15.13. 21.

BARRIERE, H., NEMES, C., DU, K. & LUKACS, G. L. 2007. Plasticity of polyubiquitin recognition as lysosomal targeting signals by the endosomal sorting machinery. *Molecular biology of the cell,* 18**,** 3952-3965.

BARRIERE, H., NEMES, C., LECHARDEUR, D., KHAN-MOHAMMAD, M., FRUH, K. & LUKACS, G. L. 2006. Molecular basis of oligoubiquitin-dependent internalization of membrane proteins in Mammalian cells. *Traffic,* 7**,** 282-297.

BELLE, L., ALI, N., LONIC, A., LI, X., PALTRIDGE, J. L., ROSLAN, S., HERRMANN, D., CONWAY, J. R., GEHLING, F. K., BERT, A. G., CROCKER, L. A., TSYKIN, A., FARSHID, G., GOODALL, G. J., TIMPSON, P., DALY, R. J. & KHEW-GOODALL, Y. 2015. The tyrosine phosphatase PTPN14 (Pez) inhibits metastasis by altering protein trafficking. *Sci Signal,* 8**,** ra18.

BUDZINSKA, M. I., VILLARROEL-CAMPOS, D., GOLDING, M., WESTON, A., COLLINSON, L., SNIJDERS, A. P. & SCHIAVO, G. 2020. PTPN23 binds the dynein adaptor BICD1 and is required for endocytic sorting of neurotrophin receptors. *J Cell Sci,* 133.

CHEN, Y.-G., WANG, Z., MA, J., ZHANG, L. & LU, Z. 2007a. Endofin, a FYVE domain protein, interacts with Smad4 and facilitates transforming growth factor-β signaling. *Journal of Biological Chemistry,* 282**,** 9688-9695.

CHEN, Y., LOW, T. Y., CHOONG, L. Y., RAY, R. S., TAN, Y. L., TOY, W., LIN, Q., ANG, B. K., WONG, C. H. & LIM, S. 2007b. Phosphoproteomics identified Endofin, DCBLD2, and KIAA0582 as novel tyrosine phosphorylation targets of EGF signaling and Iressa in human cancer cells. *Proteomics,* 7**,** 2384-2397.

CHRIST, L., RAIBORG, C., WENZEL, E. M., CAMPSTEIJN, C. & STENMARK, H. 2017. Cellular functions and molecular mechanisms of the ESCRT membrane-scission machinery. *Trends in biochemical sciences,* 42**,** 42-56.

DESROCHERS, G., KAZAN, J. M. & PAUSE, A. 2019. Structure and functions of His domain protein tyrosine phosphatase in receptor trafficking and cancer (1). *Biochem Cell Biol,* 97**,** 68-72.

DOYOTTE, A., MIRONOV, A., MCKENZIE, E. & WOODMAN, P. 2008. The Bro1-related protein HD-PTP/PTPN23 is required for endosomal cargo sorting and multivesicular body morphogenesis. *Proceedings of the National Academy of Sciences,* 105**,** 6308-6313.

EDEN, E. R., HUANG, F., SORKIN, A. & FUTTER, C. E. 2012. The role of EGF receptor ubiquitination in regulating its intracellular traffic. *Traffic,* 13**,** 329-337.

ELIAS, J. E. & GYGI, S. P. 2007. Target-decoy search strategy for increased confidence in large-scale protein identifications by mass spectrometry. *Nature methods,* 4**,** 207-214.

GAHLOTH, D., HEAVEN, G., JOWITT, T. A., MOULD, A. P., BELLA, J., BALDOCK, C., WOODMAN, P. & TABERNERO, L. 2017a. The open architecture of HD-PTP phosphatase provides new insights into the mechanism of regulation of ESCRT function. *Scientific Reports,* 7**,** 9151.

GAHLOTH, D., LEVY, C., HEAVEN, G., STEFANI, F., WUNDERLEY, L., MOULD, P., CLIFF, M. J., BELLA, J., FIELDING, A. J. & WOODMAN, P. 2016. Structural basis for selective interaction between the ESCRT regulator HD-PTP and UBAP1. *Structure,* 24**,** 2115-2126.

GAHLOTH, D., LEVY, C., WALKER, L., WUNDERLEY, L., MOULD, A. P., TAYLOR, S., WOODMAN, P. & TABERNERO, L. 2017b. Structural Basis for Specific Interaction of TGFβ Signaling Regulators SARA/Endofin with HD-PTP. *Structure*.

GAHLOTH, D., LEVY, C., WALKER, L., WUNDERLEY, L., MOULD, A. P., TAYLOR, S., WOODMAN, P. & TABERNERO, L. 2017c. Structural Basis for Specific Interaction of TGFβ Signaling Regulators SARA/Endofin with HD-PTP. *Structure,* 25**,** 1011-1024. e4.

GINGRAS, M.-C., ZHANG, Y. L., KHARITIDI, D., BARR, A. J., KNAPP, S., TREMBLAY, M. L. & PAUSE, A. 2009. HD-PTP is a catalytically inactive tyrosine phosphatase due to a conserved divergence in its phosphatase domain. *PloS one,* 4**,** e5105.

GOH, J. B., WALLACE, D. F., HONG, W. & SUBRAMANIAM, V. N. 2015. Endofin, a novel BMP-SMAD regulator of the iron-regulatory hormone, hepcidin. *Scientific reports,* 5.

HESKETH, G. G., PAPAZOTOS, F., PAWLING, J., RAJENDRAN, D., KNIGHT, J. D., MARTINEZ, S., TAIPALE, M., SCHRAMEK, D., DENNIS, J. W. & GINGRAS, A.-C. 2020. The GATOR–Rag GTPase pathway inhibits mTORC1 activation by lysosome-derived amino acids. *Science,* 370**,** 351-356.

HOU, J., DU YAN, Y. L., HUANG, P. & CUI, H. 2020. The Roles of Integrin α5β1 in Human Cancer. *OncoTargets and therapy,* 13**,** 13329.

HUANG, F., KIRKPATRICK, D., JIANG, X., GYGI, S. & SORKIN, A. 2006. Differential regulation of EGF receptor internalization and degradation by multiubiquitination within the kinase domain. *Molecular cell,* 21**,** 737-748.

ICHIOKA, F., TAKAYA, E., SUZUKI, H., KAJIGAYA, S., BUCHMAN, V. L., SHIBATA, H. & MAKI, M. 2007. HD-PTP and Alix share some membrane-traffic related proteins that interact with their Bro1 domains or proline-rich regions. *Archives of biochemistry and biophysics,* 457**,** 142-149.

IYENGAR, P. V. 2017. Regulation of Ubiquitin Enzymes in the TGF-β Pathway. *International journal of molecular sciences,* 18**,** 877.

KATOH, Y., SHIBA, Y., MITSUHASHI, H., YANAGIDA, Y., TAKATSU, H. & NAKAYAMA, K. 2004. Tollip and Tom1 form a complex and recruit ubiquitin-conjugated proteins onto early endosomes. *J Biol Chem,* 279**,** 24435-43.

KAZAN, J. M., LUKACS, G. L., APAJA, P. M. & PAUSE, A. 2019. Single Cell Fluorescence Ratio Image Analysis for Studying ESCRT Function in Receptor Trafficking. *The ESCRT Complexes.* Springer.

KHARITIDI, D., APAJA, P. M., MANTEGHI, S., SUZUKI, K., MALITSKAYA, E., ROLDAN, A., GINGRAS, M.-C., TAKAGI, J., LUKACS, G. L. & PAUSE, A. 2015. Interplay of endosomal pH and ligand occupancy in integrin α5β1 ubiquitination, endocytic sorting, and cell migration. *Cell reports,* 13**,** 599-609.

KIM, S., MISCHERIKOW, N., BANDEIRA, N., NAVARRO, J. D., WICH, L., MOHAMMED, S., HECK, A. J. & PEVZNER, P. A. 2010. The generating function of CID, ETD, and CID/ETD pairs of tandem mass spectra: applications to database search. *Molecular & Cellular Proteomics,* 9**,** 2840-2852.

KNIGHT, J. D., CHOI, H., GUPTA, G. D., PELLETIER, L., RAUGHT, B., NESVIZHSKII, A. I. & GINGRAS, A.-C. 2017. ProHits-viz: a suite of web tools for visualizing interaction proteomics data. *Nature methods,* 14**,** 645-646.

LAHAIE, S., MORALES, D., BAGCI, H., HAMOUD, N., CASTONGUAY, C. E., KAZAN, J. M., DESROCHERS, G., KLAR, A., GINGRAS, A. C., PAUSE, A., COTE, J. F. & KANIA, A. 2019. The endosomal sorting adaptor HD-PTP is required for ephrin-B:EphB signalling in cellular collapse and spinal motor axon guidance. *Sci Rep,* 9**,** 11945.

LAMBERT, J.-P., TUCHOLSKA, M., GO, C., KNIGHT, J. D. & GINGRAS, A.-C. 2015. Proximity biotinylation and affinity purification are complementary approaches for the interactome mapping of chromatin-associated protein complexes. *Journal of proteomics,* 118**,** 81-94.

LEE, J., OH, K.-J., LEE, D., KIM, B. Y., CHOI, J. S., KU, B. & KIM, S. J. 2016. Structural study of the HD-PTP Bro1 domain in a complex with the core region of STAM2, a subunit of ESCRT-0. *PloS one,* 11**,** e0149113.

LIU, G., KNIGHT, J. D., ZHANG, J. P., TSOU, C.-C., WANG, J., LAMBERT, J.-P., LARSEN, B., TYERS, M., RAUGHT, B. & BANDEIRA, N. 2016. Data independent acquisition analysis in ProHits 4.0. *Journal of proteomics,* 149**,** 64-68.

LOBERT, V. H., BRECH, A., PEDERSEN, N. M., WESCHE, J., OPPELT, A., MALERØD, L. & STENMARK, H. 2010. Ubiquitination of α5β1 integrin controls fibroblast migration through lysosomal degradation of fibronectin-integrin complexes. *Developmental cell,* 19**,** 148-159.

LOBERT, V. H. & STENMARK, H. 2012. The ESCRT machinery mediates polarization of fibroblasts through regulation of myosin light chain. *Journal of cell science,* 125**,** 29-36.

LU, Q., HOPE, L. W., BRASCH, M., REINHARD, C. & COHEN, S. N. 2003. TSG101 interaction with HRS mediates endosomal trafficking and receptor down-regulation. *Proceedings of the National Academy of Sciences,* 100**,** 7626-7631.

MA, H., WARDEGA, P., MAZAUD, D., KLOSOWSKA-WARDEGA, A., JUREK, A., ENGSTROM, U., LENNARTSSON, J. & HELDIN, C. H. 2015. Histidine-domain-containing protein tyrosine phosphatase regulates platelet-derived growth factor receptor intracellular sorting and degradation. *Cell Signal,* 27**,** 2209-19.

MAMIŃSKA, A., BARTOSIK, A., BANACH-ORŁOWSKA, M., PILECKA, I., JASTRZĘBSKI, K., ZDŻALIK-BIELECKA, D., CASTANON, I., POULAIN, M., NEYEN, C. & WOLIŃSKA-NIZIOŁ, L. 2016. ESCRT proteins restrict constitutive NF-κB signaling by trafficking cytokine receptors. *Sci. Signal.,* 9**,** ra8.

MANTEGHI, S., GINGRAS, M.-C., KHARITIDI, D., GALARNEAU, L., MARQUES, M., YAN, M., CENCIC, R., ROBERT, F., PAQUET, M. & WITCHER, M. 2016. Haploinsufficiency of the ESCRT component HD-PTP predisposes to cancer. *Cell reports,* 15**,** 1893-1900.

MIERKE, C. T., FREY, B., FELLNER, M., HERRMANN, M. & FABRY, B. 2011. Integrin α5β1 facilitates cancer cell invasion through enhanced contractile forces. *Journal of cell science,* 124**,** 369-383.

MILLER, D. S. J., BLOXHAM, R. D., JIANG, M., GORI, I., SAUNDERS, R. E., DAS, D., CHAKRAVARTY, P., HOWELL, M. & HILL, C. S. 2018. The Dynamics of TGF-beta Signaling Are Dictated by Receptor Trafficking via the ESCRT Machinery. *Cell Rep,* 25**,** 1841-1855 e5.

NORRIS, A., TAMMINENI, P., WANG, S., GERDES, J., MURR, A., KWAN, K. Y., CAI, Q. & GRANT, B. D. 2017. SNX-1 and RME-8 oppose the assembly of HGRS-1/ESCRT-0 degradative microdomains on endosomes. *Proceedings of the National Academy of Sciences,* 114**,** E307-E316.

OKIYONEDA, T., BARRIÈRE, H., BAGDÁNY, M., RABEH, W. M., DU, K., HÖHFELD, J., YOUNG, J. C. & LUKACS, G. L. 2010. Peripheral protein quality control removes unfolded CFTR from the plasma membrane. *Science,* 329**,** 805-810.

PANDEY, A., FERNANDEZ, M. M., STEEN, H., BLAGOEV, B., NIELSEN, M. M., ROCHE, S., MANN, M. & LODISH, H. F. 2000. Identification of a novel immunoreceptor tyrosine-based activation motif-containing molecule, STAM2, by mass spectrometry and its involvement in growth factor and cytokine receptor signaling pathways. *Journal of Biological Chemistry,* 275**,** 38633-38639.

PARKINSON, M. D., PIPER, S. C., BRIGHT, N. A., EVANS, J. L., BONAME, J. M., BOWERS, K., LEHNER, P. J. & LUZIO, J. P. 2015. A non-canonical ESCRT pathway, including histidine domain phosphotyrosine phosphatase (HD-PTP), is used for down-regulation of virally ubiquitinated MHC class I. *Biochemical Journal,* 471**,** 79-88.

PASHKOVA, N., GAKHAR, L., WINISTORFER, S. C., SUNSHINE, A. B., RICH, M., DUNHAM, M. J., YU, L. & PIPER, R. C. 2013. The yeast Alix homolog Bro1 functions as a ubiquitin receptor for protein sorting into multivesicular endosomes. *Developmental cell,* 25**,** 520-533.

PIPER, R. C., DIKIC, I. & LUKACS, G. L. 2014. Ubiquitin-dependent sorting in endocytosis. *Cold Spring Harbor Perspectives in Biology,* 6**,** a016808.

PLATTA, H. W. & STENMARK, H. 2011. Endocytosis and signaling. *Current opinion in cell biology,* 23**,** 393-403.

RAIBORG, C., BACHE, K. G., GILLOOLY, D. J., MADSHUS, I. H., STANG, E. & STENMARK, H. 2002. Hrs sorts ubiquitinated proteins into clathrin-coated microdomains of early endosomes. *Nature cell biology,* 4**,** 394-398.

RAIBORG, C., BACHE, K. G., MEHLUM, A., STANG, E. & STENMARK, H. 2001. Hrs recruits clathrin to early endosomes. *EMBO J,* 20**,** 5008-21.
RAIBORG, C., WESCHE, J., MALEROD, L. & STENMARK, H. 2006. Flat clathrin coats on endosomes mediate degradative protein sorting by scaffolding Hrs in dynamic microdomains. *J Cell Sci,* 119**,** 2414-24.
RODAHL, L. M., STUFFERS, S., LOBERT, V. H. & STENMARK, H. 2009. The role of ESCRT proteins in attenuation of cell signalling. *Biochem Soc Trans,* 37**,** 137-42.
ROSENBERGER, G., KOH, C. C., GUO, T., RÖST, H. L., KOUVONEN, P., COLLINS, B. C., HEUSEL, M., LIU, Y., CARON, E. & VICHALKOVSKI, A. 2014. A repository of assays to quantify 10,000 human proteins by SWATH-MS. *Scientific data,* 1**,** 1-15.
ROW, P. E., CLAGUE, M. J. & URBÉ, S. 2005. Growth factors induce differential phosphorylation profiles of the Hrs–STAM complex: a common node in signalling networks with signal-specific properties. *Biochemical Journal,* 389**,** 629-636.
SACHSE, M., URBÉ, S., OORSCHOT, V., STROUS, G. J. & KLUMPERMAN, J. 2002. Bilayered clathrin coats on endosomal vacuoles are involved in protein sorting toward lysosomes. *Molecular biology of the cell,* 13**,** 1313-1328.
SEET, L.-F. & HONG, W. 2001a. Endofin, an endosomal FYVE domain protein. *Journal of Biological Chemistry,* 276**,** 42445-42454.
SEET, L.-F. & HONG, W. 2005. Endofin recruits clathrin to early endosomes via TOM1. *Journal of cell science,* 118**,** 575-587.
SEET, L.-F., LIU, N., HANSON, B. J. & HONG, W. 2004. Endofin recruits TOM1 to endosomes. *Journal of Biological Chemistry,* 279**,** 4670-4679.
SEET, L. F. & HONG, W. 2001b. Endofin, an endosomal FYVE domain protein. *J Biol Chem,* 276**,** 42445-54.
SHI, W., CHANG, C., NIE, S., XIE, S., WAN, M. & CAO, X. 2007. Endofin acts as a Smad anchor for receptor activation in BMP signaling. *Journal of cell science,* 120**,** 1216-1224.
SIGISMUND, S., AVANZATO, D. & LANZETTI, L. 2018. Emerging functions of the EGFR in cancer. *Molecular oncology,* 12**,** 3-20.
SORKIN, A. & VON ZASTROW, M. 2009. Endocytosis and signalling: intertwining molecular networks. *Nature reviews Molecular cell biology,* 10**,** 609-622.
ST-DENIS, N., GUPTA, G. D., LIN, Z. Y., GONZALEZ-BADILLO, B., VERI, A. O., KNIGHT, J. D., RAJENDRAN, D., COUZENS, A. L., CURRIE, K. W. & TKACH, J. M. 2016. Phenotypic and interaction profiling of the human phosphatases identifies diverse mitotic regulators. *Cell reports,* 17**,** 2488-2501.
STEFANI, F., ZHANG, L., TAYLOR, S., DONOVAN, J., ROLLINSON, S., DOYOTTE, A., BROWNHILL, K., BENNION, J., PICKERING-BROWN, S. & WOODMAN, P. 2011. UBAP1 is a component of an endosome-specific ESCRT-I complex that is essential for MVB sorting. *Current Biology,* 21**,** 1245-1250.
SUNDQUIST, W. I., SCHUBERT, H. L., KELLY, B. N., HILL, G. C., HOLTON, J. M. & HILL, C. P. 2004. Ubiquitin recognition by the human TSG101 protein. *Molecular cell,* 13**,** 783-789.
SZKLARCZYK, D., GABLE, A. L., LYON, D., JUNGE, A., WYDER, S., HUERTA-CEPAS, J., SIMONOVIC, M., DONCHEVA, N. T., MORRIS, J. H. & BORK, P. 2019. STRING v11: protein–protein association networks with increased coverage, supporting functional discovery in genome-wide experimental datasets. *Nucleic acids research,* 47**,** D607-D613.

SZYMANSKA, E., BUDICK-HARMELIN, N. & MIACZYNSKA, M. 2018. Endosomal "sort" of signaling control: The role of ESCRT machinery in regulation of receptor-mediated signaling pathways. *Semin Cell Dev Biol,* 74**,** 11-20.

TEO, G., LIU, G., ZHANG, J., NESVIZHSKII, A. I., GINGRAS, A.-C. & CHOI, H. 2014. SAINTexpress: improvements and additional features in Significance Analysis of INTeractome software. *Journal of proteomics,* 100**,** 37-43.

TOYOSHIMA, M., TANAKA, N., AOKI, J., TANAKA, Y., MURATA, K., KYUUMA, M., KOBAYASHI, H., ISHII, N., YAEGASHI, N. & SUGAMURA, K. 2007. Inhibition of tumor growth and metastasis by depletion of vesicular sorting protein Hrs: its regulatory role on E-cadherin and beta-catenin. *Cancer Res,* 67**,** 5162-71.

URBÉ, S., MILLS, I. G., STENMARK, H., KITAMURA, N. & CLAGUE, M. J. 2000. Endosomal localization and receptor dynamics determine tyrosine phosphorylation of hepatocyte growth factor-regulated tyrosine kinase substrate. *Molecular and Cellular Biology,* 20**,** 7685-7692.

VIETRI, M., RADULOVIC, M. & STENMARK, H. 2020. The many functions of ESCRTs. *Nat Rev Mol Cell Biol,* 21**,** 25-42.

WANG, J., TUCHOLSKA, M., KNIGHT, J. D., LAMBERT, J.-P., TATE, S., LARSEN, B., GINGRAS, A.-C. & BANDEIRA, N. 2015. MSPLIT-DIA: sensitive peptide identification for data-independent acquisition. *Nature methods,* 12**,** 1106-1108.

WANG, T., LIU, N. S., SEET, L. F. & HONG, W. 2010. The emerging role of VHS domain-containing Tom1, Tom1L1 and Tom1L2 in membrane trafficking. *Traffic,* 11**,** 1119-1128.

WEGENER, C. S., MALERØD, L., PEDERSEN, N. M., PRODIGA, C., BAKKE, O., STENMARK, H. & BRECH, A. 2010. Ultrastructural characterization of giant endosomes induced by GTPase-deficient Rab5. *Histochemistry and cell biology,* 133**,** 41.

WEGNER, C. S., RODAHL, L. M. & STENMARK, H. 2011. ESCRT proteins and cell signalling. *Traffic,* 12**,** 1291-7.

WENZEL, E. M., SCHULTZ, S. W., SCHINK, K. O., PEDERSEN, N. M., NÄHSE, V., CARLSON, A., BRECH, A., STENMARK, H. & RAIBORG, C. 2018. Concerted ESCRT and clathrin recruitment waves define the timing and morphology of intraluminal vesicle formation. *Nature communications,* 9**,** 1-18.

YAMAGUCHI, H., WYCKOFF, J. & CONDEELIS, J. 2005. Cell migration in tumors. *Current opinion in cell biology,* 17**,** 559-564.

YAMAKAMI, M., YOSHIMORI, T. & YOKOSAWA, H. 2003. Tom1, a VHS domain-containing protein, interacts with tollip, ubiquitin, and clathrin. *J Biol Chem,* 278**,** 52865-72.

Chapter 3 - Loss of the ESCRT Complex Components Endofin and HD-PTP Enhances the Malignant Phenotypes of Triple Negative Breast Cancer Cells.

Loss of the ESCRT Complex Components Endofin and HD-PTP Enhances the Malignant Phenotypes of Triple Negative Breast Cancer Cells.

Jalal M. Kazan[1,2], Sébastien Tabariès[1,3], Ariadna Pollato Blanco[1,2], Guillaume Desrochers[1,2], Geneviève Lavoie[4,5], Philippe P. Roux[4,5], Peter M. Siegel[1,3], Arnim Pause[1,2].

1. Goodman Cancer Institute, McGill University, Montreal, Quebec, H3A 1A3, Canada.
2. Biochemistry Department, McGill University, Montreal, Quebec, H3G 1Y6, Canada.
3. Experimental Medicine Department, McGill University, Montreal, Quebec, H3G 1Y6, Canada.
4. Department of Pathology and Cell Biology, Université de Montréal, Montreal, Quebec, H3C 3J7, Canada.
5. Institute for Research in Immunology and Cancer – IRIC, Université de Montréal, Montreal, Quebec, H3T 1J4, Canada.

Key words: Endofin, HD-PTP, cell surface receptors, migration, invasion, metastasis, cancer.

3.1. Abstract:

Cell surface receptors play a critical role in cancer progression. Endofin/*ZFYVE16* directly binds to HD-PTP/*PTPN23* to regulate the lysosomal degradation of activated/internalized cell surface receptors. HD-PTP is a haploinsufficient tumor suppressor and its downregulation promotes breast tumorigenesis. However, the role of Endofin in cancer is still uncharacterized. Here, we show that Endofin and HD-PTP depletion in HeLa cells upregulated a core group of cell surface receptors and engaged gene expression programs involved in cancer metastasis. Moreover, *ZFYVE16* and *PTPN23* heterozygous deletions were shown to be most frequent in patients with basal-like breast cancer subtype and correlated with poor patient survival. Endofin and HD-PTP depletion in MDA-MB-231 cells increased total integrin α5 receptor levels, hyperactivated its downstream signaling and increased cell migration/invasion. Interestingly, HD-PTP depletion increased 4T1 lung metastasis in a syngeneic tumor mouse model. Our data demonstrates that most of the receptors with an elevated plasma membrane levels are in common upon Endofin or HD-PTP depletion, which in turn increases receptor signaling and triggers an invasive phenotype in triple negative breast cancer cells. Furthermore, HD-PTP plays a critical role in lung metastasis of triple negative breast cancer cells. Hence, Endofin might exert a tumor suppressor activity.

3.2. Introduction:

Cell surface receptors regulate several cellular processes such as proliferation, differentiation, survival and cell migration/invasion. Upon ligand stimulation, activated cell surface receptors undergo ubiquitination, internalization and will be either recycled back to the plasma membrane or sorted towards lysosomal degradation. Perturbations in sorting activated cell surface receptors towards lysosomal degradation stabilize receptors at the plasma membrane and hyperactivate their downstream signaling, a well-recognized hallmark of cancer (Mellman et al., 2013, Wegner et al., 2011). The endosomal sorting complexes required for transport (ESCRT) machinery mediates the sorting of internalized/ubiquitinated cell surface receptors towards lysosomal degradation and attenuate downstream signaling through the formation of multivesicular bodies (Raiborg et al., 2009). Therefore, ESCRT proteins exert a tumor suppressor activity (Mattissek et al., 2014).

The ESCRT protein HD-PTP/*PTPN23* regulates the lysosomal degradation of several cell surface receptors involved in tumorigenesis such as PDGFRβ, integrins, EGFR and TGFβ/BMP receptors (Ali et al., 2013, Doyotte et al., 2008, Kharitidi et al., 2015, Ma et al., 2015, Miller et al., 2018). We have previously reported that HD-PTP depletion hyperactivates integrin α5β1 signaling and increases cell migration (Kharitidi et al., 2015). In addition, we showed that *Ptpn23* exerts a haploinsufficient tumor suppressor activity since its heterozygous deletion induced spontaneous B cell lymphoma in mice (Manteghi et al., 2016). It was also shown that *PTPN23* suppression induces an invasive phenotype in mammary epithelial cells (Lin et al., 2011), and promotes breast tumorigenesis (Zhang et al., 2017). Furthermore, the decrease in *PTPN23* mRNA levels correlates with poor survival of breast cancer patients (Manteghi et al., 2016).

Endofin/*ZFYVE16*, a FYVE-domain protein recruited to early endosomes, binds directly to HD-PTP (Gahloth et al., 2017c), and regulates EGFR and integrin α5 lysosomal targeting by promoting HD-PTP interaction with ESCRT-0 and early endosomal cargo (Kazan et al., 2021). In addition, Endofin depletion increases the density and the stability of EGFR and integrin α5 at the plasma membrane, sustains receptor signaling and increases cell migration (Kazan et al., 2021). Furthermore, *ZFYVE16* heterozygous deletion and negative Z-scores, correlating with poor patient survival, are frequent in several types of human cancers, including breast cancer. Of note, the deletion of SARA, Endofin's homologue, promotes skin tumor formation and malignant progression in mice (Chang et al., 2014). However, the role of Endofin as a tumor suppressor is still uncharacterized.

In this study, we compared the impact of Endofin or HD-PTP depletion on the cell surface proteome and the downstream transcriptional pathways of HeLa cells. In addition, we investigated the effect of Endofin or HD-PTP depletion on receptor signaling, cell migration/invasion and the *in vivo* metastasis of triple negative breast cancer cells.

3.3. Results:

Individual depletion of Endofin or HD-PTP increases the cell surface localization of various receptors and engages transcriptional pathways involved in cancer metastasis:

We have previously shown that Endofin or HD-PTP depletion in HeLa cells increases the plasma membrane density of EGF and integrin α5 receptors (Kazan et al., 2021, Kharitidi et al., 2015). Moreover, *Ptpn23* heterozygous deletion in mice increased integrin β1 receptor levels at the surface of lymphoma B cells (Manteghi et al., 2016). We wanted to investigate whether

Endofin or HD-PTP depletion affects the plasma membrane density of additional receptors, thus we performed cell surface biotinylation-mass spectrometry on serum-starved Endofin- or HD-PTP-depleted HeLa cells (Figure S1A and B). Results demonstrated that alterations in the cell surface receptor proteome, upon individual depletion of Endofin or HD-PTP, were positively correlated (Figure S1C). Moreover, Endofin or HD-PTP depletion showed 38 receptors in common, with an increased plasma membrane localization (Figure S1D). Receptors that were increasingly localized to the plasma membrane in Endofin- or HD-PTP-depleted HeLa cells belonged to different cell surface receptor families, including: cell adhesion molecules (CAMs), receptor tyrosine kinases (RTKs), glucocorticoid receptors, serine/threonine kinase receptors, solute carriers, metzincin metallopeptidases, ABC transporters, cytokine receptors and G protein-coupled receptors (Figure 1A and S1E).

Further analysis of our cell surface proteomics data showed that Endofin and HD-PTP depletion in HeLa cells upregulated cell surface receptors involved in the different steps of cancer metastasis, such as: cell migration, hypoxia and cellular extravasation (Figure 1B).

Increase in receptor levels at the plasma membrane may hyperactivate downstream signaling and enhance the activation of downstream transcriptional pathways, which in turn could alter different cellular processes, such as: proliferation, differentiation, survival and migration/invasion. To investigate whether alterations in the cell surface proteome, upon Endofin or HD-PTP depletion, affects downstream transcriptional pathways, RNA-sequencing (RNAseq) was performed on serum-starved Endofin- or HD-PTP-depleted HeLa cells (Figure S2A, B and C). Indeed, results have shown that the expression of several genes related to tumorigenesis, cell migration, epithelial-to-mesenchymal transition (EMT) and hypoxia were upregulated upon individual depletion of Endofin or HD-PTP (Figure 2A, B, C and D).

Taken together, our cell surface proteomics and RNAseq data demonstrate that Endofin or HD-PTP depletion increases the cell surface localization of certain cell surface receptors, where most of the receptors are in common upon both individual depletions, and initiates gene expression programs that might enhance tumorigenesis and cancer progression.

ZFYVE16 and *PTPN23* heterozygous deletions are frequent in breast cancer patients:

We have previously shown that *ZFYVE16* and *PTPN23* heterozygous deletions are frequent in several types of human cancers (Kazan et al., 2021, Manteghi et al., 2016). In addition, we showed negative Z-scores for *ZFYVE16* and downregulation in HD-PTP protein levels in different types of human cancers, including breast cancer (Kazan et al., 2021, Manteghi et al., 2016). Therefore, we investigated *ZFYVE16* and *PTPN23* gene alteration and expression in breast cancer patients using bioinformatics approaches. Analysis of data available through the cBioPortal revealed that *ZFYVE16* heterozygous deletion in patients with breast invasive ductal carcinoma is more frequent (~ 30%) than homozygous deletions (< 2%) (Figure 3A). Of note, *ZFYVE16* homozygous deletions also occur at a very low frequency (< 3%) in several types of human cancers (Figure S3A). Moreover, breast cancer patients with *ZFYVE16* heterozygous deletion showed a decrease in overall survival rate compared to an unaltered group (Figure 3B).

Since Endofin and HD-PTP depletion delays the lysosomal degradation of activated EGFR and increases its total protein levels (Kazan et al., 2021), we assessed the correlation between *ZFYVE16* and *PTPN23* expression and EGFR in breast cancer patients. Interestingly, results showed that the expression of both *ZFYVE16* and *PTPN23* negatively correlated with EGFR expression (Spearman's correlation= -0.403 and -0.214, respectively) (Figure 3C).

Furthermore, we looked at *ZFYVE16* and *PTPN23* gene alteration in different subtypes of human breast cancer. Patients with basal-like breast cancer subtype showed higher frequency of *ZFYVE16* and *PTPN23* heterozygous deletions (Figure 3D) and a decrease in *ZFYVE16* Z-score compared to other breast cancer subtypes (Figure 3E). In addition, patients with stage IV breast cancer showed a decrease in *ZFYVE16* mRNA levels compared to other breast cancer stages (Figure S3B). In conclusion, our bioinformatics data demonstrates that *ZFYVE16* gene alteration and downregulation are frequent in breast cancer patients and correlate with poor patient survival.

HD-PTP depletion increases 4T1 lung metastasis:

PTPN23 suppression promotes breast tumorigenesis in a xenograft tumor mouse model (Zhang et al., 2017). In addition, our cell surface proteomics and RNAseq data showed an upregulation in cell surface receptors and an engagement of gene expression programs involved in cancer metastasis upon HD-PTP depletion in HeLa cells. Therefore, we knocked-down HD-PTP expression in 4T1 cells, triple negative highly metastatic murine breast cancer cells, to assess metastasis *in vivo* (Figure 4A). Upon HD-PTP depletion, integrin α5 total protein levels increased ~ 1.5-2-fold compared to NT cells (Figure 4B). In addition, adhesion of HD-PTP-depleted 4T1 cells to fibronectin coated surfaces increased ~ 1.6-2-fold compared to NT cells (Figure 4C).

Next, we injected HD-PTP-depleted 4T1 cells in the mammary fat pad of BALB/c mice to assess tumor growth and lung metastasis. HD-PTP depletion did not affect tumor growth compared to mice injected with NT cells (Figure 4D). However, HD-PTP depletion increased the area of lung metastatic lesions (~ 50-75%) compared to mice injected with NT cells (~ 25%) (Figure 4E). In addition, the number of lung metastatic lesions increased (~ 20 lesions/mouse), upon HD-PTP depletion, compared to mice injected with NT cells (~ 10 lesions/mouse) (Figure 4E).

Unfortunately, we were not able to knock-down Endofin expression more than 40% in 4T1 cells (Figure S4A), hence it was not feasible to assess Endofin-depleted 4T1 tumor growth and metastasis. In conclusion, this data clearly shows that HD-PTP depletion increases 4T1 lung metastasis.

Endofin and HD-PTP depletion in MDA-MB-231 cells hyperactivate downstream signaling and enhance cell migration/invasion:

ZFYVE16 and *PTPN23* heterozygous loss are more frequent in patients with basal-like breast cancer subtype. Endofin and HD-PTP depletion in HeLa cells upregulated cell surface receptors and genes involved in cancer progression, therefore we knocked-down Endofin and HD-PTP expression in MDA-MB-231, a triple negative basal-like highly metastatic human breast cancer cell line (Figure S4B). Endofin and HD-PTP depletion increased integrin α5 total receptor levels ~ 1.3-1.8-fold compared to NT cells (Figure 5A). However, Endofin and HD-PTP depletion in MDA-MB-231 cells showed a minimal effect on integrin α5 plasma membrane density, measured by cell surface-ELISA (Figure S4C). Interestingly, Endofin and HD-PTP depletion in unstimulated serum-starved MDA-MB-231 cells showed an increase in the levels of pSrc and pErk1/2 compared to NT cells (Figure 5B). Moreover, cell migration, measured by a real time cell analyzer, increased > 1.5-fold in Endofin- and HD-PTP-depleted MDA-MB-231 cells (Figure 5C). In addition, cell invasion increased ~ 1.4-fold and > 2-folds upon Endofin and HD-PTP depletion, respectively (Figure 5D).

Finally, this data demonstrates that Endofin and HD-PTP depletion in MDA-MB-231 breast cancer cells hyperactivate downstream signaling and increase cell migration/invasion.

3.4. Discussion:

Here we unraveled the role of Endofin and HD-PTP in regulating the plasma membrane density of several receptors known to be involved in cancer progression, a process which also regulates the activation of downstream transcriptional pathways thus affecting several cellular processes such as cell migration and invasion which are hallmarks of cancer metastasis. Our findings can be summarized as follows: i) Endofin and HD-PTP depletion in HeLa cells increased the cell surface levels of receptors in common and engaged gene expression programs involved in cancer progression. ii) *ZFYVE16* and *PTPN23* heterozygous deletions are most frequent in basal-like breast cancer subtype and correlate with poor patient survival. iii) *ZFYVE16* and *PTPN23* expressions negatively correlated with EGFR expression in breast cancer patients. iv) HD-PTP depletion increased 4T1 total integrin α5 receptor levels *in vitro* and lung metastasis *in vivo*. v) Endofin and HD-PTP depletion in MDA-MB-231 cells increased total integrin α5 receptor levels, hyperactivated its downstream signaling and increased cell migration/invasion.

CAMs such as integrins and selectins at the plasma membrane of cancer cells facilitate metastasis by mediating cell-cell and cell-extracellular matrix (ECM) interaction (Bendas et al., 2012). Upon integrin interaction with the ECM, the activation of downstream FAK or Src family kinases alter cellular morphology/polarity and migratory properties of cells (Huveneers et al., 2009). The ubiquitous presence of integrins at the cell surface of tumor, blood, endothelial and stromal cells demonstrate that integrins are essential key regulators of the metastatic cascade (Bendas et al., 2012). For instance, the expression of integrin αvβ3, αvβ5, α5β1, α6β4 at the plasma membrane of tumor cells correlates with the metastatic progression of melanoma, breast carcinoma, prostate, pancreatic and lung cancer (Desgrosellier et al., 2010). Of note, it is shown that integrin α5 expression in human breast cancer mediates bone metastasis and serves as a

therapeutic target for the treatment of osteolytic lesions (Pantano et al., 2021). Furthermore, the suppression of integrin α3β1 decreases MDA-MB-231 lung metastasis in a xenograft mouse model (Miskin et al., 2021). In line with our data HD-PTP depletion increased 4T1 total integrin α5 receptor levels *in vitro* and lung metastasis *in vivo*. In addition, integrin α5 total receptor levels and its downstream signaling increased upon Endofin and HD-PTP depletion in MDA-MB-231 cells.

Upregulation of several types of RTKs such as EGFR, VEGFR, PDGFR, IGFR and FGFR is found in different types of cancers including breast cancer (Lemmon et al., 2010, Palmieri et al., 2007, Tomiguchi et al., 2016). RTKs upregulation at the plasma membrane increase breast cancer aggressiveness and decrease overall and disease-free survival (Templeton et al., 2014). Pathways known to be activated by RTKs include ERK1/2, STAT, JAK and Akt which all have a direct role in cancer progression (Butti et al., 2018). Importantly, the upregulation and activation of RTKs such as EGFR, Her2 and IGF1R induced drug resistance through the activation of Akt and MAPK pathways (Ring et al., 2004). Moreover, VEGFR1 activation induced EMT in cancer cells thus promoting invasion and metastasis in breast cancer models (Ning et al., 2013). This coincides with the elevation of plasma membrane levels of CAMs and RTKs upon Endofin and HD-PTP depletion in HeLa cells, and with the induction of an invasive phenotype in triple negative breast cancer cells.

We have already established that Endofin/HD-PTP direct interaction is required for an efficient EGFR sorting towards lysosomal degradation (Kazan et al., 2021). Moreover, Endofin and HD-PTP depletion in HeLa cells increase the density and stability of both EGFR and integrin α5 at the plasma membrane and sustain receptor signaling (Kazan et al., 2021). HD-PTP is a haploinsufficient tumor suppressor, and *Ptpn23* heterozygous deletion in mice induces B cell

lymphoma and increases integrin β1 receptor levels at the plasma membrane of lymphoma B cells, which in turn increases cancer cell dissemination (Manteghi et al., 2016). SARA protein, Endofin's homologue, also binds directly to HD-PTP (Gahloth et al., 2017c), and its depletion delays the degradation of activated EGFR (Kostaras et al., 2013). Interestingly, SARA was also shown to exert a tumor suppressor activity since its deletion in mice promotes skin tumorigenesis and malignant progression (Chang et al., 2014). Since HD-PTP depletion increased 4T1 lung metastasis, therefore Endofin might also suppress cancer metastasis.

In this study, we show that HD-PTP depletion increased breast cancer metastasis to the lungs, and Endofin and HD-PTP depletion induced an invasive phenotype in triple negative breast cancer cells. We propose that Endofin and HD-PTP depletion favors the upregulation of cell surface receptors involved in cancer progression. Therefore, the downstream receptor signaling is hyperactivated leading to the engagement of gene expression programs involved in cancer metastasis. Future studies are required to understand whether certain receptor candidates, upregulated upon HD-PTP depletion, are directly involved in the increase of 4T1 lung metastasis (e.g., integrin α5), and whether Endofin exerts the same effect as HD-PTP on cancer metastasis.

3.5. Materials and Methods:

Constructs, reagents and cell culture:

4T1 (ATCC® CRL-2539™) and MDA-MB-231 (Peter Siegel's Lab) cells were cultured in RPMI, 10% FBS (Wisent). MISSION® shRNA Lentiviral plasmids pLKO.1-puro for human Endofin (clone ID: NM_014733.2-4263s1c1 (sh54), NM_014733.3-3858s21c1 (sh75)), human HD-PTP (clone ID: NM_015466.x-571s1c1 (sh47), NM_015466.x-887s1c1 (sh51)), murine HD-

PTP (clone ID: XM_135197 (sh43), XM_135197 (sh46)) and empty vector (MISSION® pLKO.1-puro Empty Vector Control Plasmid DNA, SHC001) were purchased from Sigma.

Purification and enrichment of cell-surface proteins:

Two proteomic procedures for the enrichment of cell-surface proteins were adapted from previously published methods (Weekes et al., 2010). For Cell Surface Sapture (CSC), cells were chilled on ice, rinsed twice with ice-cold biotinylation buffer [phosphate buffered saline (PBS), pH 7.4, supplemented with 1mM CaCl2 and 0.5mM MgCl2], and then incubated with 1 mM sodium (meta)periodate (Sigma-Aldrich) at 4 °C for 30 min in the dark. The mildoxidation reaction was quenched by addition of glycerol at a final concentration of 1 mM. Cells were then washed twice with ice-cold PBS (pH 7.4) supplemented with 5% (v/v) FBS, and biotinylated for 1 h at 4 °C with a mix of 100 μM aminooxybiotin (Biotium Inc.) and 10mM aniline (Sigma-Aldrich) in ice-cold PBS (pH 6.7) supplemented with 5% FBS. Cells were then washed once with ice-cold PBS pH 7.4/ 5% FBS, and then once with ice-cold biotinylation buffer. Biotinylated cells were incubated in Surfaceome Lysis Buffer [noted as SLB; 1% Triton X-100, 150mM NaCl, 10mM Tris–HCl, pH 7.6, 5mM iodoacetamide (Sigma-Aldrich), 1× protease inhibitor (cOmplete, without EDTA, Roche), 1mM sodium orthovanadate (Na3VO4), and 1mM phenylmethylsulfonyl fluoride (PMSF)] for 30 min at 4 °C. Cell debris and nuclei were removed by successive centrifugation for 10 min at 4 °C, initially at 2800 × g and then 16,000 × g. Next, biotinylated proteins were isolated from 10 mg total protein by incubating cell lysates with high-capacity streptavidin agarose resin (Thermo Fisher Scientific) for 2 h at 4 °C. Beads were washed extensively with intermittent centrifugation at 1000 × g for 5 min to eliminate all potential contaminants bound to biotinylated proteins. Three washes were performed with SLB, once with PBS pH 7.4/0.5% (w/v) sodium dodecyl sulfate (SDS), and then beads were incubated with PBS/0.5% SDS/100mM dithiothreitol

(DTT), for 20 min at RT. Further washes were performed with 6M urea in 100mM Tris–HCl pH 8.5, followed by incubation with 6M urea/100mM Tris–HCl pH 8.5/50mM iodoacetamide, for 20 min at RT. Additional washes were performed with 6M urea/100mM Tris–HCl pH 8.5, PBS pH 7.4 and then water. Biotinylation efficiency was confirmed by blotting aliquots of cell lysates with streptavidin horseradish peroxidase (HRP) (Dilution 1:50,000). For proteomic analysis, beads were rinsed thrice with 50mM ammonium bicarbonate (NH4HCO3) pH 8.5, and re-suspended in 400 µL of 50mM NH4HCO3 pH 8.5 containing 4 µg of proteomics grade trypsin (Sigma-Aldrich), overnight at 37 °C. The proteins were further digested with an additional 4 µg trypsin for 4 h at 37 °C. The resulting tryptic peptides were then collected by centrifugation at 10,000 × g, for 10 min at RT. The beads were washed twice with MS grade water and the tryptic fractions pooled. The tryptic fractions were dried to completion in a SpeedVac and re-suspended in MS solvent (5% aqueous Acetonitrile (ACN), 0.2% FA). For Cell Surface Biotinylation (CSB), cells were chilled on ice, washed twice with ice-cold biotinylation buffer, and incubated with 1 mg/mL Sulfo-NHS LCbiotin (resuspended in biotinylation buffer) for 1 h at 4 °C. The biotinylation reaction was quenched by addition of 100mM glycine for 10 min at 4 °C, followed by two washes with ice-cold biotinylation buffer. Biotinylated cells were lysed in SLB, proteins isolated and digested for MS analysis as described above.

Mass spectrometry and database searches:

Samples were loaded on a 1.5 µL C18 pre-column (Optimize Technologies) connected directly to the switching valve. They were separated on a homemade reversed-phase column (150 µm i.d. by 150 mm) with a 56-min gradient from 10 to 30% ACN/0.2% FA and a 600-nl/min flow rate on a Ultimate 3000 LC system (Eksigent, Dublin, CA) connected to an QExactive Plus (Thermo Fisher Scientific, San Jose, CA). Each full MS spectrum acquired at a resolution of

70,000 was followed by 12 tandem-MS (MS–MS) spectra on the most abundant multiply charged precursor ions. Tandem-MS experiments were performed using collision-induced dissociation (CID) at a collision energy of 27%. Proteomic samples were analyzed as biological, back-to-back triplicates per condition. Peptides were identified using PEAKS 7.0 (Bioinformatics Solutions, Waterloo, ON) and peptide sequences were blasted against the Rat Uniprot database. Mass tolerances on precursor and fragment ions were 10 ppm and 0.01 Da, respectively. The false discovery rate (FDR) for peptide and protein was set to 0.5%. The minimum number of peptides per protein was set to 2, and minimum peptide length was set to ~6 amino acids. Search criteria included a static modification of cysteine residues of +57.0214 Da; a variable modification of +15.9949 Da to include potential oxidation of methionines; and a modification of +79.966 on serine, threonine, or tyrosine for the identification of phosphorylation. The data were visualized with Scaffold 4.4.6. Normalized Spectral abundance factors (NSAF) for the significantly upregulated or downregulated cell-surface proteins by shEndofin or shHD-PTP (Log2 FC values), for each of the replicates of CSC or CSB technique, were extracted from Scaffold 4.4.6.

Label-free quantification and data processing:

Peptide precursor intensities were extracted using an integral algorithm of PEAKS® software 8.05. Proteins were then selected based on their detection in at least two replicates of the same biological condition (either Control or shEndofin/shHD-PTP), with a minimum of two unique peptides, which were verified for uniqueness and leucine/isoleucine switch using the neXt-Prot checker54. These proteins were considered as identified with high-confidence. Gene Ontology Cellular Component (GO.CC) terms and functional annotations were queried for all identified proteins using g:profiler (http://biit.cs.ut.ee/gprofiler/ index.cgi) to get an objective estimation about the number of proteins specific to the cell surface. We then manually sorted all

identified proteins such that we kept those that contain at least one cell surface-exposed domain, which could be potentially biotinylated. To do so, we analyzed proteins identified with highconfidence by querying them against the UniProt online database (http://www. uniprot.org/). We then defined proteins as integral to plasma membrane proteins when they contained at least one transmembrane domain and an extracellular region (e.g., CAMs, RTKs), as belonging to secretory or extracellular components when they were known to be secreted and potentially interact with the cell surface (e.g., growth factors, cytokines), and as potential contaminants when they corresponded to proteins that do not possess an extracellular domain (e.g., abundant intracellular proteins that may interact with streptavidin beads, plasma membranetethered proteins that interact intracellularly with a biotinylated protein). Proteins were considered differentially upregulated by shEndofin/shHD-PTP if log2 FC (shEndofin or shHD-PTP /Control) values were ≥ 2, and downregulated if ≤ -2. Some proteins were only identified in the shEndofin/shHD-PTP or Control condition, making it impossible to calculate fold-change values. The value "±1.4 (Log2FC=±0.5)" was chosen as it was higher than our highest and lowest sh54Endofin or sh47HD-PTP/Control fold-change, respectively.

RNA-sequencing:

For transcriptome analysis, total RNA was extracted using RNeasy mini Kit (Qiagen). Presence of contamination was assessed by NanoDrop (ThermoFisher Scientific) using 260/280 and 260/230 ratios. Quantification of total RNA was made by QuBit (ABI) and 500 ng of total RNA was used for library preparation. Quality of total RNA was assessed with the BioAnalyzer Nano (Agilent) and all samples had a RIN above 9.8. Library preparation was done with the KAPA mRNA-seq stranded kit (KAPA, Cat no. KK8420). Ligation was made with 9 nM final concentration of Illumina index and 10 PCR cycles was required to amplify cDNA libraries.

Libraries were quantified by QuBit and BioAnalyzer. All libraries were diluted to 10 nM and normalized by qPCR using the KAPA library quantification kit (KAPA; Cat no. KK4973). Libraries were pooled to equimolar concentration. Sequencing was performed with the Illumina Hiseq2000 using the Hiseq Reagent Kit v3 (200 cycles, paired-end) using 1.8 nM of the pooled library. Around 120M paired-end PF reads were generated per sample. Library preparation and sequencing was made at the Institute for Research in Immunology and Cancer's (IRIC) Genomics Platform. Sequence data were mapped to the reference genome using the Illumina Casava 1.8.1 package and Refseq release 63. Expression levels of mRNA were displayed as reads per kilobase per million (RPKM), these RPKM values were used to analyze the functional enrichment of genes associated with the sequencing data by gene set enrichment analysis (GSEA). Data are representative of three independent biological experiments. RPKM values of each biological replicate were averaged for Control and shEndofin or shHD-PTP conditions, and Log2 FC (shEndofin or shHD-PTP/Control) values were calculated. Transcripts were considered differentially upregulated by shEndofin or shHD-PTP if log2 FC (shEndofin or shHD-PTP /Control) values were ≥ 2, and downregulated if ≤ -2 ($P < 0.05$).

Human data analysis:

All bioinformatics data were extracted from the cBioPortal database from different studies listed in Figure 3 legend.

***In vivo* metastasis assay:**

4T1 cells (500 cells) were injected with matrigel in the mammary fat pad of BALB/c mice. Tumor growth was measured by a caliber. Four weeks post-injection and when tumor reached ~ 500 mm^3 volume, tumors were resected. Mice were left two weeks post-resection and

then euthanized. Lungs were collected for H and E staining. Lung metastatic lesion area/tissue area was quantified using Imagescope software (Aperio). The mice were housed in facilities managed by McGill University Animal Resources Centre and all animal experiments were conducted under a McGill University-approved Animal Use Protocol (AUP #4722), which was reviewed by the Facility Animal Care Committee for the Faculty of Medicine (Committee A). All projects involving live animals were subjected to peer review for scientific merit, in accordance with guidelines established by the Canadian Council on Animal Care.

Cell surface measurements using cs-ELISA:

Cell-surface ELISA-based assays were performed in live cells as described by Apaja et al. (Apaja et al., 2010). Briefly, cells were starved for 2 h in serum-free RPMI media, labeled with integrin α5 antibody on ice, and detected with horseradish peroxidase (HRP)-conjugated secondary antibody (Jackson ImmunoResearch) and Amplex Red (Life Technologies). Antibodies are listed in Table S1.

Cell migration/invasion assays:

Migration/invasion assays were performed using xCELLigence system (ACEA Biosciences). 30,000 MDA-MB-231 cells in serum-free RPMI media were allowed to migrate for 24 h or to invade for 48 h towards 10% FBS medium serving as a chemoattractant. As a negative control, serum-free media was used. Rate of cellular migration/invasion was analyzed by plotting for the slope of the real-time migration/invasion curve of each cell line tested.

Signaling experiment:

MDA-MB-231 cells were collected and lysed on ice in buffer B (50 mM Tris pH 7.5, 150 mM NaCl, 1,5 mM MgCl2, 1 mM EDTA, 1% triton x-100, 5% glycerol, 20 mM NaF, 5 mM NaPPi, 1 mM Na3VO4, 2 mM imidazole, 175 µg/ml PMSF and cOmplete (Roche) protease inhibitors). Protein extracts were separated by SDS-PAGE and analyzed by Western blotting. Antibodies are listed in Table S1.

Quantification and Statistical Analysis:

Western blots were quantified using imageJ software. Statistical analysis was performed using Microsoft Excel software. Significance was determined by paired two-tailed Student's t test, and data with p values: *<0.05, **<0.01 and ***<0.001 are considered to be significant.

Acknowledgements:

J.M.K holds Fonds de Recherche Sante (FRQS) doctoral award. This work was supported by the Canadian Institutes for Health Research (CIHR) grant 245969 and the Canadian Cancer Society Research Institute (CCSRI) grant 245095.

Author Contributions:

J.M.K., S.T, A.P.B. P.M.S. and A.P. carried out the study conceptualization and experimental design. J.M.K., S.T., A.P.B. and G.L. and performed experiments and analysis. J.M.K., P.P.R., P.M.S. and A.P. wrote and edited the manuscript.

Declarations of Interest:

The authors declare no competing financial interests.

3.6. Figures and Figure Legends:

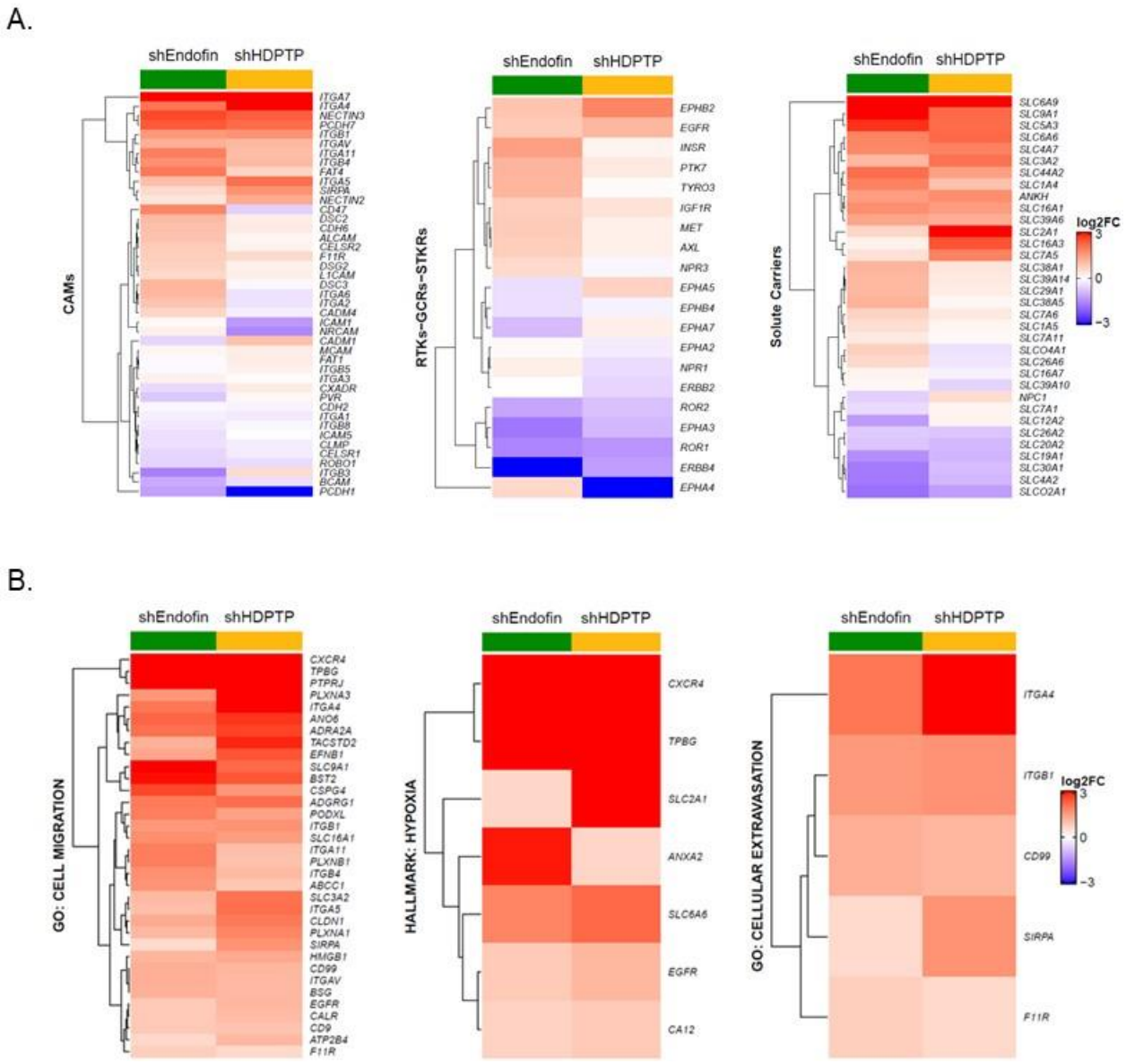

Figure 1: Endofin and HD-PTP depletion upregulate cell surface receptors involved in cancer metastasis.

(A) Cell surface proteomics heat maps showing the expression levels of cell adhesion molecules (CAMs), receptor tyrosine kinases (RTKs), glucocorticoid receptors (GCRs), serine/threonine kinase receptors (STKRs) and solute carriers in Endofin- or HD-PTP-depleted HeLa cells normalized to control cells. (B) Cell surface proteomics heat maps for receptors involved in cell migration (GO: 0016477), hypoxia and cellular extravasation (GO: 0045123) upregulated in Endofin- and HD-PTP- depleted HeLa cells normalized to control cells. Scale bar shows expression levels in Log2FC. The Log2FC value (shEndofin/control or shHD-PTP/control) above 0.5 or below -0.5 (±1.4-fold) were considered as significantly upregulated (red) or downregulated (blue), respectively.

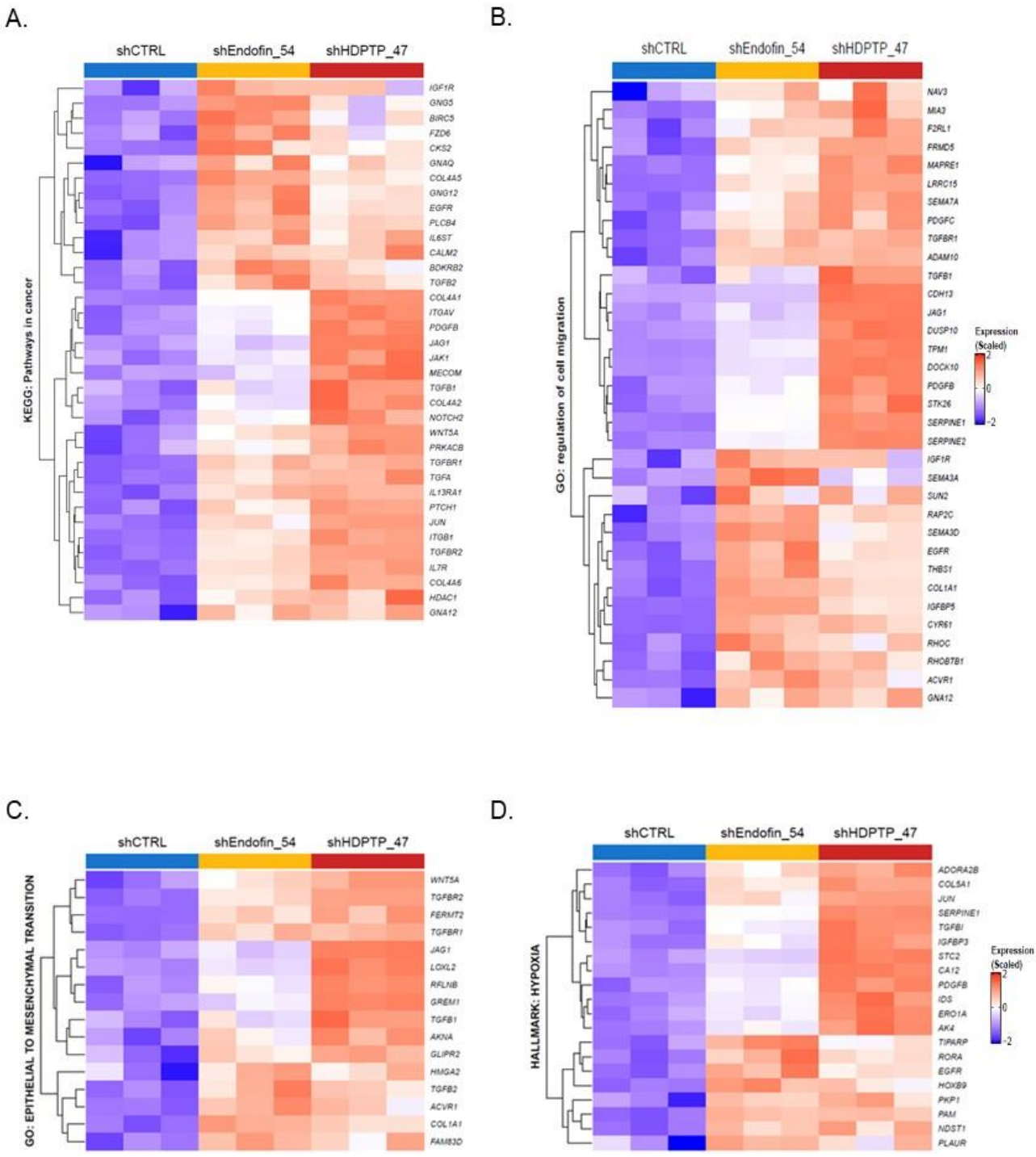
A.
shCTRL
shEndofin_54
shHDPTP_47
KEGG: Pathways in cancer
IGF1R
GNG5
BIRC5
FZD6
CKS2
GNAQ
COL4A5
GNG12
EGFR
PLCB4
IL6ST
CALM2
BDKRB2
TGFB2
COL4A1
ITGAV
PDGFB
JAG1
JAK1
MECOM
TGFB1
COL4A2
NOTCH2
WNT5A
PRKACB
TGFBR1
TGFA
IL13RA1
PTCH1
JUN
ITGB1
TGFBR2
IL7R
COL4A6
HDAC1
GNA12
B.
shCTRL
shEndofin_54
shHDPTP_47
GO: regulation of cell migration
NAV3
MIA3
F2RL1
FRMD5
MAPRE1
LRRC15
SEMA7A
PDGFC
TGFBR1
ADAM10
TGFB1
CDH13
JAG1
DUSP10
TPM1
DOCK10
PDGFB
STK26
SERPINE1
SERPINE2
IGF1R
SEMA3A
SUN2
RAP2C
SEMA3D
EGFR
THBS1
COL1A1
IGFBP5
CYR61
RHOC
RHOBTB1
ACVR1
GNA12
Expression (Scaled)
2
0
-2
C.
shCTRL
shEndofin_54
shHDPTP_47
GO: EPITHELIAL TO MESENCHYMAL TRANSITION
WNT5A
TGFBR2
FERMT2
TGFBR1
JAG1
LOXL2
RFLNB
GREM1
TGFB1
AKNA
GLIPR2
HMGA2
TGFB2
ACVR1
COL1A1
RAMB3D
D.
shCTRL
shEndofin_54
shHDPTP_47
HALLMARK: HYPOXIA
ADORA2B
COL5A1
JUN
SERPINE1
TGFBI
IGFBP3
STC2
CA12
PDGFB
IDS
ERO1A
AK4
TIPARP
RORA
EGFR
HOXB9
PKP1
PAM
NDST1
PLAUR
Expression (Scaled)
2
0
-2

Figure 2: Endofin and HD-PTP depletion engage gene expression programs involved in cancer metastasis.

(A-D) RNAseq heat maps showing upregulated genes involved in the regulation of pathways in cancer (KEGG: hsa05200) (A), cell migration (GO: 0030334) (B), epithelial-to-mesenchymal transition (GO: 0001837) (C) and hypoxia (D) in Endofin- and HD-PTP-depleted HeLa cells compared to control cells. Scale bar shows expression levels in Log2FC. The Log2FC value (shEndofin/control or shHD-PTP/control) above 0.5 or below -0.5 (±1.4-fold) were considered as significantly upregulated (red) or downregulated (blue), respectively.

A.

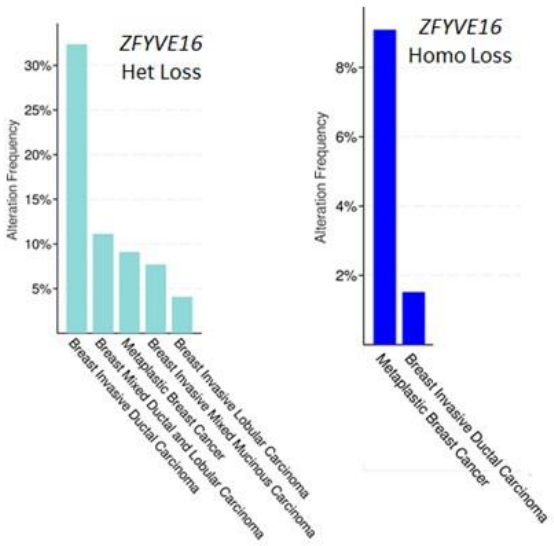
ZFYVE16
Het Loss
Alteration Frequency
30%
25%
20%
15%
10%
5%
Breast Invasive Ductal Carcinoma
Breast Mixed Ductal and Lobular Carcinoma
Metaplastic Breast Cancer
Breast Invasive Mixed Mucinous Carcinoma
Breast Invasive Lobular Carcinoma
ZFYVE16
Homo Loss
Alteration Frequency
8%
6%
4%
2%
Metaplastic Breast Cancer
Breast Invasive Ductal Carcinoma

B.

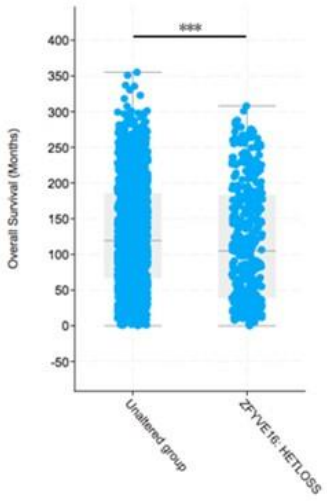
***
Overall Survival (Months)
400
350
300
250
200
150
100
50
0
-50
Unaltered group
ZFYVE16: HETLOSS

C.

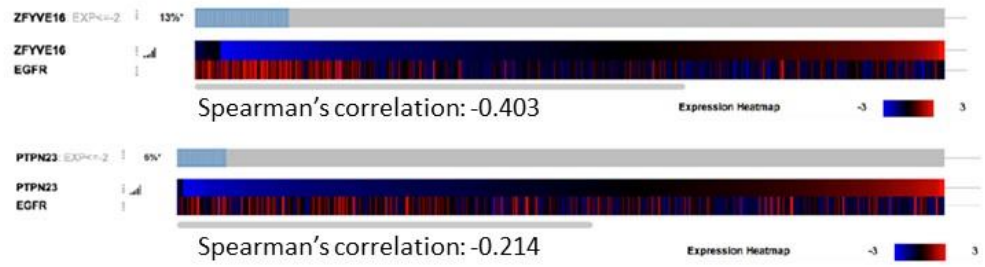
ZFYVE16
13%*
ZFYVE16
EGFR
Spearman's correlation: -0.403
Expression Heatmap
-3
3
PTPN23
6%*
PTPN23
EGFR
Spearman's correlation: -0.214
Expression Heatmap
-3
3

D.

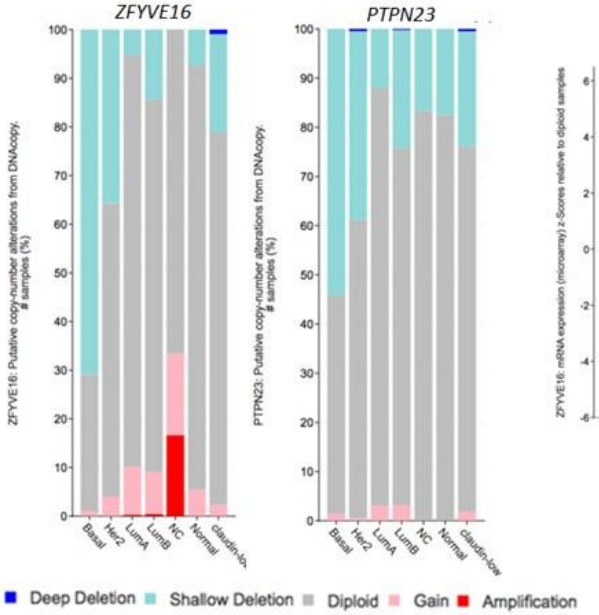
ZFYVE16
PTPN23
ZFYVE16: Putative copy-number alterations from DNAcopy: # samples (%)
PTPN23: Putative copy-number alterations from DNAcopy: # samples (%)
Basal
Her2
LumA
LumB
NC
Normal
Claudin-low
Deep Deletion
Shallow Deletion
Diploid
Gain
Amplification

E.

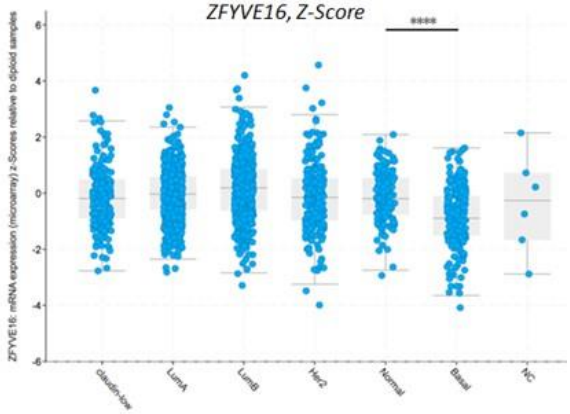
ZFYVE16, Z-Score
****
ZFYVE16: mRNA expression (microarray) z-Scores relative to diploid samples
Claudin-low
LumA
LumB
Her2
Normal
Basal
NC

Figure 3: ZFYVE16 heterozygous deletion and downregulation are more frequent in human patients with basal-like breast cancer subtype and negatively correlate with EGFR expression.

(A) Frequency of *ZFYVE16* heterozygous deletion (left panel) and homozygous deletion (right panel) in different types of human breast cancer (cBioPortal, Breast Invasive Carcinoma, TCGA, Firehose Legacy). (B) Overall survival of human breast cancer patients with *ZFYVE16* heterozygous deletion compared to unaltered group (cBioPortal, Breast Cancer, METABRIC, Nature 2012 and Nat Commun 2016). (C) Correlation between *ZFYVE16*, *PTPN23* and EGFR mRNA expression in breast cancer patients (*ZFYVE16* and *PTPN23* expression< -2 folds) (cBioPortal, Breast Invasive Carcinoma, TCGA, Firehose Legacy). (D) Frequency of *ZFYVE16* and *PTPN23* homozygous deletion (dark blue), heterozygous deletion (light blue), diploidy (grey), gain (pink) and gene amplification (red) in patients with different breast cancer subtypes (basal: basal-like, Her2: Her2 positive, LumA: luminal A, LumB: luminal B, NC: non-classified, Normal: normal breast-like and claudin-lo: claudin-low subtype) (cBioPortal, Breast Cancer, METABRIC, Nature 2012 and Nat Commun 2016). (E) *ZFYVE16* Z-score in patients with different subtypes of breast cancer. Data were downloaded from cBioPortal.

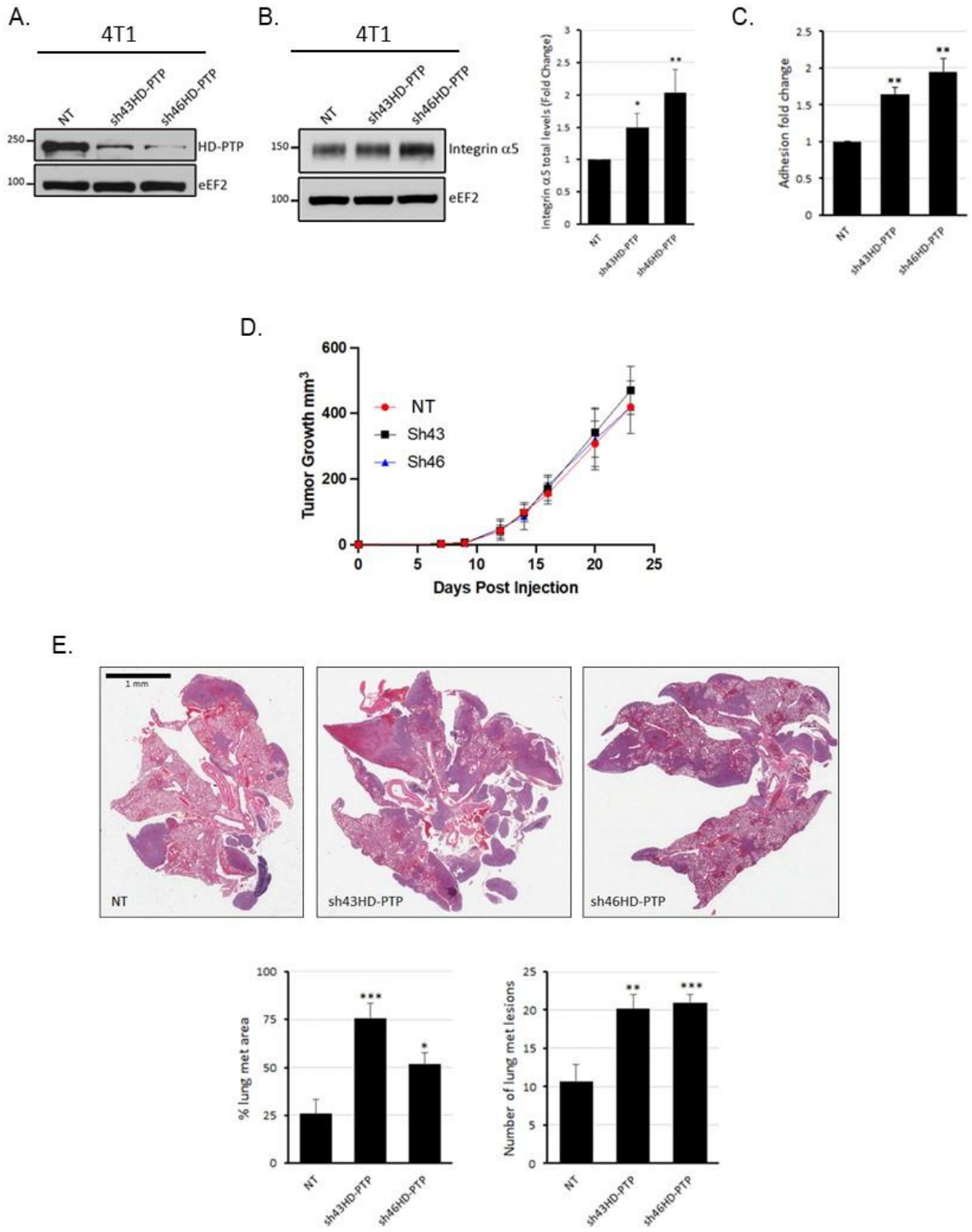
A.
4T1
NT
sh43HD-PTP
sh46HD-PTP
250
HD-PTP
100
eEF2
B.
4T1
NT
sh43HD-PTP
sh46HD-PTP
150
Integrin α5
100
eEF2
Integrin α5 total levels (Fold Change)
C.
Adhesion fold change
D.
Tumor Growth mm³
NT
Sh43
Sh46
Days Post Injection
E.
1 mm
NT
sh43HD-PTP
sh46HD-PTP
% lung met area
Number of lung met lesions

Figure 4: HD-PTP depletion increases 4T1 lung metastasis.

(A-B) Western blots showing HD-PTP (A) and integrin α5 (B) expression levels in HD-PTP-depleted 4T1 cells compared to control cells (NT). HD-PTP is knocked-down using two different shRNAs, and NT cells are infected with a non-targeting shRNA. eEF2 blot is used as a loading control. Quantification was performed using imageJ. (C) Fibronectin adhesion assay (1 h, 37^{o}C) compared to NT cells. (D) Tumor volumes of HD-PTP-depleted 4T1 cells compared to control (NT) cells injected in the mammary fat pad of BALB/c mice. (E) H and E stains of lung tissues from an orthotopic syngeneic tumor mouse model injected with HD-PTP-depleted 4T1 cells compared to NT cells. Four weeks post-injection, tumors were resected, and mice were kept for two additional weeks before euthanasia and tissue collection. Scale bar is 1 mm. Percentage of metastatic lesions area and number of metastatic lesions were quantified using ImageScope. *In vitro* data are mean ± SEM of n≥3 independent experiments. *In vivo* data are mean ± SEM of n=10 mice/cohort. Unpaired student t-test: * $p<0.05$, ** $p<0.01$, *** $p<0.001$.

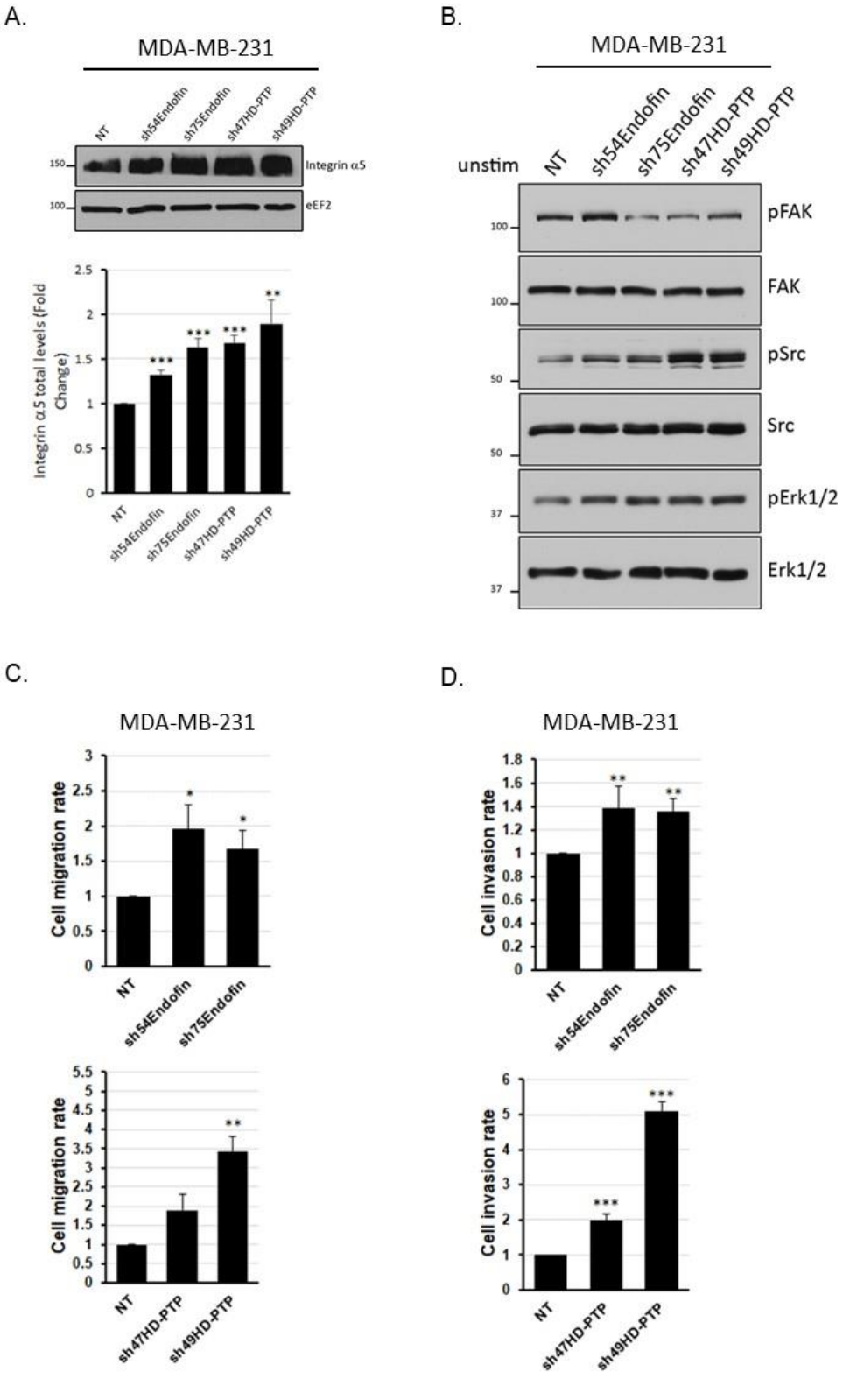
A.
MDA-MB-231
NT
sh54Endofin
sh75Endofin
sh47HD-PTP
sh49HD-PTP
150
Integrin α5
100
eEF2
Integrin α5 total levels (Fold Change)
B.
MDA-MB-231
unstim
NT
sh54Endofin
sh75Endofin
sh47HD-PTP
sh49HD-PTP
pFAK
FAK
pSrc
Src
pErk1/2
Erk1/2
C.
MDA-MB-231
Cell migration rate
NT
sh54Endofin
sh75Endofin
Cell migration rate
NT
sh47HD-PTP
sh49HD-PTP
D.
MDA-MB-231
Cell invasion rate
NT
sh54Endofin
sh75Endofin
Cell invasion rate
NT
sh47HD-PTP
sh49HD-PTP

Figure 5: Endofin and HD-PTP depletion in MDA-MB-231 cells increase cell migration, invasion, total integrin α5 receptor levels and its downstream signaling.

(A) Western blot of integrin α5 receptor in Endofin- and HD-PTP-depleted MDA-MB-231 cells. eEF2 blot is used as a loading control. Quantification was performed using imageJ. (B) Western blot of integrin α5 receptor downstream signaling components pFAK, pSrc and pErk1/2 in unstimulated Endofin- and HD-PTP-depleted MDA-MB-231 cells. (C-D) Real time cell analysis of Endofin- and HD-PTP-depleted MDA-MB-231 cell migration (C) and invasion (D) compared to NT cells. Cell migration and invasion were triggered by a chemoattractant gradient (FBS) and compared to NT cells. A negative control (no FBS gradient) was used to assess migration. Invasion was assessed by seeding cells on top of a matrigel layer. Data are mean ± SEM of $n \geq 3$ independent experiments. Unpaired student t-test: * $p<0.05$, ** $p<0.01$, *** $p<0.001$.

3.7. Supplemental Figures:

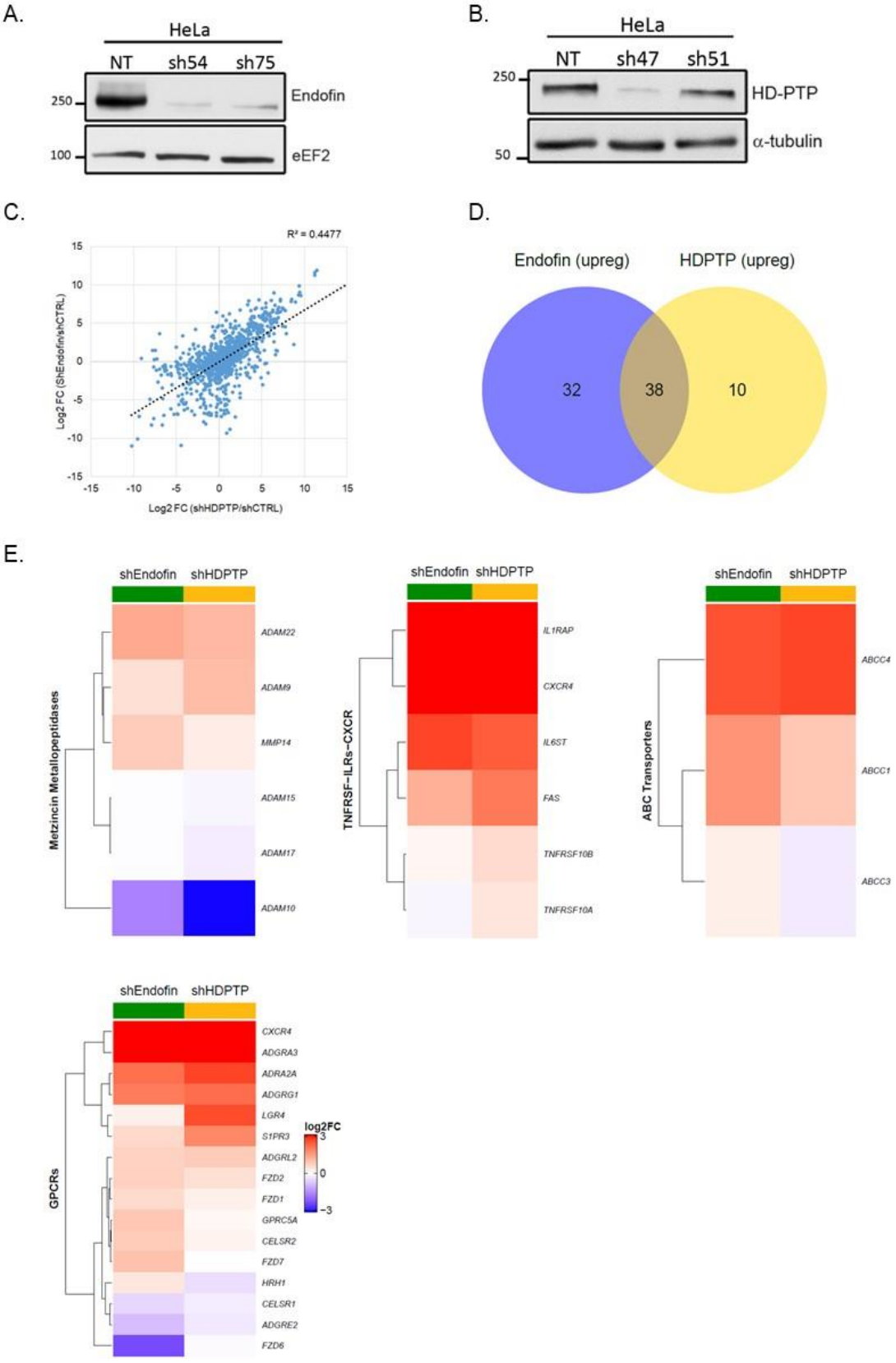

Figure S1: Endofin and HD-PTP depletion in HeLa cells upregulate various cell surface proteins. Related to Figure 1.

(A-B) Western blots showing Endofin (A) and HD-PTP (B) depletion in HeLa cells using two different shRNAs. Control cells (NT) were infected with a non-targeting shRNA. eEF2 (A) and α-tubulin (B) were used as loading controls. (C) Correlation of cell surface protein expression (Log2FC) in Endofin- and HD-PTP-depleted HeLa cells normalized to control cells. (D) Venn diagram showing the number of upregulated receptors which are either in common or unique for Endofin or HD-PTP depletion. (E) Cell surface proteomics heat maps showing the expression levels of metzincin metallopeptidases, cytokine receptors (TNFRSF-ILRs-CXCR), ABC transporters, G protein-coupled receptors (GPCRs) in Endofin- and HD-PTP-depleted HeLa cells normalized to control cells. Scale bar shows expression levels in Log2FC. The Log2FC value (shEndofin/control or shHD-PTP/control) above 0.5 or below -0.5 (±1.4-fold) were considered as significantly upregulated (red) or downregulated (blue), respectively.

A.

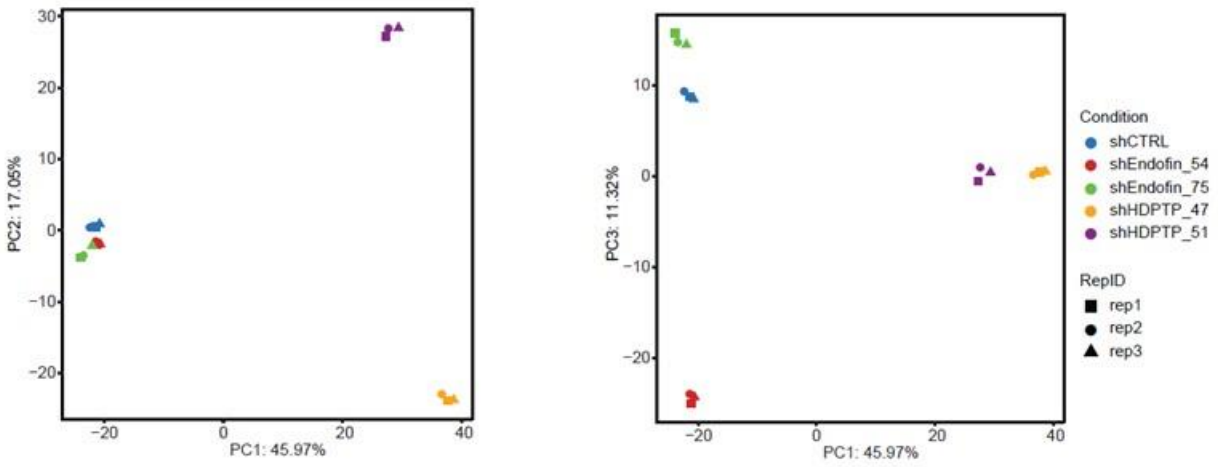
PC2: 17.05%
PC1: 45.97%
PC3: 11.32%
PC1: 45.97%
Condition
shCTRL
shEndofin_54
shEndofin_75
shHDPTP_47
shHDPTP_51
RepID
rep1
rep2
rep3

B.

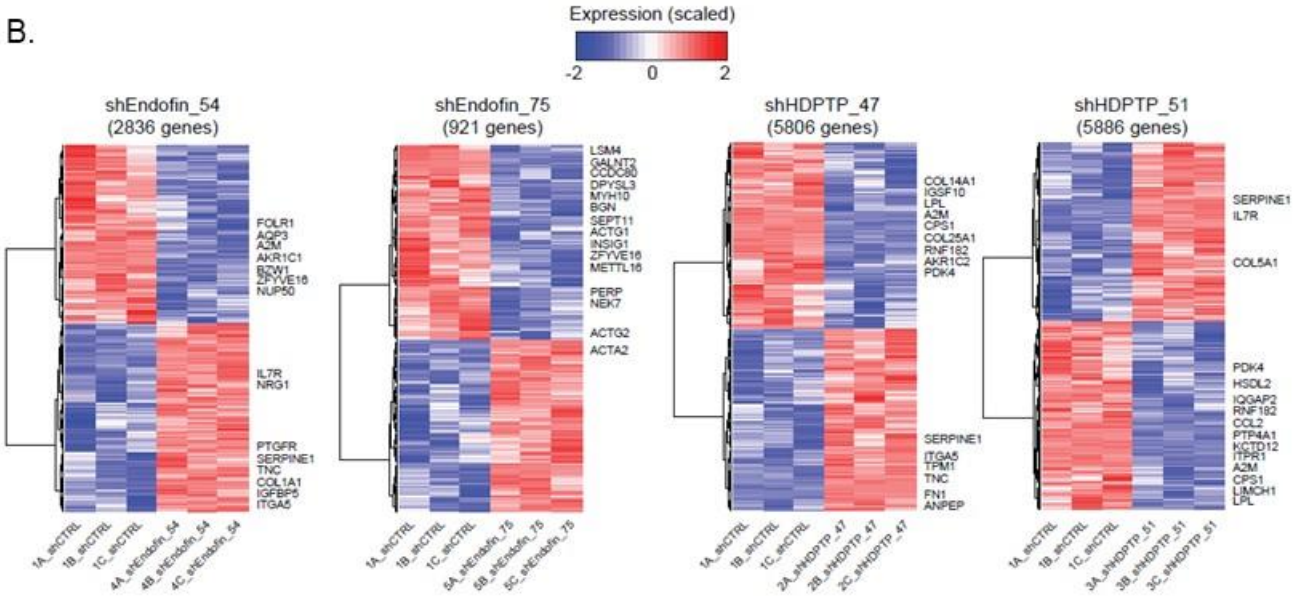
Expression (scaled)
shEndofin_54
(2836 genes)
shEndofin_75
(921 genes)
shHDPTP_47
(5806 genes)
shHDPTP_51
(5886 genes)

C.

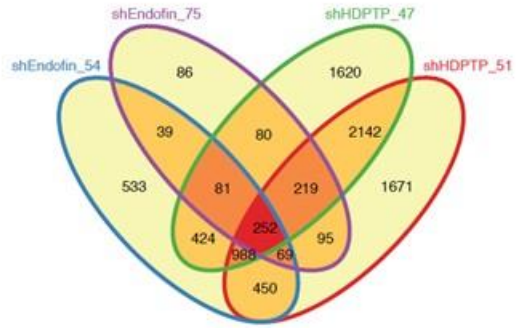
shEndofin_75
shHDPTP_47
shEndofin_54
shHDPTP_51
86
1620
39
80
2142
533
81
219
1671
424
252
95
988
69
450

Figure S2: RNAseq data analysis from Endofin- and HD-PTP-depleted HeLa cells. Related to Figure 2.

(A) Principal component analysis (PCA) of gene expression data from all samples. (Left) PC1 (x-axis) separate control from the sh47HDPTP and sh51HDPTP samples. (Right) PC3 (y-axis) further separates control from sh54Endofin and sh75Endofin samples. (B) RNAseq heat maps showing gene clustering as upregulated and downregulated upon Endofin and HD-PTP depletion in HeLa cells compared to control cells. Gene clustering for each cell line are shown in triplicates. Scale bar shows expression levels in Log2FC. (C) Venn diagram for 4 sets showing common/different RNAseq hits between Endofin- and HD-PTP-depleted HeLa cells.

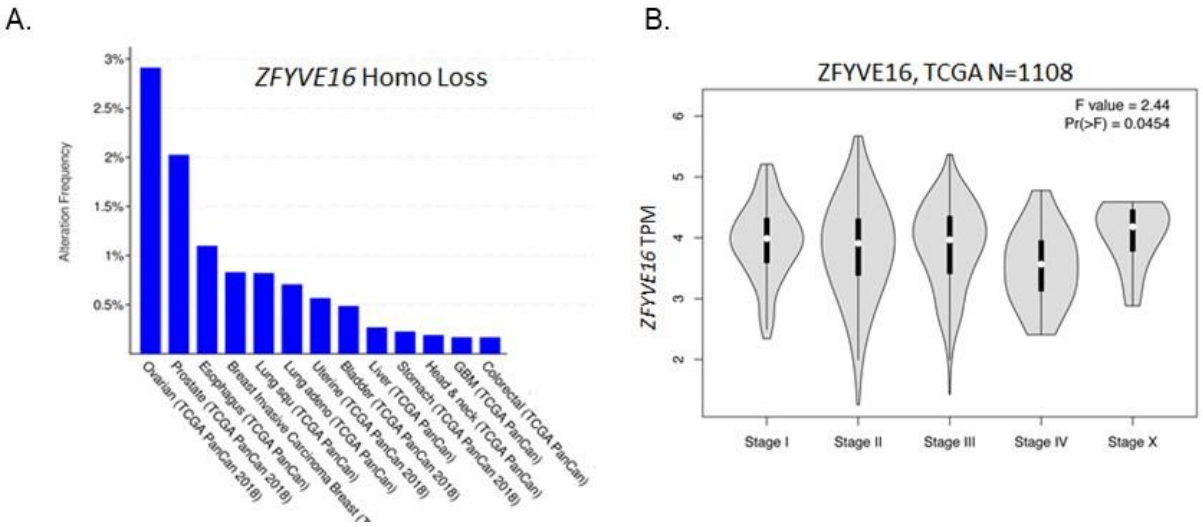

Figure S3: ZFYVE16 mRNA expression decreases with advanced stages of human breast cancer. Related to Figure 3.

(A) Frequency of *ZFYVE16* homozygous deletions in different types of human cancers (cBioPortal). (B) *ZFYVE16* mRNA expression (TPM: transcript per million) in patients with different stages of breast cancer (TCGA).

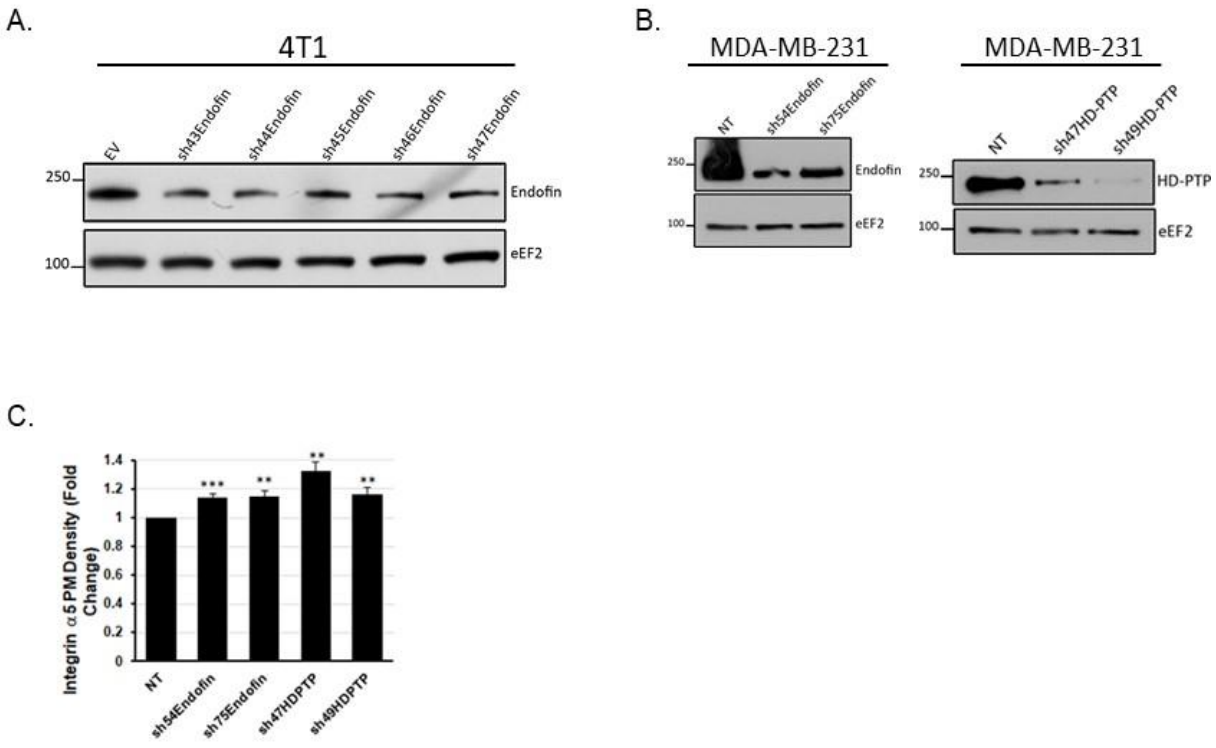

Figure S4: Endofin and HD-PTP depletion in MDA-MB-231 cells has a minimal effect on integrin α5 plasma membrane levels. Related to Figure 4.

(A) Western blot showing Endofin depletion in 4T1 cells using shRNA. (B) Western blots showing Endofin (left panel) and HD-PTP (right panel) depletion in MDA-MB-231 cells compared to NT cells. Endofin and HD-PTP are knocked-down using two different shRNAs, and NT cells are

infected with a non-targeting shRNA. eEF2 blot is used as a loading control. (C) Cell surface-ELISA measuring the plasma membrane density of integrin α5 receptor at steady states in Endofin- and HD-PTP-depleted MDA-MB-231 cells compared to NT cells. Data are mean ± SEM of n≥3 independent experiments. Unpaired student t-test: ** $p<0.01$, *** $p<0.001$.

3.8. References:

Ali, N., Zhang, L., Taylor, S., Mironov, A., Urbé, S., & Woodman, P. (2013). Recruitment of UBPY and ESCRT exchange drive HD-PTP-dependent sorting of EGFR to the MVB. *Current biology, 23*(6), 453-461.

Bendas, G., & Borsig, L. (2012). Cancer cell adhesion and metastasis: selectins, integrins, and the inhibitory potential of heparins. *International journal of cell biology, 2012*.

Butti, R., Das, S., Gunasekaran, V. P., Yadav, A. S., Kumar, D., & Kundu, G. C. (2018). Receptor tyrosine kinases (RTKs) in breast cancer: signaling, therapeutic implications and challenges. *Molecular cancer, 17*(1), 1-18.

Chang, H.-M., Lin, Y.-Y., Tsai, P.-C., Liang, C.-T., & Yan, Y.-T. (2014). The FYVE domain of Smad Anchor for Receptor Activation (SARA) is required to prevent skin carcinogenesis, but not in mouse development. *PLoS One, 9*(8), e105299.

Desgrosellier, J. S., & Cheresh, D. A. (2010). Integrins in cancer: biological implications and therapeutic opportunities. *Nature Reviews Cancer, 10*(1), 9-22.

Doyotte, A., Mironov, A., McKenzie, E., & Woodman, P. (2008). The Bro1-related protein HD-PTP/PTPN23 is required for endosomal cargo sorting and multivesicular body morphogenesis. *Proceedings of the National Academy of Sciences, 105*(17), 6308-6313.

Gahloth, D., Levy, C., Walker, L., Wunderley, L., Mould, A. P., Taylor, S., . . . Tabernero, L. (2017). Structural Basis for Specific Interaction of TGFβ Signaling Regulators SARA/Endofin with HD-PTP. *Structure*.

Huveneers, S., & Danen, E. H. (2009). Adhesion signaling–crosstalk between integrins, Src and Rho. *Journal of cell science, 122*(8), 1059-1069.

Kazan, J. M., Desrochers, G., Martin, C. E., Jeong, H., Kharitidi, D., Apaja, P. M., . . . Lukacs, G. L. (2021). Endofin is Required for HD-PTP and ESCRT-0 Interdependent Endosomal Sorting of Ubiquitinated Transmembrane Cargoes. *iScience*, 103274.

Kharitidi, D., Apaja, P. M., Manteghi, S., Suzuki, K., Malitskaya, E., Roldan, A., . . . Pause, A. (2015). Interplay of endosomal pH and ligand occupancy in integrin α5β1 ubiquitination, endocytic sorting, and cell migration. *Cell reports, 13*(3), 599-609.

Lemmon, M. A., & Schlessinger, J. (2010). Cell signaling by receptor tyrosine kinases. *Cell, 141*(7), 1117-1134.

Lin, G., Aranda, V., Muthuswamy, S. K., & Tonks, N. K. (2011). Identification of PTPN23 as a novel regulator of cell invasion in mammary epithelial cells from a loss-of-function screen of the ‘PTP-ome'. *Genes & development, 25*(13), 1412-1425.

Ma, H., Wardega, P., Mazaud, D., Klosowska-Wardega, A., Jurek, A., Engstrom, U., . . . Heldin, C. H. (2015). Histidine-domain-containing protein tyrosine phosphatase regulates platelet-derived growth factor receptor intracellular sorting and degradation. *Cell Signal, 27*(11), 2209-2219. doi:10.1016/j.cellsig.2015.07.020

Manteghi, S., Gingras, M.-C., Kharitidi, D., Galarneau, L., Marques, M., Yan, M., . . . Witcher, M. (2016). Haploinsufficiency of the ESCRT component HD-PTP predisposes to cancer. *Cell reports, 15*(9), 1893-1900.

Mattissek, C., & Teis, D. (2014). The role of the endosomal sorting complexes required for transport (ESCRT) in tumorigenesis. *Molecular membrane biology, 31*(4), 111-119.

Mellman, I., & Yarden, Y. (2013). Endocytosis and cancer. *Cold Spring Harbor Perspectives in Biology, 5*(12), a016949.

Miller, D. S. J., Bloxham, R. D., Jiang, M., Gori, I., Saunders, R. E., Das, D., . . . Hill, C. S. (2018). The Dynamics of TGF-beta Signaling Are Dictated by Receptor Trafficking via

the ESCRT Machinery. *Cell Rep, 25*(7), 1841-1855 e1845. doi:10.1016/j.celrep.2018.10.056

Miskin, R. P., Warren, J. S., Ndoye, A., Wu, L., Lamar, J. M., & DiPersio, C. M. (2021). Integrin α3β1 promotes invasive and metastatic properties of breast cancer cells through induction of the Brn-2 transcription factor. *Cancers, 13*(3), 480.

Ning, Q., Liu, C., Hou, L., Meng, M., Zhang, X., Luo, M., . . . Zhao, X. (2013). Vascular endothelial growth factor receptor-1 activation promotes migration and invasion of breast cancer cells through epithelial-mesenchymal transition. *PLoS One, 8*(6), e65217.

Palmieri, D., Bronder, J. L., Herring, J. M., Yoneda, T., Weil, R. J., Stark, A. M., . . . Halverson, D. (2007). Her-2 overexpression increases the metastatic outgrowth of breast cancer cells in the brain. *Cancer research, 67*(9), 4190-4198.

Pantano, F., Croset, M., Driouch, K., Bednarz-Knoll, N., Iuliani, M., Ribelli, G., . . . Bonin, F. (2021). Integrin alpha5 in human breast cancer is a mediator of bone metastasis and a therapeutic target for the treatment of osteolytic lesions. *Oncogene, 40*(7), 1284-1299.

Raiborg, C., & Stenmark, H. (2009). The ESCRT machinery in endosomal sorting of ubiquitylated membrane proteins. *Nature, 458*(7237), 445-452.

Ring, A., & Dowsett, M. (2004). Mechanisms of tamoxifen resistance. *Endocrine-related cancer, 11*(4), 643-658.

Templeton, A. J., Diez-Gonzalez, L., Ace, O., Vera-Badillo, F., Šeruga, B., Jordán, J., . . . Ocaña, A. (2014). Prognostic relevance of receptor tyrosine kinase expression in breast cancer: a meta-analysis. *Cancer treatment reviews, 40*(9), 1048-1055.

Tomiguchi, M., Yamamoto, Y., Yamamoto-Ibusuki, M., Goto-Yamaguchi, L., Fujiki, Y., Fujiwara, S., . . . Inao, T. (2016). Fibroblast growth factor receptor-1 protein expression is associated with prognosis in estrogen receptor-positive/human epidermal growth factor receptor-2-negative primary breast cancer. *Cancer science, 107*(4), 491-498.

Weekes, M. P., Antrobus, R., Lill, J. R., Duncan, L. M., Hör, S., & Lehner, P. J. (2010). Comparative analysis of techniques to purify plasma membrane proteins. *Journal of biomolecular techniques: JBT, 21*(3), 108.

Wegner, C. S., Rodahl, L. M., & Stenmark, H. (2011). ESCRT proteins and cell signalling. *Traffic, 12*(10), 1291-1297. doi:10.1111/j.1600-0854.2011.01210.x

Zhang, S., Fan, G., Hao, Y., Hammell, M., Wilkinson, J. E., & Tonks, N. K. (2017). Suppression of protein tyrosine phosphatase N23 predisposes to breast tumorigenesis via activation of FYN kinase. *Genes & development, 31*(19), 1939-1957.

Chapter 4 – General Discussion

4.1. Endofin functions as an ESCRT protein in ubiquitinated endo-lysosomal cargo sorting:

The ESCRT machinery is involved in several cellular processes such as: cytokinesis, viral budding and lysosomal membrane repair, as well as ubiquitinated plasma membrane transmembrane cargo sorting along the endo-lysosomal organelles. The latter mechanism also contributes to ubiquitinated PM receptor downregulation, a critical process not only in the termination of a large number of receptors signaling (Wegner et al., 2011) and elimination of non-native PM proteins to preserve proteostasis (Apaja et al., 2014), but to thwart oncogenic receptors uncontrolled signaling in various types of cancer. The loss-of-expression or -function of selected ESCRT components stabilizes receptors at the PM and in early endosomes, which in turn increases their signaling, a known cancer hallmark. Hyperactivated signaling pathways trigger oncogenic cellular responses such as: increased proliferation, migration and survival. Moreover, perturbations in the ESCRT machinery might also increase the cell surface availability of other receptors related to cell migration/invasion and drug resistance. Hence, deletions/mutations of ESCRT components can enhance tumorigenesis and cancer progression. To have a better insight on how the levels of cell surface receptors and their downstream signaling are regulated under normal physiological and pathological conditions (e.g., cancer), the interactions and the functional role of individual components of the ESCRT machinery have to be mapped and understood.

In this thesis, I uncovered a previously unknown role of Endofin as a component of the ESCRT machinery with critical role in a subset of cell surface receptor trafficking (e.g., EGFR and integrin), signaling and cell migration. Therefore, I propose that Endofin plays a critical role in tumor suppression at cellular and organism levels. I also shed some light on the role of Endofin and HD-PTP in cancer metastasis. Several questions need to be addressed: 1) Endofin functional and physical relation to HD-PTP and to other constituents of ESCRT-0/-III complexes? 2) How

does Endofin association/dissociation from the ESCRT machinery aids receptor sorting towards MVBs and lysosomes. 3) What are the consequences of Endofin downregulation/haploinsufficiency on receptor recycling and lysosomal targeting, as well as on cellular oncogenicity? 4) What is the molecular, cellular and clinical relevance of the altered cell surface proteome upon Endofin depletion in cancer? 5) How does Endofin depletion might enhance cancer progression at a systematic (organism) level? The relevance of these topics and their potential as research avenues are discussed here.

4.2. The role of Endofin/HD-PTP interaction in the ESCRT machinery:

Tom1, a ubiquitin and a clathrin binding protein, is shown to recruit clathrin to early endosomes through its direct interaction with Endofin (Katoh et al., 2004, Seet et al., 2005, Seet et al., 2004, Shiba et al., 2004). Clathrin recruitment to early endosomes is indispensable for cargo sorting towards lysosomal degradation (Raiborg et al., 2006, Sachse et al., 2002). Moreover, the Tom1 ortholog in *Dictyostelium discoideum*, ddTom1 serves as an ancestral ESCRT-0 component in the absence of the classical ESCRT-0 complex, Hrs/STAM (Blanc et al., 2009). However, the incapability of FYVE-Tom1 chimera to restore EGFR lysosomal delivery, showed that Tom1 is dispensable for the role of Endofin in receptor trafficking. Of note, Tom1 is also recruited to early endosomes by Tollip protein (Ankem et al., 2011). Therefore, Tollip activity might serve as a compensatory mechanism for clathrin recruitment to early endosomes in an Endofin-depleted cellular context. Alternatively, Hrs clathrin binding capacity may ensure sufficient recruitment of clathrin molecules to form the double layered clathrin layer on the surface of sorting endosomes as an initial site of ESCRT assembly and ubiquitinated cargo concentration (Raiborg et al., 2002, Sachse et al., 2002).

Although it is shown that L202D/I206D-HD-PTP variant prevented its recruitment to early endosomes even upon its co-expression with myc-Endofin (Gahloth et al., 2017c), I thought that this experiment does not directly characterize the importance of Endofin/HD-PTP association in receptor trafficking. In fact, L202D/I206D mutation disrupts HD-PTP interaction with several proteins such as Endofin, SARA, CHMP4B and STAM2, which in turn recruit HD-PTP to early endosomes (Gahloth et al., 2017c). Thus, it was essential to assess EGFR lysosomal delivery upon complementation with Endofin mutants lacking the interaction with HD-PTP or the localization to early endosomes. Furthermore, both BioID and APMS proteomics data showed a significant interaction of HD-PTP to clathrin. This interaction whether it is direct or indirect, it is still unknown and requires further research. However, it is shown that HD-PTP and clathrin are recruited to early endosomes in the early stages of an ESCRT wave just before the sharp recruitment of ESCRT-III (CHMP4B) (Wenzel et al., 2018). Therefore, Endofin might either form an alternative ESCRT complex consisting of HD-PTP, clathrin and ESCRT-III, or Endofin might be mediating the recruitment of HD-PTP to the proper microdomain at early endosomes to facilitate its interaction/colocalization with the cargo and ESCRT-0 complex for an efficient cargo sorting towards MVBs and lysosomes. The real time recruitment of wild-type and mutant Endofin to early endosomes and its association with HD-PTP and other ESCRT components could be assessed by live imaging microscopy. This would allow us to figure whether Endofin recruitment/interaction with the ESCRT machinery occurs during early or late phases of the ESCRT wave. Since Endofin is identified as a phosphorylation target upon EGF stimulation (Chen et al., 2007b), further structural/biochemical analysis (e.g., phosphorylation/dephosphorylation and conformational changes) permits us to better understand the importance of Endofin/HD-PTP association/dissociation in sorting cargo towards MVBs and lysosomes.

4.3. Compositional changes of cell surface receptor profile upon Endofin and HD-PTP depletion:

Internalized/ubiquitinated cargo at the surface of early endosomes are recognized by the ESCRT ubiquitin binding proteins, such as Hrs, STAM2, Tsg101 and UBAP1, then sorted towards MVB formation (Agromayor et al., 2012, Bache et al., 2003, Raiborg et al., 2002, Sundquist et al., 2004). HD-PTP and Tom1 are also ubiquitin binding proteins recognizing both poly- and mono-ubiquitinated cargo (Akutsu et al., 2005, Pashkova et al., 2013, Wang et al., 2010), but the ability of Endofin to bind ubiquitinated cargo is still uncharacterized. It is well-known that Hrs, Tsg101 and UBAP1 depletion disrupt receptor trafficking and delay their lysosomal degradation (Kharitidi et al., 2015, Lu et al., 2003, Stern et al., 2007). However, the effect of depleting individual ESCRT components on the global cell surface proteome is still undetermined.

Our cell surface proteomics data showed that Endofin and HD-PTP depletion upregulated several receptors at the PM, while some of the receptors' density remained either unaltered or downregulated. This suggests that other factors such as receptor posttranslational modifications (e.g., ubiquitination), receptor interactome formation upon ligand-stimulation as well as indirect effects via transcriptomic alterations likely play a complex/partially understood role in the biochemical consequences of Endofin and/or HD-PTP downregulation and their effect on the cell surface receptors' distribution pattern.

The effect of Endofin and HD-PTP depletion on the lysosomal targeting of poly- versus tetrameric mono-ubiquitinated CD4 cargo models supports this notion (Kazan et al., 2021, Kharitidi et al., 2015). Moreover, Endofin showed a strong interaction with EGFR upon EGF stimulation, and it also might be interacting with other internalized cell surface receptors to mediate their ESCRT-dependent lysosomal targeting. Furthermore, the crosstalk between cell

surface receptors, for instance the blockage of integrin αvβ3 triggers VEGFR2 recycling (Reynolds et al., 2009), might also affect the cell surface proteome upon Endofin and HD-PTP depletion. I suggest that all these factors directly affect receptor sorting and further explain the alteration in the cell surface proteome upon Endofin and HD-PTP depletion.

One of the limitations is that the effect of Endofin depletion on the cell surface proteome should not only be compared to HD-PTP depletion, but also to the depletion of other classical ESCRTs such as Hrs, Tsg101, UBAP1 or CHMP4B. It would be important to know whether Endofin and classical ESCRT depletions have similar, partially overlapping or distinct impact on the cell surface proteome. Hence, Endofin might have a similar or a different impact on downstream receptor signaling and transcriptional activation. This permits us to better understand the role of Endofin in ESCRT machinery function and the regulation of selective cargo trafficking.

4.4. The role of Endofin in cell surface receptor recycling from early endosomes:

The interaction of SNXs with the specific sorting motifs of activated/internalized cell surface receptors, segregates cargoes into different microdomains on the surface of early endosomes and directs them either towards tubulovesicular recycling routes, Golgi complex or towards the MVB/lysosomal degradative pathway (Norris et al., 2017). For instance, SNX17 binds integrin α5β1, suppresses its lysosomal degradation and favors its recycling (Brahme et al., 2012). HD-PTP is shown to favor the sorting of activated integrin α5β1 towards lysosomal degradation and to suppress its recycling route (Kharitidi et al., 2015). This role coincides with the role of the classical ESCRT-I protein UBAP1, where its depletion favors the recycling of integrin α5β1 back to the cell surface (Kharitidi et al., 2015). This phenotype is the reverse of USP9x deubiquitinating (DUB) enzyme depletion, which promoted integrin α5β1 ubiquitination and destabilization at the

PM (Homan et al., 2014). Endofin might also play a critical role in receptor recycling through 1) its interaction with the receptor (e.g., EGFR), which might block the interaction of SNXs with the specific sorting motifs of a receptor and its subsequent recycling. 2) Endofin promotes HD-PTP interaction/colocalization with ESCRT-0 and cargo to mediate an efficient sorting towards lysosomal degradation, thus suppressing receptor recycling. 3) Endofin might also block the recruitment and DUB activity of USP9x to deubiquitinate cargo on the surface of early endosomes, thus promoting its lysosomal targeting by stabilizing cargo ubiquitination.

It is shown that tumor cells of cancer patients with p53 mutations exhibit an enhanced recycling of both integrin and EGFR, which in turn results in continuous activation of their downstream signaling (Muller et al., 2009). In addition, these tumor cells show enhanced metastatic behavior (Muller et al., 2009). Moreover, the upregulation of proteins mediating integrin recycling such as Rab-coupled protein, are shown to correlate with poor survival and cancer aggressiveness in patients with luminal B breast cancer subtype (Zhang et al., 2009b). Endofin depletion favored integrin α5 and EGFR recycling, sustained their downstream signaling and increased cell migration. Moreover, Endofin depletion in MDA-MB-231 breast cancer cells increased their migration and invasive abilities. Importantly, HD-PTP depletion favors integrin α5β1 recycling and increases cell migration (Kharitidi et al., 2015). In addition, the heterozygous loss of *Ptpn23* in mice induced spontaneous B cell lymphoma, increased integrin β1 levels at the surface of lymphoma B cells and enhanced cancer cell dissemination (Manteghi et al., 2016). Hence, Endofin might exert a tumor suppressor activity through its role in sorting activated/internalized cell surface receptors towards lysosomal degradation, thus suppressing receptor recycling and their downstream signaling pathways.

4.5. Cellular oncogenicity upon Endofin depletion:

Cell surface receptors play a critical role in cancer progression. CAMs facilitate cancer metastasis by mediating cell interaction with stromal cells and ECM triggering downstream signaling cascades, which in turn influence cell morphology, polarity and migratory behavior (Bendas et al., 2012, Huveneers et al., 2009). For instance, integrins are involved in almost every step of cancer progression including cancer cell proliferation, local invasion and intravasation, survival of tumor circulating cells and extravasation into the secondary metastatic site (Hamidi et al., 2018). Cell surface proteomics showed an increase in cell surface levels of integrin β1, αv, α5 and α7 upon Endofin and HD-PTP depletion. Most β1 integrins are necessary for breast tumorigenesis with a growth-promoting function (White et al., 2004). Moreover, integrin α5β1 upregulation in lung cancer is linked to poor prognosis and cancer progression (Roman et al., 2010). It is also shown that the increase in integrin αvβ3 expression in breast and lung cancer increases metastasis (Desgrosellier et al., 2009). Integrin α7 plays a critical role in the growth and invasiveness of glioblastoma stem-like cells, and its high expression negatively correlates with the survival of glioma patients (Haas et al., 2017). Endofin and HD-PTP depletion also upregulated the cell surface levels of RTKs receptors and multi drug resistance proteins. Although I directly link the regulation of cell surface receptor levels to the role of Endofin and HD-PTP, however it also shown that the crosstalk between receptors affects their trafficking and signaling. For instance, the upregulation of integrin β3 may promote TGFβ activation and TGFβ-mediated EMT in breast cancer (Truong et al., 2014). It is also shown that blocking integrin αvβ3 with Cilengitide triggers the rapid recycling of VEGFR2, which in turn enhance endothelial migration and tumor vascularization (Reynolds et al., 2009). Moreover, integrin α6β4 cooperate with EGFR and HER2 receptors to amplify their downstream signaling in several carcinomas (Guo et al., 2006, Mariotti et al., 2001, Trusolino et al., 2001). In addition, the interaction of integrin α5β1 with fibronectin is

shown to be sufficient to induce MET activation in ovarian cancer and to enhance metastasis (Mitra et al., 2011). Integrins can also induce Src family kinases to phosphorylate RTKs, thus sustaining their downstream signaling (Cooper et al., 2019). Therefore, the sustained signaling observed upon Endofin and HD-PTP depletion might not only be due to the accumulation of activated/internalized receptors at early endosomes, but the bidirectional crosstalk between receptors might also hyperactivate and sustain downstream signaling pathways.

In line with the sustained signaling observed, our RNAseq data showed that different downstream transcriptional pathways are upregulated upon Endofin and HD-PTP depletion, driving HeLa cells towards enhanced migratory phenotype. Of note, it is well-known that the activation of MEK, Src and Erk signaling cascades trigger the activation of transcriptional pathways related to cell proliferation and migration/invasion, which are hallmarks of tumorigenesis and cancer progression (Guo et al., 2020).

4.6. Endofin depletion (or haploinsufficiency) might enhance metastasis formation:

In this study, I have shown that HD-PTP depletion significantly increased 4T1 total integrin α5 receptor levels and lung metastasis. In addition, Endofin depletion increased MDA-MB-231 total integrin α5 receptor levels, cell migration and invasion. It is shown that the upregulation of integrin β1/Src signaling promotes resistance to HER2 and PI3K inhibitors (Hanker et al., 2017). Moreover, blocking integrin α5β1, in triple negative breast cancer, inhibits EGFR and FAK signaling pathways and hampers metastasis (Shen et al., 2019). Our cell surface proteomics data showed an increase in the cell surface levels of ABCC transporters and matrix metallopeptidases which play direct roles in drug resistance and cell invasion, respectively.

Breast cancer patients with high expression of integrin β1 and fibronectin show a significant decrease in overall survival (Yao et al., 2007). Moreover, integrin α5 expression in

human breast cancer mediates bone metastasis and serves as a therapeutic target for the treatment of osteolytic lesions (Pantano et al., 2021). Furthermore, the overexpression of integrin αv in cancer cells originally exhibiting low integrin αv levels, accelerated cell migration *in vitro* and increased brain metastasis *in vivo* (Wu et al., 2017). In addition, EGFR overexpression in triple negative breast cancer enhances metastasis and decreases survival rates (Park et al., 2014, Tischkowitz et al., 2007). Despite the different RNAi approaches used, an efficient Endofin knock-down in 4T1 cells was not attainable. Hence, I decided to knock-down the expression of Endofin and HD-PTP in MDA-MB-231 cells and to assess metastasis in a xenograft tumor mouse model. I expect Endofin depletion to enhance cancer metastasis similar to HD-PTP depletion in 4T1 cells. It would be interesting to assess cell surface proteome alterations in Endofin- and HD-PTP-depleted MDA-MB-231 cells to better understand which receptor or family of receptors contribute to the expected enhanced metastatic phenotype. This could be further validated by knocking-down the expression of a candidate receptor and assessing metastasis upon Endofin and HD-PTP depletion.

Despite the inefficient downregulation of Endofin in 4T1 cells (40% depletion), these cells were injected in the mammary fat pad of a syngeneic tumor mouse model. Results did not show any significant differences in tumor growth and lung metastasis compared to control cells (data not shown). However, bioinformatics showed high frequency of heterozygous deletion of both *ZFYVE16* and *PTPN23* in basal-like breast cancer subtype. This infers that the level of Endofin downregulation might be critical to alter the metastatic potential of cancer cells and might also differ between different cell types and cancers. Furthermore, the alterations in the cell surface receptor profile upon Endofin depletion, might also differ between different cell types and different

cancers leading to different consequences and phenotypes. This requires further research to elucidate the role of Endofin in cancer progression at both cellular and systematic levels.

4.7. Proposed woking model for the role of Endofin in receptor trafficking and cancer development:

The ESCRT machinery has been long established as a key mechanism to downregulated ubiquitinated cell surface receptors via lysosomal targeting and proteolysis. Here, I introduce Endofin as a previously unrecognized player in ESCRT-mediated cargo sorting mechanism through its interaction with the haploinsufficient tumor suppressor protein, HD-PTP. Furthermore, I implicate that haploinsufficiency of Endofin has an indispensable role in a subset of activated/internalized ubiquitinated cell surface receptors accumulation at the cell surface and in cancer metastasis. I propose the following model for the molecular mechanism of Endofin action. Upon receptor activation/internalization, Endofin is recruited to early endosomes via its FYVE-domain to mediate HD-PTP interaction/colocalization with the cargo and ESCRT-0 thus catalyzing the efficient sorting of cargo towards lysosomal degradation. In an Endofin-depleted cellular context, recycling of internalized cell surface receptors is favored which in turn alters the cell surface proteome and sustains downstream receptor signaling. Due to the crosstalk between cell surface receptors, recycling and signaling of some other receptors could be indirectly affected by Endofin depletion. It is well-known that hyperactivated receptor signaling is a cancer hallmark driving tumor cells towards more aggressive phenotypes.

It is essential to better understand the association/dissociation of Endofin/HD-PTP complex and its impact on receptor trafficking. This might be attained through advanced live imaging and protein structural analysis, which might elucidate the real time

recruitment/dissociation of Endofin to/from the ESCRT machinery and what biochemical or conformational changes regulate Endofin's activity.

All in all, these notions discussed here introduce Endofin as an important component of the ESCRT machinery and a potential regulator of the cell surface proteome, which in turn might regulate several cellular processes playing critical roles in several human diseases, including cancer.

4.8. References:

Agromayor, M., Soler, N., Caballe, A., Kueck, T., Freund, S. M., Allen, M. D., . . . McDonald, B. (2012). The UBAP1 subunit of ESCRT-I interacts with ubiquitin via a SOUBA domain. *Structure, 20*(3), 414-428.

Akutsu, M., Kawasaki, M., Katoh, Y., Shiba, T., Yamaguchi, Y., Kato, R., . . . Wakatsuki, S. (2005). Structural basis for recognition of ubiquitinated cargo by Tom1-GAT domain. *FEBS letters, 579*(24), 5385-5391.

Ankem, G., Mitra, S., Sun, F., Moreno, A. C., Chutvirasakul, B., Azurmendi, H. F., . . . Capelluto, D. G. (2011). The C2 domain of Tollip, a Toll-like receptor signalling regulator, exhibits broad preference for phosphoinositides. *Biochemical Journal, 435*(3), 597-608.

Apaja, P. M., & Lukacs, G. L. (2014). Protein homeostasis at the plasma membrane. *Physiology, 29*(4), 265-277.

Bache, K. G., Raiborg, C., Mehlum, A., & Stenmark, H. (2003). STAM and Hrs are subunits of a multivalent ubiquitin-binding complex on early endosomes. *Journal of Biological Chemistry, 278*(14), 12513-12521.

Bendas, G., & Borsig, L. (2012). Cancer cell adhesion and metastasis: selectins, integrins, and the inhibitory potential of heparins. *International journal of cell biology, 2012*.

Blanc, C., Charette, S. J., Mattei, S., Aubry, L., Smith, E. W., Cosson, P., & Letourneur, F. (2009). Dictyostelium Tom1 participates to an ancestral ESCRT-0 complex. *Traffic, 10*(2), 161-171.

Brahme, N. N., & Calderwood, D. A. (2012). Cell adhesion: a FERM grasp of the tail sorts out integrins. *Current biology, 22*(17), R692-R694.

Chen, Y., Low, T. Y., Choong, L. Y., Ray, R. S., Tan, Y. L., Toy, W., . . . Lim, S. (2007). Phosphoproteomics identified Endofin, DCBLD2, and KIAA0582 as novel tyrosine phosphorylation targets of EGF signaling and Iressa in human cancer cells. *Proteomics, 7*(14), 2384-2397.

Cooper, J., & Giancotti, F. G. (2019). Integrin signaling in cancer: mechanotransduction, stemness, epithelial plasticity, and therapeutic resistance. *Cancer Cell, 35*(3), 347-367.

Desgrosellier, J. S., Barnes, L. A., Shields, D. J., Huang, M., Lau, S. K., Prévost, N., . . . Cheresh, D. A. (2009). An integrin α v β 3–c-Src oncogenic unit promotes anchorage-independence and tumor progression. *Nature medicine, 15*(10), 1163-1169.

Gahloth, D., Levy, C., Walker, L., Wunderley, L., Mould, A. P., Taylor, S., . . . Tabernero, L. (2017). Structural Basis for Specific Interaction of TGFβ Signaling Regulators SARA/Endofin with HD-PTP. *Structure*.

Guo, W., Pylayeva, Y., Pepe, A., Yoshioka, T., Muller, W. J., Inghirami, G., & Giancotti, F. G. (2006). β4 integrin amplifies ErbB2 signaling to promote mammary tumorigenesis. *Cell, 126*(3), 489-502.

Guo, Y. J., Pan, W. W., Liu, S. B., Shen, Z. F., Xu, Y., & Hu, L. L. (2020). ERK/MAPK signalling pathway and tumorigenesis. *Experimental and therapeutic medicine, 19*(3), 1997-2007.

Haas, T. L., Sciuto, M. R., Brunetto, L., Valvo, C., Signore, M., Fiori, M. E., . . . Boe, A. (2017). Integrin α7 is a functional marker and potential therapeutic target in glioblastoma. *Cell Stem Cell, 21*(1), 35-50. e39.

Hamidi, H., & Ivaska, J. (2018). Every step of the way: integrins in cancer progression and metastasis. *Nature Reviews Cancer, 18*(9), 533-548.

Hanker, A. B., Estrada, M. V., Bianchini, G., Moore, P. D., Zhao, J., Cheng, F., . . . Sánchez, V. (2017). Extracellular matrix/integrin signaling promotes resistance to combined inhibition of HER2 and PI3K in HER2+ breast cancer. *Cancer research, 77*(12), 3280-3292.

Homan, C. C., Kumar, R., Nguyen, L. S., Haan, E., Raymond, F. L., Abidi, F., . . . Gecz, J. (2014). Mutations in USP9X are associated with X-linked intellectual disability and disrupt neuronal cell migration and growth. *The American Journal of Human Genetics, 94*(3), 470-478.

Huveneers, S., & Danen, E. H. (2009). Adhesion signaling–crosstalk between integrins, Src and Rho. *Journal of cell science, 122*(8), 1059-1069.

Katoh, Y., Shiba, Y., Mitsuhashi, H., Yanagida, Y., Takatsu, H., & Nakayama, K. (2004). Tollip and Tom1 form a complex and recruit ubiquitin-conjugated proteins onto early endosomes. *J Biol Chem, 279*(23), 24435-24443. doi:10.1074/jbc.M400059200

Kazan, J. M., Desrochers, G., Martin, C. E., Jeong, H., Kharitidi, D., Apaja, P. M., . . . Lukacs, G. L. (2021). Endofin is Required for HD-PTP and ESCRT-0 Interdependent Endosomal Sorting of Ubiquitinated Transmembrane Cargoes. *iScience*, 103274.

Kharitidi, D., Apaja, P. M., Manteghi, S., Suzuki, K., Malitskaya, E., Roldan, A., . . . Pause, A. (2015). Interplay of endosomal pH and ligand occupancy in integrin α5β1 ubiquitination, endocytic sorting, and cell migration. *Cell reports, 13*(3), 599-609.

Lu, Q., Hope, L. W., Brasch, M., Reinhard, C., & Cohen, S. N. (2003). TSG101 interaction with HRS mediates endosomal trafficking and receptor down-regulation. *Proceedings of the National Academy of Sciences, 100*(13), 7626-7631.

Manteghi, S., Gingras, M.-C., Kharitidi, D., Galarneau, L., Marques, M., Yan, M., . . . Witcher, M. (2016). Haploinsufficiency of the ESCRT component HD-PTP predisposes to cancer. *Cell reports, 15*(9), 1893-1900.

Mariotti, A., Kedeshian, P. A., Dans, M., Curatola, A. M., Gagnoux-Palacios, L., & Giancotti, F. G. (2001). EGF-R signaling through Fyn kinase disrupts the function of integrin α6β4 at hemidesmosomes: role in epithelial cell migration and carcinoma invasion. *The Journal of cell biology, 155*(3), 447-458.

Mitra, A., Sawada, K., Tiwari, P., Mui, K., Gwin, K., & Lengyel, E. (2011). Ligand-independent activation of c-Met by fibronectin and α 5 β 1-integrin regulates ovarian cancer invasion and metastasis. *Oncogene, 30*(13), 1566-1576.

Muller, P. A., Caswell, P. T., Doyle, B., Iwanicki, M. P., Tan, E. H., Karim, S., . . . Gosselin, P. (2009). Mutant p53 drives invasion by promoting integrin recycling. *Cell, 139*(7), 1327-1341.

Norris, A., Tammineni, P., Wang, S., Gerdes, J., Murr, A., Kwan, K. Y., . . . Grant, B. D. (2017). SNX-1 and RME-8 oppose the assembly of HGRS-1/ESCRT-0 degradative microdomains on endosomes. *Proceedings of the National Academy of Sciences, 114*(3), E307-E316.

Pantano, F., Croset, M., Driouch, K., Bednarz-Knoll, N., Iuliani, M., Ribelli, G., . . . Bonin, F. (2021). Integrin alpha5 in human breast cancer is a mediator of bone metastasis and a therapeutic target for the treatment of osteolytic lesions. *Oncogene, 40*(7), 1284-1299.

Park, H. S., Jang, M. H., Kim, E. J., Kim, H. J., Lee, H. J., Kim, Y. J., . . . Kim, I. A. (2014). High EGFR gene copy number predicts poor outcome in triple-negative breast cancer. *Modern pathology, 27*(9), 1212-1222.

Pashkova, N., Gakhar, L., Winistorfer, S. C., Sunshine, A. B., Rich, M., Dunham, M. J., . . . Piper, R. C. (2013). The yeast Alix homolog Bro1 functions as a ubiquitin receptor for protein sorting into multivesicular endosomes. *Developmental cell, 25*(5), 520-533.

Raiborg, C., Bache, K. G., Gillooly, D. J., Madshus, I. H., Stang, E., & Stenmark, H. (2002). Hrs sorts ubiquitinated proteins into clathrin-coated microdomains of early endosomes. *Nature cell biology, 4*(5), 394-398.

Raiborg, C., Wesche, J., Malerod, L., & Stenmark, H. (2006). Flat clathrin coats on endosomes mediate degradative protein sorting by scaffolding Hrs in dynamic microdomains. *J Cell Sci, 119*(Pt 12), 2414-2424. doi:10.1242/jcs.02978

Reynolds, A. R., Hart, I. R., Watson, A. R., Welti, J. C., Silva, R. G., Robinson, S. D., . . . Jones, M. C. (2009). Stimulation of tumor growth and angiogenesis by low concentrations of RGD-mimetic integrin inhibitors. *Nature medicine, 15*(4), 392-400.

Roman, J., Ritzenthaler, J. D., Roser-Page, S., Sun, X., & Han, S. (2010). α5β1-integrin expression is essential for tumor progression in experimental lung cancer. *American journal of respiratory cell and molecular biology, 43*(6), 684-691.

Sachse, M., Urbé, S., Oorschot, V., Strous, G. J., & Klumperman, J. (2002). Bilayered clathrin coats on endosomal vacuoles are involved in protein sorting toward lysosomes. *Molecular biology of the cell, 13*(4), 1313-1328.

Seet, L.-F., & Hong, W. (2005). Endofin recruits clathrin to early endosomes via TOM1. *Journal of cell science, 118*(3), 575-587.

Seet, L.-F., Liu, N., Hanson, B. J., & Hong, W. (2004). Endofin recruits TOM1 to endosomes. *Journal of Biological Chemistry, 279*(6), 4670-4679.

Shen, M., Jiang, Y.-Z., Wei, Y., Ell, B., Sheng, X., Esposito, M., . . . Rowicki, M. (2019). Tinagl1 suppresses triple-negative breast cancer progression and metastasis by simultaneously inhibiting integrin/FAK and EGFR signaling. *Cancer Cell, 35*(1), 64-80. e67.

Shiba, Y., Katoh, Y., Shiba, T., Yoshino, K., Takatsu, H., Kobayashi, H., . . . Nakayama, K. (2004). GAT (GGA and Tom1) domain responsible for ubiquitin binding and ubiquitination. *Journal of Biological Chemistry, 279*(8), 7105-7111.

Stern, K. A., Visser Smit, G. D., Place, T. L., Winistorfer, S., Piper, R. C., & Lill, N. L. (2007). Epidermal growth factor receptor fate is controlled by Hrs tyrosine phosphorylation sites that regulate Hrs degradation. *Molecular and Cellular Biology, 27*(3), 888-898.

Sundquist, W. I., Schubert, H. L., Kelly, B. N., Hill, G. C., Holton, J. M., & Hill, C. P. (2004). Ubiquitin recognition by the human TSG101 protein. *Molecular cell, 13*(6), 783-789.

Tischkowitz, M., Brunet, J.-S., Bégin, L. R., Huntsman, D. G., Cheang, M. C., Akslen, L. A., . . . Foulkes, W. D. (2007). Use of immunohistochemical markers can refine prognosis in triple negative breast cancer. *BMC cancer, 7*(1), 1-11.

Truong, H. H., Xiong, J., Ghotra, V. P., Nirmala, E., Haazen, L., Le Devedec, S. E., . . . Vreugdenhil, E. (2014). β1 integrin inhibition elicits a prometastatic switch through the tgfβ–mir-200–zeb network in e-cadherin–positive triple-negative breast cancer. *Science signaling, 7*(312), ra15-ra15.

Trusolino, L., Bertotti, A., & Comoglio, P. M. (2001). A signaling adapter function for α6β4 integrin in the control of HGF-dependent invasive growth. *Cell, 107*(5), 643-654.

Wang, T., Liu, N. S., Seet, L. F., & Hong, W. (2010). The emerging role of VHS domain-containing Tom1, Tom1L1 and Tom1L2 in membrane trafficking. *Traffic, 11*(9), 1119-1128.

Wegner, C. S., Rodahl, L. M., & Stenmark, H. (2011). ESCRT proteins and cell signalling. *Traffic, 12*(10), 1291-1297. doi:10.1111/j.1600-0854.2011.01210.x

Wenzel, E. M., Schultz, S. W., Schink, K. O., Pedersen, N. M., Nähse, V., Carlson, A., . . . Raiborg, C. (2018). Concerted ESCRT and clathrin recruitment waves define the timing and morphology of intraluminal vesicle formation. *Nature communications, 9*(1), 1-18.

White, D. E., Kurpios, N. A., Zuo, D., Hassell, J. A., Blaess, S., Mueller, U., & Muller, W. J. (2004). Targeted disruption of β1-integrin in a transgenic mouse model of human breast cancer reveals an essential role in mammary tumor induction. *Cancer Cell, 6*(2), 159-170.

Wu, Y. J., Pagel, M. A., Muldoon, L. L., Fu, R., & Neuwelt, E. A. (2017). High αv integrin level of cancer cells is associated with development of brain metastasis in athymic rats. *Anticancer research, 37*(8), 4029-4040.

Yao, E. S., Zhang, H., Chen, Y.-Y., Lee, B., Chew, K., Moore, D., & Park, C. (2007). Increased β1 integrin is associated with decreased survival in invasive breast cancer. *Cancer research, 67*(2), 659-664.

Zhang, J., Liu, X., Datta, A., Govindarajan, K., Tam, W. L., Han, J., . . . Phua, T. Y. (2009). RCP is a human breast cancer–promoting gene with Ras-activating function. *The Journal of clinical investigation, 119*(8), 2171-2183.